Dissecting the Stress Recruitment of BNST CRF Neurons:

Regulation of Glutamatergic Inputs via Gi-coupled GPCR Signaling

By

Tracy Lynne Fetterly

Dissertation

Submitted to the Faculty of the

Graduate School of Vanderbilt University

in partial fulfillment of the requirements

for the degree of

DOCTOR OF PHILOSOPHY

in

Neuroscience

September 30, 2018

Nashville, TN

Approved:

Sachin Patel, M.D./Ph.D.

Brad A. Grueter, Ph.D.

David H. Wasserman, Ph.D.

Danny G. Winder, Ph.D.

To my grandmother, Leota
Who saw my potential long before I could

And

To my brother, Matt
For more than you will ever know

ACKNOWLEDGEMENTS

First, I would like to acknowledge my funding sources that supported the work presented in this dissertation. I would like to thank the Molecular Endocrinology Training Program (T32 DK007563) for funding my first two years in lab and continued support throughout my graduate career. This work was additionally funded by grants awarded to Danny Winder from the National Institute on Drug Abuse (R01 DA042475) and National Institute on Alcohol Abuse and Alcoholism (R37 AA019455). Additionally, I would like to thank the Vanderbilt Diabetes Research and Training Center for Pilot Project funding awarded to Danny Winder. I would also like to thank the Vanderbilt Brain Institute and Neuroscience Graduate Program for their support, including Roz Johnson and Beth Sims for everything they do for us.

I would like to thank my mentor, Danny Winder, for his unwavering support and guidance throughout my graduate career. I thank you for your time, patience, and mentorship. Most of all I thank you for always pushing me to believe in my abilities. I would also like to thank the members of my thesis committee: Sachin Patel (chair), Brad Grueter, and David Wasserman. I appreciate all of your time and advice in guiding my project. I especially appreciate the support I received when I switched projects three years into my thesis work.

Next, I would like to thank the members of the Winder Lab. To Katie Holleran, Tiffany Wills, Megan Williams, Stephanie Flavin, and Yuval Silberman, thank you for teaching me the ropes as a young graduate student. To Oliver Vranjkovic, Sam Centanni, Kellie Williford, and Anel Jarmillo, thank you for your continued guidance and friendship. To Elana Milano, thank you for always being there. And thank you to Nick Harris, I could not have asked for a better labmate and friend to walk through the ups and downs of graduate school with. To all the members of the Winder Lab, past and present, thank you for all of your support and for always making the lab a welcoming place to work.

Having been a student at Vanderbilt for a decade, I would also like to thank the many people who saw me all the way through my time here. To Kate Kerbel and Hillary Cansler, your

constant support from afar was key to my success. To Morgan Zienkiewicz and Olivia Roman, thank you for always believing in me and knowing when I need a break. And thank you to my fellow graduate students in the IGP.

Finally, I would like to thank my family. First, to my parents, Gordon and Terry Fetterly, thank you for raising me to believe I can do anything and for your never-ending support. Thank you to Yadi and Eva for seeing me through many rough times. And thank you to my brother, Matt. You have always motivated, supported, and challenged me. I would never have made it here without all of you!

TABLE OF CONTENTS

LIST OF FIGURES

LIST OF ABBREVIATIONS

2-AG	2-arachidonyl glycerol
AAV	adeno-associated virus
ACTH	adrenocorticotropic hormone
AEA	anandamide
AMPA	α-amino-3-hydroxy-5-methyl-4-isoxazolepropionic acid
ANOVA	analysis of variance
ANS	autonomic nervous system
AR	adrenergic receptor
BLA	basolateral amygdala
BNST	bed nucleus of the stria terminalis
cAMP	cyclic adenosine monophosphate
CB1R	cannabinoid 1 receptor
CB2R	cannabinoid 2 receptor
CCK	cholecystokinin
CeA	central amygdala
CGRP	calcitonin gene related peptide
ChR2	channelrhodposin-2
CNS	central nervous system
CRF	corticotropin releasing factor
CRFR1	corticotropin releasing factor receptor 1
CRFR2	corticotropin releasing factor receptor 2
dBNST	dorsal bed nucleus of the stria terminalis
DREADD	designer receptors exclusively activated by designer drugs
eCB	endocannabinoid

EPM	elevated plus maze
EPSC	excitatory post-synaptic current
GABA	γ-aminobutyric acid
GABAA	γ-aminobutyric acid A receptor
GLP1	glucagon-like peptide 1
GPCR	G protein-coupled receptor
HPA	hypothalamic pituitary adrenal
IP	intraperitoneal
LC	locus coeruleus
LH	lateral hypothalamus
MAG	monoacylglycerol
MeA	medial amygdala
NE	norepinephrine
NIH	novelty-induced hypophagia
NMDA	N-methyl-D-aspartate
NPY	neuropeptide Y
NSFT	novelty-suppressed feeding test
NTS	nucleus of the solitary tract
oEPSC	optical excitatory post-synaptic current
PACAP	pituitary adenlyate cyclase activating polypeptide
PBN	parabrachial nucleus
PKCδ	protein kinase C delta
PPR	paired-pulse ratio
PTSD	post-traumatic stress disorder
PVN	paraventricular nucleus

PVT	paraventricular nucleus of the thalamus
vBNST	ventral bed nucleus of the stria terminalis
VNAB	ventral noradrenergic bundle
VTA	ventral tegmental area

Chapter 1

Introduction

Defining the Physiological and Behavioral Effects of Stress

The Adaptive Stress Response

Hans Selye first described the biological stress response in 1936, where he discussed the body's common response to "diverse nocuous agents" (Selye, 1936). This response is considered evolutionarily adaptive, as it provides a mechanism for responding to disruptions in homeostasis (Chrousos and Gold, 1992; Chrousos, 2009). The stress response triggers alterations in signaling in both the central nervous system (CNS) and throughout the periphery. Acute stress results in increased arousal, including increases in attention, allowing for focused cognition. Conversely, drives to feed and reproduce are blunted. Peripherally, increases in cardiovascular tone, respiratory rate, gluconeogenesis, and lipolysis are all observed. Additionally, the growth axis is blunted and immune system activity is altered. Globally, the body works to redirect energy sources to systems necessary for addressing the disruption in homeostasis (Chrousos and Gold, 1992).

As the stress response alters processes throughout the body, a wide variety of signaling pathways work in concert to exert the many effects discussed above. One major component of the stress response is the hypothalamic-pituitary-adrenal (HPA) axis. Within the HPA axis, corticotropin releasing factor (CRF) released from neurons in the paraventricular nucleus (PVN) of the hypothalamus acts in the anterior pituitary to stimulate the release of adrenocorticotropic hormone (ACTH). ACTH can then act on the adrenal glands, resulting in release of glucocorticoid hormones, including cortisol in humans and corticosterone in rodents, into the bloodstream (Figure 1). The connection between hypothalamic signaling molecules and pituitary/adrenal stimulation was initially observed in the 1950s (Guillemin and Rosenberg, 1955; Saffran and Schally, 1955). Identifying the factor that stimulated ACTH release proved

difficult, with the first thorough characterization of CRF occurring in 1981 by Wiley Vale (Vale et al., 1981). An additional signaling component of the HPA axis is the negative feedback loop in which glucocorticoids can signal at the level of both the hypothalamus and pituitary, resulting in decreased release of CRF and production of ACTH (Calogero et al., 1988). The HPA axis can interact with other peripheral systems, influencing metabolic, cardiovascular, and immune function (Chrousos, 2009). Additionally, the hypothalamus provides a direct connection to other brain regions within the CNS, including cortical, hippocampal, and amygdalar circuits (Chrousos, 2009). The wide reaching influence of the HPA axis helps in the coordination of a whole body stress response.

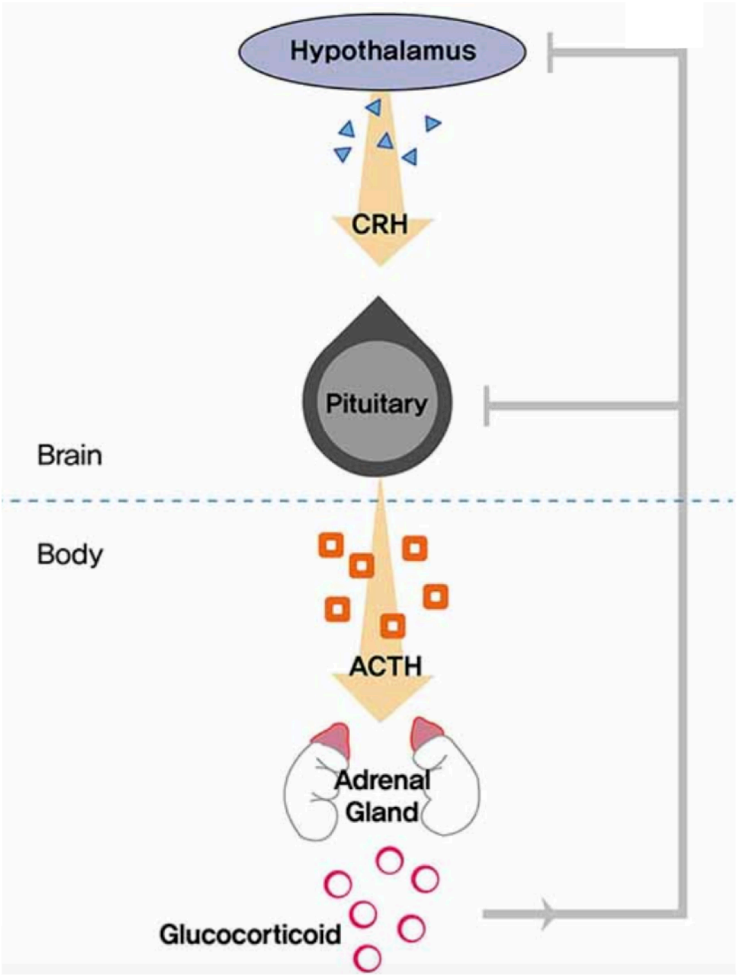

Figure 1. Schematic of Hypothalamic-Pituitary-Adrenal Axis Signaling Cascade.
Adapted from Paul et al., 2015.

Another key component activated by stress is the brainstem norepinephrine (NE) system (Chrousos and Gold, 1992). Although a relatively small number of neurons divided into sub-nuclei within the brainstem make-up the entirety of the NE system (Aston-Jones et al., 1986; Aston-Jones et al., 2000; Robertson et al., 2013), these neurons project widely throughout the CNS. In addition to local connections within the brainstem, these neurons project to the cortex, hippocampus, amygdala, hypothalamus, thalamus, basal ganglia, and cerebellum (Robertson, et al., 2013). As seen with the HPA axis, the NE system also provides a connection between the CNS and the periphery as it plays a role in the autonomic nervous system (ANS) and influencing the release of catecholamines into the bloodstream from the medullary portion of the adrenal glands (Chrousos and Gold, 1992). The ANS, specifically the sympathetic division, is thought to orchestrate the "fight or flight" response first described by Walter Cannon (1915).

While both the HPA axis and brainstem structures are activated by disruptions in homeostasis, these systems are not working independently. The vast connectivity with the rest of the CNS allows for modulation of these two systems by other brain regions and other neurotransmitter systems (Chrousos and Gold, 1992). Furthermore, CRF and NE signaling interact with one another, providing a positive feedback loop. For instance, in rats, an antagonist of a CRF receptor (CRFR1) can block the stress-induced alterations in locus coeruleus (LC; a NE sub-nuclei) neuronal activity (Valentino and Wehby, 1988). Similarly, local NE administration in the hypothalamus results in increase in plasma corticosterone levels in rats, as well as activation of the hypothalamus, as marked by the immediate early gene *Fos* (Cole and Sawchenko, 2002). This cross-talk between the hypothalamus and brainstem provides another layer to an already complex stress response that includes signaling systems throughout the entire body.

The Maladaptive Stress Response: The Influence of Stress in Clinical Disorders

The stress response as discussed above is important for re-establishing homeostasis and protecting the body during acute stress. However, particularly intense stressors and/or chronic stressors can result in alterations in the signaling pathways, as the body works to compensate for prolonged homeostatic disruptions (Chrousos, 2009). These compensatory mechanisms may lead to maladaptive responses to stress and in turn contribute to the pathophysiology of a wide-variety of clinical disorders. Indeed, stress has been associated with illnesses affecting both the nervous system and peripheral systems in the body; these include anxiety (Bystritsky and Kronemyer, 2014), depression (Nestler et al., 2002; Yang et al., 2015), post-traumatic stress disorder (PTSD; Newport and Nemeroff, 2000; Pitman et al., 2012), addiction (Koob, 2008), eating disorders (Hardaway et al., 2015), metabolic syndrome (Tamashiro et al., 2011), cardiovascular disease (Inoue, 2014), and immune alterations (Vitlic et al., 2014).

The link between stress and anxiety/depression has long been studied in both humans and animal models of disease. Elevated levels of glucocorticoids, as well as elevations in catecholamine signaling, have been connected to altered cognition in both rodent models and humans (McEwen and Sapolsky, 1995). However, the effects of elevated glucocorticoids on cognition depend on both the magnitude and duration of elevation, as cognitive performance follows an inverted U-shape, such that performance is best during mild elevation of glucocorticoids (de Kloet et al., 1999; Lupien et al., 2007). These cognitive effects have been attributed to changes in plasticity and signaling in a variety of brain regions, including the hippocampus (Diamond et al., 1992; McEwen, 2016), cortex (Young et al., 1999), and amygdala (Roozendaal, 2002). Structural and functional changes in these brain regions have been observed in patients diagnosed with anxiety (Chen and Etkin, 2013), depression (Rosso et al., 2005; Nifosi et al., 2010), and PTSD (Bremner et al., 1995; Liberzon et al., 1999; Shin et al., 1999). Furthermore, differences in HPA axis activity have been observed in patients diagnosed

with Major Depressive Disorder and PTSD (Yehuda et al., 1991; Strohle and Holsboer, 2003; Wichmann et al., 2017). Similar support for the role of stress signaling in these disorders has been observed in animal models. Norepinephrine and corticosterone levels in the prefrontal cortex and hippocampus in mice predict PTSD-like symptoms (Kao et al., 2015). Overexpressing CRF in the forebrain during development results in anxiety-like phenotypes in adult mice (Toth et al., 2014). Furthermore, chronic stress has been shown to alter CRF gene expression in multiple brain regions in rats (Sterrenburg et al., 2011) and chronic social defeat stress in rats leads to an upregulation of the norepinephrine transporter in the brainstem, hippocampus, amygdala, and frontal cortex (Chen et al., 2012). Taken together, evidence from both clinical and pre-clinical studies point to the importance of stress signaling systems in understanding anxiety and depression.

Stress has also been clinically relevant in understanding substance use disorders. Of note, addiction is often found to be comorbid with other psychiatric disorders including anxiety, depression, and PTSD (Kandel et al., 1997; Brady and Sinha, 2005; Reed et al., 2007). There is evidence that early-life stress may make individuals more vulnerable to addiction (Wills et al., 1992; Sher et al., 1997). Indeed, animal models have demonstrated alterations in the brain reward pathway following both early-life stress and chronic stress (Kosten et al., 2000; Cleck and Blendy, 2008; Sinha, 2008). For example, neonatal rats that are exposed to maternal separation show changes in the development of the CRF system in both the hypothalamus and the LC, as well as alterations in dopamine signaling in the mesolimbic reward pathway (Meaney et al., 2002). Beyond vulnerability and the development of addiction, stress has also been shown to play an important role during the withdrawal and relapse stages of addiction. A negative affective state that develops during withdrawal from drugs of abuse has been associated with changes in stress signaling pathways (Koob et al., 2004; Koob and Kreek, 2007; Koob, 2008) and indeed stress is a major risk factor for relapse to drugs of abuse in humans (Sinha, 2007). Animal models of stress-induced reinstatement of drug-seeking behavior

have indicated roles for both the brain CRF (George et al., 2007; Mantsch et al., 2008) and NE (Le et al., 2005) systems in relapse. Based on substantial pre-clinical research, clinical studies of drug craving have targeted both the CRF and NE systems, with varying outcomes (Fox et al., 2014; Kwako et al., 2015; Schwandt et al., 2016; Pomrenze et al., 2017). These systems continue to be studied in an effort to further dissect the role of these signaling systems in influencing drug-seeking behavior, and will hopefully lead to the development of better-targeted therapies in humans.

The connection between stress and reward signaling also extends beyond drugs of abuse, to natural rewards such as food. Stress has been implicated in a wide range of eating disorders spanning anorexia nervosa to binge eating disorder (Rosenberg et al., 2013; Guarda et al., 2015). CRF signaling itself has been linked to both sides of this spectrum. Rats exposed to stress or central administration of CRF develop an anorectic phenotype (Ciccocioppo et al., 2001), while CRF system recruitment has also been implicated in driving compulsive eating (Cottone et al., 2009). Similarly, catecholamine (dopamine, serotonin, and NE) signaling is altered in animal models of eating disorders (van Gestel et al., 2014) and a human polymorphism in the NE transporter is associated with increased risk for developing a subtype of anorexia nervosa (Urwin et al., 2002). While the mechanisms underlying stress-induced eating as compared to stress-induced hypophagia are not well understood (Oliver and Wardle, 1999), it is clear that stress is an important factor in regulating feeding behavior.

Beyond the central nervous system, stress is also a contributing factor to many other peripheral phenotypes (Chrousos, 2009). For example, chronic stress has been linked to the development of metabolic disorders (Rosmond, 2005; Tamashiro, et al., 2011). Additionally, stress interacts with other factors to play a role in the development of cardiovascular disease (Inoue, 2014). More generally, stress plays an important role in the function of the immune system. While adaptive changes in immune signaling following stress are important for addressing threats to the body, long-term stress can also suppress immune function and result

in maladaptive signaling (Dhabhar, 2014). Together, these studies emphasize that while the stress response is important for maintaining homeostasis, altered stress signaling affects processes throughout the body and is an important variable in understanding the pathophysiology of a wide-variety of clinical phenotypes.

Top-Down Regulation of the HPA axis

While the HPA axis and brainstem NE nuclei comprise the core components of the stress response that link the CNS with the periphery, the complicated connectivity of these regions throughout the brain point to the importance in understanding the role of other brain areas in the stress response. Indeed many brain regions implicated in stress-related psychiatric disorders are key mediators of hypothalamic signaling, resulting in top-down regulation of the HPA axis by these higher brain regions (Figure 2). For example, hippocampal lesions have been shown to enhance basal glucocorticoid levels in rodents, partially through increases in CRF mRNA in the hypothalamus (Knigge, 1961; Herman et al., 1995). These same lesions also result in an enhanced stress response, with prolonged increases in corticosterone and ACTH levels following restraint stress (Herman, et al., 1995). Similarly, in humans, stimulating the hippocampus results in decreased HPA axis activity (Rubin et al., 1966). Like with the hypothalamus, rodents with lesions of the prelimbic prefrontal cortex also show increased HPA axis activity, as well as an increased *Fos* response in the PVN following restraint stress (Figueiredo et al., 2003). Conversely, infralimbic prefrontal cortex lesions have been shown to dampen HPA axis activity (Sullivan and Gratton, 1999), suggesting more ventral regions of the prefrontal cortex may be involved in activation of the stress response. The amygdala is also thought to play a role in activating the HPA axis. Damage to the central amygdala leads to a decreased response to immobilization stress, with lower corticosterone and ACTH levels (Beaulieu et al., 1986). Furthermore, stimulating the medial amygdala increases corticosterone release in rats (Dunn and Whitener, 1986). Interestingly, all of these regions send sparse, if any,

projections to the PVN in the hypothalamus, suggesting that their effects on HPA axis activity rely on an intermediary brain region (Herman et al., 2003). The bed nucleus of the stria terminalis (BNST) receives direct input from all of the regions described above and projects directly to the PVN (Ju and Swanson, 1989; McDonald et al., 1999; Dong et al., 2001a; Dong et al., 2001b), suggesting that the BNST may be an important relay station involved in the integration of top-down signals regulating HPA axis activity.

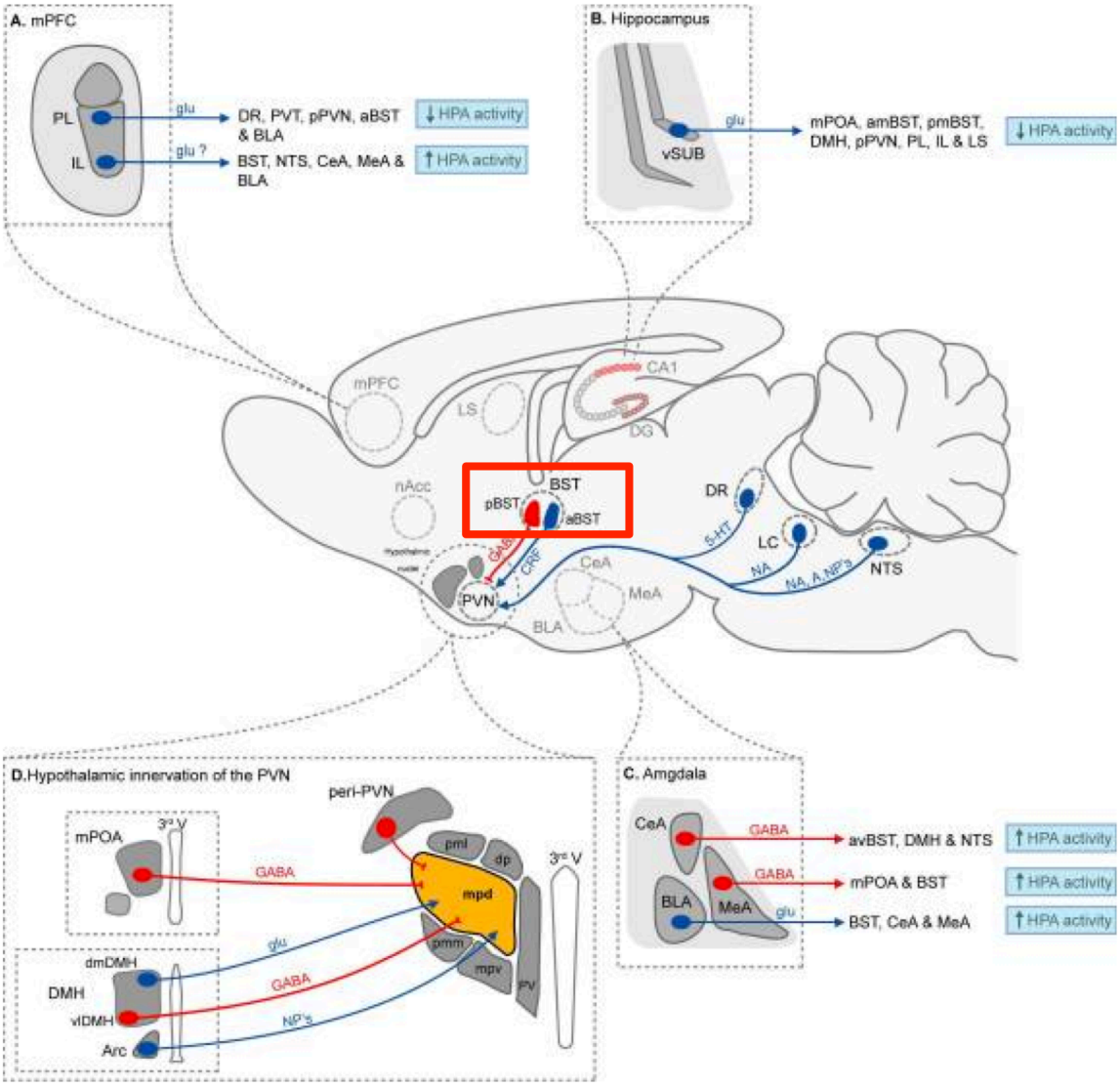

Figure 2. The BNST acts as a central hub of CNS circuitry regulating the HPA axis.
Adapted from Gunn et al., 2015

A Role for the Bed Nucleus of the Stria Terminalis in Understanding Stress-Related Phenotypes

A region of the extended amygdala, the BNST is a key hub and regulator of stress responsivity. The concept of the extended amygdala was first described by several scientists, including Leonard Heimer and George Alheid, following-up on anatomical observations dating back to the 1920s (Johnston, 1923; Alheid and Heimer, 1988). Studies of the BNST have largely been restricted to animal models due to limitations in human imaging techniques. Recently, however, advances have been made in neuroimaging, allowing for studies of smaller brain regions such as the BNST (Avery et al., 2014). Anatomical studies using rodents have shown the BNST to be interconnected with many regions including cortical regions, the amygdala, hypothalamus, and brainstem nuclei (McDonald, et al., 1999; Dong, et al., 2001a; Dong, et al., 2001b; Dong and Swanson, 2004; Dobolyi et al., 2005; Dong and Swanson, 2006). Human neuroimaging studies have begun to confirm connectivity findings from the rodent literature (Avery, et al., 2014), emphasizing the role of the BNST as an integral hub in the brain.

Due to its vast connectivity with other regions in the brain, the BNST is well positioned to directly influence the HPA axis (Crestani et al., 2013). Indeed, studies have shown that BNST lesions in rats result in alterations in HPA axis output, including changes in ACTH and corticosterone levels, along with alterations in PVN neuronal activity (Choi et al., 2007). Additionally, the BNST receives norardrenergic input from NE nuclei in the brainstem (Swanson and Hartman, 1975; Phelix et al., 1992) and stress can increase NE levels in the BNST (Pacak et al., 1995). This noradrenergic projection to the BNST has also been shown to be behaviorally relevant, such as in studies of opiate withdrawal (Aston-Jones et al., 1999; Delfs et al., 2000). Indeed, the BNST has been implicated in a variety of stress-related psychiatric illnesses (Lebow and Chen, 2016), including stress-induced reinstatement to drugs of abuse (Erb et al., 2001; McReynolds et al., 2014; Harris and Winder, 2018), anxiety (Davis et al., 2010; Avery et al., 2016), depression (Louderback et al., 2013; Fitzgerald et al., 2018), and PTSD (Lebow et al.,

2012; Brinkmann et al., 2017). As a whole, the vast rodent literature on BNST structure and function, combined with new neuroimaging studies of the human BNST, support the idea that understanding this small, but complex brain region will be important for continuing to develop effective treatment strategies for stress-related disorders.

Dissecting the Heterogeneous Bed Nucleus of the Stria Terminalis

While a role for the BNST in stress circuitry has been established, determining the precise function of the BNST in various behaviors has proven difficult, as the BNST is not a homogenous region. This heterogeneity can result in what may seem like conflicting behaviors produced by distinct circuits, neurons, and molecules in the BNST. For example, depending on the subregion being investigated, the BNST can both increase and decrease HPA axis output (Choi, et al., 2007). CRF signaling in the BNST has been implicated in both decreased and increased feeding behavior (Krahn et al., 1986; Micioni Di Bonaventura et al., 2014). Neurons that project from the BNST to the ventral tegmental area (VTA) can regulate both rewarding and aversive motivational states depending on the fast neurotransmitter expressed (Jennings et al., 2013). Similarly, neurons projecting to the lateral hypothalamus (LH) regulate divergent emotional states based on the neuropeptide expressed (Giardino et al., 2018). There are many ways to begin to dissect the heterogeneity of the BNST; these include, investigating specific BNST subregions, using expression of specific genes/proteins as markers of cell populations, examining cell populations based on input- and output-specificity, and probing the signaling mechanisms of various neuromodulatory systems within the BNST.

Anatomical Sub-Nuclei of the BNST

One of the earliest examples of BNST heterogeneity comes from the division of the BNST into sub-nuclei based on the cytoarchitecture of the cells in the region (Ju and Swanson, 1989; Ju et al., 1989; Dong, et al., 2001a; Dong, et al., 2001b; Dong and Swanson, 2004; Dong

and Swanson, 2006; Bota et al., 2012). The largest subdivisions of this region include separating it into anterior and posterior divisions based on the divide created by the main bundles of the stria terminals (Ju and Swanson, 1989). The anterior division is further divided into dorsal (dBNST) and ventral (vBNST) regions, which are separated by the anterior commissure. Grossly, the anterior division includes anterolateral cell groups and anteromedial cell groups. The anterolateral region includes the following sub-nuclei: oval, fusiform, juxtacapsular, and rhomboid nuclei (Ju and Swanson, 1989; Dong, et al., 2001a). The posterior division of the BNST can also be divided into sub-nuclei, including the principal, interfasicular, transverse, premedullary, and dorsal nuclei (Ju and Swanson, 1989). Of note, this work was primarily done using rats and there do exist known species differences in the BNST, as discussed later in this chapter.

BNST Circuitry: Inputs

While the cytoarchitecture was used to define the sub-nuclei, these divisions do not necessarily align with differences in functionality within the BNST. Beyond the location of a neuron in the BNST, it can be helpful to define cell populations by looking at specific connectivity patterns. Indeed, the BNST receives inputs from a wide-variety of brain regions, while sending outputs to an equally diverse set of regions. Understanding the connectivity of a given cell population can provide additional information concerning diverse functionality within the BNST. Interestingly, while there have been efforts to map specific inputs/outputs onto specific sub-nuclei in the brain, the vast overlap in connectivity between these regions suggests that the circuitry does not necessarily fit into these cytoarchitectural boundaries. The BNST receives inputs from throughout the brain from many different types of cells. Excitatory (glutamatergic) inputs include the insular and infralimbic cortex (McDonald, et al., 1999), basolateral amygdala (BLA; Kim et al., 2013), ventral subiculum of the hippocampus (Cullinan et al., 1993), parabrachial nucleus (PBN; Dobolyi, et al., 2005), and the paraventricular nucleus of

the thalamus (PVT; Penzo et al., 2015). Inhibitory (GABAergic) inputs include the medial and central amygdala (MeA/CeA; Dong, et al., 2001a), the globus pallidus (Arluison et al., 1990), and regions of the hypothalamus including the PVN (Dabrowska et al., 2011) and the arcuate nucleus (Betley et al., 2013). Here, these inputs have been defined based on the fast neurotransmitter expressed, but this does not preclude the release of other molecules, including neuropeptides. The BNST also receives input from several neuromodulatory regions, such as dopaminergic inputs from the VTA (Meloni et al., 2006), serotonergic inputs from the dorsal raphe nucleus (Phelix, et al., 1992), and noradrenergic inputs from the ventral noradrenergic bundle (VNAB; Forray and Gysling, 2004). Chapters 2 and 3 will focus on two glutamatergic inputs to the BNST, the insular cortex and PBN, which are discussed below.

The insula is largely thought to play a role in interoceptive processing or sensing the internal state of the body (Craig, 2002). As a rather large structure, the insula is a cortical hub in the brain, integrating information from sensory, limbic, motivation/reward, cognitive, and neuromodulatory systems (Gogolla, 2017). The insula has been implicated in several stress-related psychiatric illnesses, including anxiety disorders, depression, and addiction. Individuals with high-trait anxiety have increased insular activity, which has been linked to self-reports of decreased perceived control (Alvarez et al., 2015). Similarly, a functional brain imaging study of females with major depressive disorder showed changes in gray matter volume in the anterior insular cortex (Liu et al., 2014). Relatedly, the evidence for a role for the insula in addiction continues to build, particularly focused around drug craving. Several studies have shown insula activation during cue-induced urges for multiple drugs, including cigarettes (McBride et al., 2006), cocaine (Bonson et al., 2002), and alcohol (Myrick et al., 2004). Furthermore, a study of addicted smokers with brain lesions found that those with a lesion encompassing part of the insula were >100 times more likely to have their addiction disrupted, including the ability to quit, without relapse, and without the urge to smoke (Naqvi et al., 2007). Based on this evidence from human studies, animal models have begun to more thoroughly investigate the role of the

insula in these disorders (Kusumoto-Yoshida et al., 2015; Arguello et al., 2017). The insula and BNST are both significantly involved in anxiety and stress-related psychopathology, yet little is understood about the mechanistic signaling underlying the connectivity of these two regions. As a conserved connection across species (McDonald, et al., 1999; Avery, et al., 2014), the insula to BNST circuit remains a prime area of interest for current research.

While the insula relays interoceptive information via top-down signaling from the cortex, the PBN is located in the brainstem and plays a role in bottom-up processing, as it transmits visceral sensory information to higher brain regions. Studies of PBN signaling have largely been performed in rodents, but there is evidence to support similar visceral processing occurring in the human (de Lacalle and Saper, 2000). The PBN is an important brain structure for responding to homeostatic threats as it relays many aversive signals from the periphery to the rest of the CNS (Palmiter, 2018). These signals include information about visceral malaise, as well as taste, temperature, and pain signals. PBN signaling is involved in a wide-range of behaviors, including feeding, anxiety and fear signals, and pain sensitization. Activation of PBN neurons can suppress feeding, while hypothalamic feeding signals can inhibit this anorexigenic activity (Carter et al., 2013; Essner et al., 2017). These anorectic signals can be in response to peripheral signals (CCK, GLP1, leptin) to terminate normal meals (Campos et al., 2016), but can also be responding to visceral malaise signals, such as experienced during food poisoning, thus promoting conditioned taste aversion (Reilly, 1999; Carter et al., 2015). Similar to learned taste aversion, PBN signaling is involved in the fear conditioning response and may promote fear memory (Sato et al., 2015), while encoding danger signals (Campos et al., 2018). Further, PBN projections to the BNST have specifically been shown to play a role in stress and anxiety responses, including signaling through neurons that express the calcitonin gene-related peptide (CGRP; Gungor and Pare, 2014), as well as neurons expressing the pituitary adenlyate cyclase activating polypeptide (PACAP; Hammack and May, 2015). Thus, the BNST is a site of integration for signals relaying bodily state from both the insular cortex and the brainstem PBN.

BNST Circuitry: Outputs

In addition to receiving a diverse array of inputs, BNST projection neurons synapse in a wide-variety of brain regions (Lebow and Chen, 2016). Within the extended amygdala, the BNST sends projections back to the CeA (Dong, et al., 2001b). The BNST is also reciprocally connected to the hypothalamic stress system via projections to the PVN (Roland and Sawchenko, 1993; Dong, et al., 2001b; Dong and Swanson, 2006), as well as projections to other hypothalamic regions such as the LH (Dong and Swanson, 2004). Motivational and reward centers including the VTA and substantia nigra are also innervated by projections from the BNST (Georges and Aston-Jones, 2001; Dong and Swanson, 2004; Kim, et al., 2013). While the majority of reported projection neurons express the inhibitory neurotransmitter GABA, glutamatergic projections from the BNST have also been reported (Jennings, et al., 2013). The complex interconnectivity of the BNST with other brain regions highlights the importance of the BNST as a relay station, resulting in influence over an immense number of different behavioral phenotypes.

BNST Cell Populations as Defined by Genetic Markers

While the majority of BNST neurons express the fast neurotransmitter GABA, these neurons do not act as a homogenous population, as emphasized by the differences in cytoarchitecture and circuitry described above. As a way to further define these cell populations, it is useful to study BNST neurons based on the expression of various signaling molecules. Advances in genetic technology in rodents have pushed forward these studies, as researches are now able to use these genetically modified animals to identify and manipulate neurons expressing a given protein of interest. In addition to releasing GABA, neurons in the BNST can also release various neuropeptides, although the mechansims of release may differ (van den Pol, 2012; Kash et al., 2015). These neuropeptides, as well as other signaling molecules, are

commonly used as genetic markers to identify sub-populations of BNST neurons. Several of these markers will be discussed below.

Perhaps the most widely studied neuropeptide in the BNST is CRF. Although CRF was first described for its role in the PVN as part of the HPA axis, CRF is also expressed outside the hypothalamus, particularly in the extended amygdala. CRF neurons in the BNST are involved in multiple stress-related behaviors/pathologies. For example, overexpression of CRF in the BNST of rats alters conditioned-anxiety responses (Sink et al., 2013). Furthermore, CRF receptor signaling in the BNST plays a role in processing both anxiety and pain (Tran et al., 2014). The involvement of the BNST in stress-induced hypophagia is also linked specifically to BNST CRF cells (Ciccocioppo et al., 2003). Additionally, a large literature exists examining the role of BNST CRF neurons in addiction (Koob, 2009), particularly their role in stress-induced reinstatement to drug-seeking behaviors (Erb and Stewart, 1999; McReynolds, et al., 2014). CRF cells may be uniquely sensitive to regulation by monoamines, as serotonin, dopamine, and norepinephrine signaling can all modulate these neurons (Guo et al., 2009; Silberman and Winder, 2013). The actions of CRF within the BNST are complex. While CRF has been shown to increase GABAergic transmission in the BNST (Kash and Winder, 2006), CRF is also able to increase glutamatergic drive onto neurons in the BNST (Silberman et al., 2013). CRF binds two receptors, CRFR1 and CRFR2, both of which are G-protein coupled receptors (GPCRs) coupled to Gs, resulting in increased cAMP levels in the cell (Dautzenberg and Hauger, 2002). Some evidence suggests actions at CRFR1 and CRFR2 may work in opposition to each other as seen by their opposing actions in modulating anxiety-like behavior and autonomic/endocrine responses to stress (Tran, et al., 2014). While BNST CRF neurons have been implicated in many behaviors, these cells do not represent a homogenous population. CRF cells can be found throughout multiple sub-nuclei in the BNST and vary in their electrophysiological properties (Silberman, et al., 2013), suggesting that multiple populations of CRF cells may exist.

Another stress-related peptide in the BNST is Neuropeptide Y (NPY). Broadly, NPY is thought to work in opposition to the CRF system, decreasing stress responsivity and returning the system to homeostasis (Heilig et al., 1994). For instance, intracerebroventricular administration of NPY was able to block yohimbine (a pharmacological stressor) induced reinstatement to alcohol seeking (Cippitelli et al., 2010). Specifically in the BNST, NPY decreases GABAergic transmission, acting in opposition to CRF (Kash and Winder, 2006). Similarly, NPY administration in the BNST is able to block pain-induced conditioned place aversion, which is promoted by CRF (Ide et al., 2013). Based on the contrasting effects of NPY and CRF signaling in the BNST, these neuropeptides provide promising markers for helping to dissect heterogeneous cell populations in this region.

A less-well studied signaling molecule in the BNST is Protein Kinase C δ (PKCδ), however, this marker has been commonly used in another region of the extended amygdala, the CeA, to dissect the behavioral and physiological role of different cell populations. Interestingly, PKCδ neurons in the CeA are largely distinct from CRF-expressing neurons (Haubensak et al., 2010). PKCδ-expressing neurons in the CeA have been implicated in conditioned responses to fear, with PKCδ neurons in the lateral division of the CeA being shown to inhibit ouput neurons in the medial division (Haubensak, et al., 2010). Some studies have classified these neurons as being part of a “fear-off” circuit (Ciocchi et al., 2010), while others show somewhat opposing effects, with PKCδ neurons being involved in conveying aversive signals, as well as acquisition of aversive learning (Yu et al., 2017). Beyond fear circuitry, these neurons in the CeA are also activated by anorexigenic signals (Cai et al., 2014). Together, these studies show the potential of using PKCδ as a marker of unique neuronal populations and suggest similar insight may be attained when investigating stress and anxiety circuits in the BNST.

Neuromodulatory Systems in the BNST

Defining inputs and outputs to BNST cells is an important step to understanding the overall circuitry. Once connections have been identified, it is possible to investigate how the synaptic activity between these connections can be altered, including through neuromodulatory systems. While fast neurotransmission, including GABA and glutamate signaling, largely act via ligand-gated ion channels (e.g. AMPA, NMDA, and GABAA), slower neuromodulatory systems commonly signal through GPCRs to regulate synaptic transmission. Understanding how these systems interact can provide insight into drug targets for treating various psychopathologies.

As NE signaling is a key component of the stress response, it is important to understand the neuromodulatory effects of NE throughout the brain. The BNST is innervated directly by NE via fibers from the VNAB (Forray and Gysling, 2004). NE expression in terminals is found throughout the BNST, with the densest innervation located in the vBNST (Phelix, et al., 1992; Egli et al., 2005). The brainstem NE input to the BNST is largely from the nucleus of the solitary tract (NTS; Riche et al., 1990; Forray et al., 2000), but input from the LC has also been observed (Phelix, et al., 1992; Forray, et al., 2000). While basal NE levels in the BNST provide a noradrenergic tone (Forray et al., 1997), stress can increase NE levels in the BNST (Pacak, et al., 1995). NE signaling in the BNST is directly involved in the regulation of multiple behaviors. Adrenergic ligands in the BNST can alter the neuroendocrine output of the HPA axis, as seen by blunted stress-induced plasma ACTH levels in rats (Cecchi et al., 2002). NE signaling also directly affects the role of the BNST in stress-induced reinstatement to drug-seeking paradigms (Wang et al., 2001), at least partially through interactions with the CRF system (Brown et al., 2009; McReynolds, et al., 2014). The effects of NE on neurotransmission in the BNST can be quite complex, as NE signals through multiple classes of GPCRs. Adrenergic receptors (ARs) are divided into three classes: α_1, α_2, and β (Bylund et al., 1994). Broadly, α_1-ARs are coupled to Gq signaling, while α_2-ARs are Gi/o-linked, and β-ARs signal through Gs (Hein, 2006). Based on the diverse coupling of these GPCRs, NE signaling can have varying effects based on the

predominant AR class that is activated. The BNST expresses all three classes of ARs (Rainbow et al., 1984; Scheinin et al., 1994; Day et al., 1997). The expression of α_2-ARs is particularly widespread in the BNST, with these receptors being found in both pre- and post-synaptic compartments within the BNST (Shields et al., 2009; Flavin et al., 2014). Dissecting the complex actions of NE in the BNST will provide opportunities for uncovering ways to bias NE signaling to alter physiology and behavior.

Another stress-related neuromodulatory system in the CNS is the endocannabinoid (eCB) system. This system consists of two endogenous ligands, anandamide (AEA) and 2-arachidonyl glycerol (2-AG), as well as the Gi/o-coupled cannabinoid receptors (CB1R and CB2R). CB1 receptors are widely expressed throughout the CNS (Herkenham et al., 1990), particularly in axon terminals (Kano et al., 2009). Activation of CB1Rs leads to increases in adenylyl cyclase activity, inhibition of voltage-gated calcium channels, and activation of G protein-gated inwardly rectifying potassium channels, resulting in decreased neurotransmitter release from axon terminals (Howlett et al., 2002; Kano, et al., 2009). Uniquely, the ligands AEA and 2-AG are synthesized post-synaptically and then activate pre-synaptic CB1Rs, traveling in a retrograde manner (Kano, et al., 2009; Ohno-Shosaku and Kano, 2014). The role of the eCB system in stress signaling has been well documented (Morena et al., 2016), with both human studies (Green et al., 2003) and rodent studies (Patel et al., 2004; Bellocchio et al., 2013; Shonesy et al., 2014) providing evidence for CB1R signaling in dampening stress and anxiety. CB1Rs are expressed in the BNST (Puente et al., 2010) and have been shown to influence plasticity and excitability within this region (Grueter et al., 2006; Massi et al., 2008). Furthermore, eCB signaling in the BNST plays a role in stress responsivity, including regulating cardiovascular responses to acute stress (Gomes-de-Souza et al., 2016). As the therapeutic potential of targeting the eCB system continues to be explored (Morena, et al., 2016; Volkow et al., 2017) it will be important to continue to examine the specific circuits and signaling pathways regulated by the eCB system in the BNST. Understanding the varied roles and interactions of

neuromodulatory systems within the context of BNST circuitry will improve methods for targeting aberrant synaptic activity underlying psychiatric disorders.

Known Species Differences in BNST Anatomy

Broadly, the connectivity and functionality of the BNST fundamentally appears similar across current mouse, rat, primate, and human studies. However, there have been noted species differences in animal studies. First, the anatomical studies first identifying the many sub-nuclei of the BNST, while also mapping inputs and outputs, were all performed in rats (Ju and Swanson, 1989; Dong, et al., 2001a; Dong, et al., 2001b; Dong and Swanson, 2004; Dong and Swanson, 2006). While similar circuitry has been confirmed in mouse studies, the cytoarchitectural sub-nuclei divisions are not as clear in the mouse BNST and differences between specific nuclei are perhaps less well understood. For instance, in the rat BNST CRF is largely localized to the oval nucleus in the dBNST (Cummings et al., 1983; Hazra et al., 2011; Dabrowska et al., 2013), while the CRF cells in the mouse BNST are distributed throughout the dBNST (Silberman, et al., 2013). Additionally, these cells differ in their electrophysiological characteristics. In the rat, three types of neurons (Type I, II, III) were described based on varying physiological properties (Hammack et al., 2007). In the rat, BNST CRF cells appear to share many characteristics with Type III neurons (Hazra, et al., 2011). However, in the mouse, more than three types of neurons were identified, with CRF cells being spread throughout all of these categories (Silberman, et al., 2013). Additionally, a study comparing the physiology of neurons in mouse, rat, and primate BNST demonstrates that the distribution of Type I-III neurons varies between species (Daniel et al., 2017). Similar to the mouse, neurons in the primate BNST could be divided into more than three classes. Additionally, while Type II cells were most prevalent in the rat BNST, Type III cells were most common in mouse and primate BNST. Beyond differences in cell types, there is also evidence of differences in functional connectivity between species. When comparing the BNST projection to the VTA in mice and

rats, researchers found a stronger projection in mice, while rats exhibited a stronger excitatory influence over dopamine neurons in the VTA (Kaufling et al., 2017). Additionally, while advances in neuroimaging have largely confirmed similar BNST connectivity in humans and rodents, newly identified connections in the human have been reported, such as a function connection with the paracingulate gyrus (Avery, et al., 2014). Many features of the BNST have are similar across species, but it is important to keep in mind potential differences, particularly when considering the potential for the translation of animal studies to clinical treatments.

The Importance of Sex as a Biological Factor in Stress Responsivity

Historically, preclinical studies using animal models have relied largely on males, with a notably strong bias within the field of neuroscience (Beery and Zucker, 2011). Interestingly, the prevalence of male studies may have started following observations of altered phenotypes that were dependent on stages of the estrus cycle (Wang, 1923), leading to concerns over variability in female animals. Recent efforts in preclinical research have worked to rid the field of this bias as more studies begin to uncover that female mice do not have inherently higher trait variability (Mogil and Chanda, 2005; Becker et al., 2016) and that sex hormones alone often do not explain observed differences in females (Cahill, 2006). Translation of preclinical studies into successful treatment in humans relies upon a thorough understanding of differences in sex as a biological variable. Indeed, the stress system is an excellent example of sexual dimorphism, as many components of this system contain sex-based differences, as discussed below.

Sex Differences in Clinical Diagnoses of Stress-Related Psychiatric Disorders

Epidemiological studies have shown that women have higher rates of depression and many types of anxiety disorders (Kessler et al., 1994; Kessler et al., 1995; Weissman et al., 1996; Kessler et al., 2012). Beyond rates of diagnosis, women also exhibit differential symptomology. For example, not only were women shown to have a higher risk for developing

PTSD following an adverse event, but the duration of symptoms was also shown to be longer in women (Breslau, 2002). Similarly, women diagnosed with depression are more likely to have atypical symptoms (mood reactivity, hypersomnia, hyperphagia) or elevated anxiety levels (Posternak and Zimmerman, 2001). Furthermore, even in populations that do not reach clinical criteria for diagnosis, symptoms of anxiety and depression are more common in women (Nolen-Hoeksema et al., 1999; Hankin, 2009). While these disparities in risk are acknowledged, the mechanistic underpinnings of these differences are not thoroughly understood. A better understanding of sex-specific alterations in brain circuitry and signaling pathways will allow for more targeted clinical treatment of individuals diagnosed with these stress-related disorders.

Sex Differences in the HPA axis

Male and female differences in stress activation of the HPA axis have been observed in both rodent and human populations. In the rodent literature, higher basal levels of corticosterone have been reported in females (Kitay, 1961; Sterrenburg et al., 2012; Babb et al., 2013), with differences being most notable at the onset of the dark phase of the light cycle (Atkinson and Waddell, 1997). Female rodents also show increased corticosterone levels in response to stress as compared to males, including following restraint stress (Aloisi et al., 1998; Babb, et al., 2013) and after both predictable and unpredictable stressors (Heinsbroek et al., 1991). The timecourse of corticosterone elevation also differs, with females exhibiting quicker increases in response to stress and prolonged elevation of corticosterone levels (Iwasaki-Sekino et al., 2009). Interestingly, these effects may be linked to differential corticosterone sensitivity in males and females (Atkinson and Waddell, 1997). Additionally, there is evidence of greater ACTH secretion following stress in females (Iwasaki-Sekino, et al., 2009; Babb, et al., 2013). Of note, female rodents have heavier adrenal glands, along with a greater capacity for corticosterone synthesis, and thus produce more corticosterone in response to similar levels of ACTH stimulation (Malendowicz, 1976; Malendowicz, 1980). Sex differences have also been

noted at the level of the hypothalamus. In the basal state, higher transcript levels of *Crh* have been observed in the PVN of female rodents (Duncko et al., 2001). Stress activation of PVN neurons has been investigated using *Fos*, an immediate early gene, as a marker of neuronal activation. Following restraint stress, females exhibit larger numbers of PVN neurons expressing *Crh* and *Fos* as compared to males (Babb, et al., 2013). Together, these rodent studies demonstrate sex-specific differences throughout the components of the HPA axis.

The human literature has similarly looked at sex differences in the HPA axis; however, the conclusions have been less straightforward. Depending on the test used to activate the HPA axis, both males and females have shown larger increase in cortisol levels (Kirschbaum et al., 1999; Stroud et al., 2002). Females appear to show greater HPA activation when using social stress of physical stress tests (Gerra et al., 1992; Jezova et al., 1994). Pharmacological stimulation of the HPA axis also generally results in greater activation in females. Administration of ovine CRF resulted in increased ACTH levels and a prolonged cortisol response in females (Gallucci et al., 1993). Similarly, dexamethasone (a corticosteroid) administration also increased cortisol levels more in females (Heuser et al., 1994). These human studies further support a role for increased activation of the HPA axis in females that has been well documented in rodents. Continued research focused on sex differences may provide insight into female susceptibility to anxiety and depression-related disorders.

Sex Differences in the NE Brainstem System

Further evidence for increased stress responsivity in females comes from research investigating brainstem NE nuclei such as the LC. Both structural and functional sex differences have been observed in the rodent LC. Structurally, the LC is larger in female rats, possibly due to greater numbers of neurons, although this was dependent on the specific strain of rats utilized (Luque et al., 1992; Pinos et al., 2001; Garcia-Falgueras et al., 2005; Garcia-Falgueras et al., 2006). These extra neurons may arise from LC neurogenesis that continues during

puberty in females but not in males (Pinos, et al., 2001). Additionally, LC neuronal structure is more complex in females, with longer dendritic extensions and increased branching (Bangasser et al., 2011). These more complex dendritic trees may also receive more synaptic input, as they have increased levels of a synaptic vesicle protein, synaptophysin, as seen by immunohistochemical staining (Bangasser, et al., 2011). In addition to these structural differences, NE signaling is also sensitive to regulation by ovarian hormones. Studies using ovariectomized rats showed that treatment with estradiol could increase NE levels in multiple brain regions, including the cortex, hippocampus, and hypothalamus (Alfinito et al., 2009; Lubbers et al., 2010). Furthermore, these hormones may also be altering NE signaling through changes in adrenergic receptor expression (Karkanias et al., 1997; Meitzen et al., 2013). Sex differences in the LC also connect back to the HPA axis and CRF signaling. LC neurons in female rats are more sensitive to activation by CRF in the basal state, as larger doses of CRF are needed to activate LC neurons in males (Curtis et al., 2006). Furthermore, while prior stress is able to shift the CRF response of LC neurons in males, decreasing the CRF dose necessary for activation, prior stress does not alter this response in females (Curtis, et al., 2006; Bangasser et al., 2010). Combined, these rodent studies demonstrate sex-specific differences in both structure and function of the NE system.

Compared to the rodent literature, far fewer studies have addressed sex-specific NE brainstem differences in the human. While never directly compared, one lab published two studies quantifying LC neurons, finding more neurons in females (Busch et al., 1997; Ohm et al., 1997). A neuroimaging study also found increased activation of an emotional-arousal circuit, composed of the amygdala and LC, following exposure to noxious stimuli (Labus et al., 2008). Future research in humans will be needed to better understand sex-specific brainstem NE differences, as well as potential interactions with the HPA axis.

Sex Differences in the Bed Nucleus of the Stria Terminalis

The BNST is one of the most sexually dimorphic regions in the brain, with particularly strong evidence coming form early studies of the posterior portion of the BNST. Specifically, the principal nucleus of the posterior BNST is larger in male rodents and contains more neurons (del Abril et al., 1987; Hines et al., 1992). The greater number of neurons is partially due to increased vasopressin expressing cells in males (van Leeuwen et al., 1985). The development of this sexually dimorphic region is driven by sex hormones, including estradiol and testosterone (Kanaya et al., 2014). Differences in expression of receptors for these hormones have been observed in the BNST of mature rodents, with decreased levels of the estrogen receptor found in males (Kelly et al., 2013). There is also evidence of sex-specific differences in both synaptic inputs and outputs of the posterior BNST. Immunohistochemical staining for synaptophysin is denser in female rats, suggesting stronger presynaptic innervation (Carvalho-Netto et al., 2011). Chronic variable stress reduces this synaptophysin staining in females, but does not alter it in males (Carvalho-Netto, et al., 2011). Conversely, when looking at outputs from the posterior BNST, males show increased GABAergic innervation of the anteroventral periventricular nucleus of the hypothalamus as compared to females (Polston et al., 2004). Importantly, observed sex differences are not limited to the posterior portion of the BNST. Several studies have shown sex-specific effects in anterior regions of the BNST, particularly when investigating the CRF system and its response to stress. For instance, following restraint stress, female rats show increased neuronal activation as marked by increases in *Fos* expression in the oval nucleus of the BNST (Sterrenburg, et al., 2012). Interestingly, in this study males were shown to have increased *Crh* mRNA following stress, but there were no differences in overall protein levels in both males and females. While the oval nucleus is part of the dBNST, other groups have looked at changes in the vBNST. As seen in the oval nucleus, restraint stress led to greater increases in *Fos* expression in female rats, this time in the anteroventral region of the BNST (Babb, et al., 2013). Additionally, in this region females also showed increased *Crh*

mRNA levels following stress, as well as an increase in the number of cells co-expressing *Crh* and *Fos* (Babb, et al., 2013). While a lot of attention has been given to the sexual dimorphism of the posterior BNST, it is clear that there are sex-differences throughout the rodent BNST that should be considered in future studies.

Due to its location and small size in the human brain, much less is understood about sex-specific aspects of the human BNST. However, there are several studies demonstrating structural differences in the male and female BNST in post-mortem human brain tissue. In one study, researchers found a region of the human BNST ("darkly staining posteromedial") to be 2.47 times larger in volume in males as compared to females (Allen and Gorski, 1990). Similarly, a region of the BNST termed the "central subdivision" was also shown to be larger in males than females (Zhou et al., 1995). As neuroimaging techniques continue to evolve, more information will be gained about the sexual dimorphism of the human BNST and how this compares to the sex differences reported in the rodent literature.

Summary

Stressful events are a part of everyday life, making a stress response system a necessary component of the body. While the stress response itself is evolutionarily advantageous, alterations in this response are thought to underlie the psychopathology of multiple disorders, particularly in response to chronic stress. Direct connections between the brain and the periphery, such as the HPA axis and the brainstem, have long been implicated in controlling the stress response. However, decades of research have continued to build on these circuits, complicating our understanding and providing a role for many regions throughout the brain. As a result of these studies, regions such as the BNST have become popular areas of study in recent years. Unfortunately, the heterogeneity of the BNST has often made it very difficult to study. The connectivity of the BNST is quite complex and many different populations of cells have been identified, often leading to difficulties in drawing conclusions about the role of

the BNST in specific behaviors. Chapter 2 describes an effort to dissect the heterogeneity of the BNST, to better understand regulation of the activation of the BNST by stress. This includes investigation of specific excitatory inputs to BNST CRF cells, as well as exploration of the regulation of these connections by neuromodulatory systems. Chapter 3 continues this effort by focusing on sex-specific effects in the BNST stress circuitry, focusing on the identification of a unique subpopulation of neurons in the female BNST that is uncovered by stress. Overall, this dissertation aims to provide a more thorough understanding of the stress recruitment of BNST neurons in males and females, while elucidating potential targets for dampening this stress activation.

Chapter 2

Neuromodulation of insular and parabrachial input to stress sensitive BNST CRF cells

Adapted from: *Fetterly et al., α_{2A}-adrenergic receptor activation decreases parabrachial nucleus excitatory drive onto BNST CRF neurons and reduces their activity in vivo*

Introduction

Stress is a major contributor to many psychiatric diseases, including depression, eating disorders, and addiction (Chrousos, 2009). While the stress response is necessary for maintaining homeostasis in the body, chronic stress can become maladaptive over time. The bed nucleus of the stria terminalis (BNST), a region within the extended amygdala, plays a critical role in physiological and behavioral responses to stress (Casada and Dafny, 1991; Sullivan et al., 2004; Crestani, et al., 2013; Tran, et al., 2014). Within the BNST, the corticotropin releasing factor (CRF) system is thought to promote negative affective responses to stress (Koob, 1999). BNST CRF signaling is enhanced following both acute and chronic stress exposure (Choi et al., 2006; Funk et al., 2006) and may be more stress reactive in females (Sterrenburg, et al., 2012; Babb, et al., 2013). Understanding the regulation of BNST CRF neurons during both acute and chronic stress could lead to better ways to address stress-induced pathologies.

Previous work has demonstrated an interaction between norepinephrine (NE) and glutamatergic inputs into the BNST (Egli, et al., 2005; Shields, et al., 2009; Flavin, et al., 2014). However, the heterogeneity of BNST neurons remains a large obstacle in dissecting the impact of specific BNST inputs. We previously identified the parabrachial nucleus (PBN) as a functional glutamatergic input into the BNST that is sensitive to the clinically well-tolerated α_{2A}-AR agonist guanfacine. Clinically, guanfacine has shown promise for the treatment of attention-deficit/hyperactivity disorder (Sallee et al., 2009). The PBN is known to form axosomatic synapses with BNST neurons, potentially allowing for increased influence over neuronal activity

(Shimada et al., 1989; Dobolyi, et al., 2005). Functionally, PBN projection neurons play a role in regulating many behaviors, including anxiety responses, fear conditioning, taste aversion, feeding, and pain sensitization (Carter, et al., 2013; Carter, et al., 2015; Sato, et al., 2015; Chen et al., 2017; Campos, et al., 2018). Here we find PBN afferents synapse onto BNST CRF cells, and that these CRF neurons are inhibited by α_{2A}-AR activation. Together, these studies suggest a role for the PBN in modulating stress activation of BNST CRF neurons.

Another glutamatergic input to the BNST is the insular cortex (McDonald, et al., 1999). As a cortical hub, the insula is involved in interoceptive processing (Craig, 2002). Changes in insular function have been linked to several stress-related psychiatrc disorders, including anxiety, depression, and substance use disorders (Myrick, et al., 2004; Naqvi, et al., 2007; Liu, et al., 2014; Alvarez, et al., 2015) Interestingly, data suggests that this input may be insensitive to α_{2A}-AR regulation (S. Flavin, unpublished data), but can be regulated by endocannabionid (eCB) signaling (S. Centanni, unpublished data), another neuromodulatory sytem in the BNST. Activation of the eCB system can decrease stress and anxiety responses (Patel, et al., 2004; Bellocchio, et al., 2013; Shonesy, et al., 2014), making this a therapeutically relevant system (Morena, et al., 2016). While little is known about insula modulation of BNST CRF cells, these studies suggest that the eCB system may be involved in the stress regulation of this input.

In this study we assess the recruitment of BNST CRF cells following acute restraint stress, and explore regulation of these cells by neuromodulatory systems. We specifically investigate glutamatergic drive onto CRF neurons to provide insight into mechanisms that decrease stress activation of these neurons. Utilizing cFos as a marker of neuronal activation, we find that activation of α_{2A}-adrenergic receptors (AR) can decrease the activation of BNST CRF neurons in both stressed and unstressed conditions. Further, we use electrophysiology to understand the modulation of glutamatergic drive onto these CRF neurons by the NE system. Additionally, we show that increasing eCB signaling can decrease stress activation of BNST CRF neurons, an effect that may be regulated by the insular cortex input. Moreover, we found

evidence of highly sex-dependent responses of BNST CRF cells, both in terms of afferent control of stress responses as well as sensitivity to neuromodulation. Together, these studies provide a better mechanistic understanding of ways to dampen the stress response in BNST CRF neurons. These insights will be important for future efforts in more effectively developing drugs that can alter maladaptive responses to stress.

Methods

Animals

Adult male and female C57BL/6J mice (>7 weeks of age; The Jackson Laboratory; RRID: IMSR_JAX:000664) were used for all fluorescence *in situ* hybridization studies. CRF neurons were identified for electrophysiological analysis and immunohistochemistry experiments through the use of previously described male and female CRF-tdtomato reporter mice (Silberman, et al., 2013). The CRF-Cre line utilized in these studies has been extensively evaluated and reliably reports CRF mRNA-expressing neurons (Chen et al., 2015). All mice were group housed (2-5 animals per cage) and maintained on a 12 hour light/dark cycle (lights on 0600-1800) under controlled temperature (20-25 °C) and humidity (30-50%) levels. Food and water were available *ad libitum*. All procedures were approved by the Institutional Animal Care and Use Committee at Vanderbilt University (Nashville, TN).

Restraint Stress Exposure

Mice were restrained during the light cycle (0600-1800) using 50 mL conical tubes (Fisher Scientific) altered to have holes throughout the tube and cap to allow for airflow (McElligott et al., 2010). Order of restraint was counterbalanced within experimental groups, to account for differences in time of day. Prior to undergoing restraint, mice were handled for five days as described previously (Olsen and Winder, 2010). Mice were allowed to acclimate to the test location in their home cage for one hour in a sound- and light-attenuating box (Med Associates Inc.). During restraint, mice were placed inside separate sound- and light-attenuating

boxes for one hour before being returned to their home cage for 30 minutes. In some experiments, mice were treated with guanfacine (1mg/kg IP; Fisher Scientific) or Clozapine-N-oxide (CNO; 3mg/kg IP) 30 min prior to restraint stress. For the final experiment, mice were treated with JZL184 (8 mg/kg IP; Cayman Chemical) 2 hr prior to restraint stress).

Fluorescent Immunohistochemistry

Under isoflurane anesthesia, mice were transcardially perfused with 10 mL cold phosphate buffered saline (PBS) followed by 20 mL 4% paraformaldehyde (PFA) in PBS. Brains were extracted, post-fixed for 24 hours at 4 °C in the same fixative, and then cryoprotected with 30% sucrose in PBS for a minimum of 48 hours. Coronal sections were cut on a cryostat (Leica, CM3050S) at a thickness of 40 µm and stored in PBS prior to immunohistochemical staining. For cFos experiments, free-floating brain slices containing the BNST (Bregma +0.14) were washed in PBS (4 x 10 min), permeabilized with 0.5% Triton X-100 in PBS (1 hour), and then blocked with 5% Normal Donkey Serum and 0.5% Bovine Serum Albumin (1 hour); all steps were at room temperature. Sections were then incubated in cFos primary antibody (1:2000, sc-52, Santa Cruz Biotechnology Inc., RRID: AB_2106783) in blocking solution for 24 hours at room temperature. Slices then underwent PBS washes (4 x 10 min) followed by incubation in donkey Alexa Fluor 488 anti-rabbit (1:500, Jackson ImmunoResearch, RRID:AB_2313584) fluorescent dye-conjugated secondary antibody for 24 hours at 4 °C in PBS with 0.1% Triton X-100. Slices were then washed with PBS (4 x 10 min), mounted on positively charged slides (Fisher Scientific), and coverslipped with PolyAquamount (Polysciences) when dry. Modifications were made to the staining protocol for visualizing CGRP terminals surrounding CRF cells in CRF-tdtomato mice, including an altered blocking buffer (10% Normal Donkey Serum), primary incubation step in CGRP primary antibody (1:400, ab36001, Abcam, RRID:AB_725807) for 3 days at 4 °C, and secondary amplification using donkey Cy5 anti-goat (1:400, Jackson ImmunoResearch, RRID:AB_2340415) overnight at 4 °C. For visualizing DREADD viral injection sites, no amplification steps were utilized. Images of injections sites and

antibody-labeled tissue were obtained using a Zeiss 710 scanning confocal microscope and a 20x/0.75 NA lens, keeping acquisition parameters consistent within an experiment. For cFos cell quantification, the number of cFos+ cells per dBNST was averaged over two coronal slices. For ChR2 injection verification (without amplification), images were obtained using an Olympus SZX12 stereo microscope. Images were analyzed using ImageJ software (NIH; RRID: SCR_003070), with the same brightness and contrast settings applied across all images.

RNA in situ hybridization

Fluorescence *in situ* hybridization assays were performed using the RNAScope Fluorescent Multiplex Reagent Kit (Advanced Cell Diagnostics) to visualize RNA transcripts in BNST coronal sections. Probes used include Mm-Crh-C1, Mm-Fos-C2, and Mm-Prkcd-C3. Mice were put under isoflurane anesthesia and brains were quickly extracted, submerged in ice-cold, oxygenated (95% O_2/5% CO_2) artificial cerebrospinal fluid (ACSF; in mM: 124 NaCl, 4.4 KCl, 2.5 $CaCl_2$, 1.3 $MgSO_4$, 1 NaH_2PO_4, 10 glucose, 26 $NaHCO_3$), and flash-frozen in Optimal Cutting Temperature Solution (VWR) using Super Friendly Freeze-It Spray (Fisher Scientific). Embedded brains were stored at -80 °C prior to being cut on a cryostat (Leica, CM3050S). Slices (16 µm) were adhered to charged slides (Denville Scientific) and immediately frozen with dry ice and stored at -80 °C until staining. Fixation, dehydration, hybridization, and staining protocols for fresh frozen tissue were carried out according to ACD's online specifications. Z-stack BNST images were obtained with a 63x/1.4 NA oil lens on a Zeiss 710 scanning confocal microscope. Three images were taken to cover the dorsal, medial, and lateral areas of the dorsal BNST (Bregma +0.14). Negative control images (negative control probe: DapB) were used to determine brightness and contrast parameters for experimental images. Max intensity projections were used for analysis with ImageJ software (NIH). Counts were combined for the three BNST regions and then averaged with the counts for the contralateral BNST in the slice. Transcripts were identified as individual dots within a cell, using DAPI-labeled nuclei to identify individual cells. A blinded reviewer identified cells as positive for zero, one, or two of the

following transcripts: *Crh and Fos*. Negative control images were used to determine thresholding parameters that excluded non-specific fluorescence.

Microinjection Surgeries

Mice that were >6 weeks of age were used for viral injections studies. Mice were anesthetized with isoflurane and injected intracranially with AAV constructs expressing either ChR2 or DREADD as described below. For the optical stimulation experiments, 200-300 nL of AAV5-CamKIIα-ChR2:YFP (University of North Carolina Viral Vector Core) was injected at 40 nL/min into one of two regions based on coordinates from the (Franklin and Paxinos, 2007) mouse brain atlas: insula (AP: 0.02, ML: ±3.66, DV: -4.30) or PBN (AP: -5.34, ML: ±1.31, DV: -4.30; 15.03° angle). For both the restraint stress and electrophysiological control PBN DREADD experiments, 200-300 nL of AAV5-hSyn-hM4D(Gi)-mCherry (Addgene) was injected at 40 nL/min into the PBN (coordinates above). For the insula DREADD experiment, 200-300 nL of AAV5-hSyn-hM4D(Gi)-YFP (University of North Carolina Viral Vector Core) was injected into the insula (coordinates above) of one hemisphere, with the control virus AAV5-hSyn-GFP (University of North Carolina Viral Vector Core) injected into the contralateral hemisphere. Mice were treated with 5 mg/kg of ketoprofen once every 24 hours for 48 hours following surgery. Virally injected mice were killed 6 –12 weeks after surgery for anatomical and electrophysiological analysis.

Electrophysiology

Brain slice preparation - Brain slices containing the BNST (Bregma +0.14 – 0.26) were prepared from adult CRF-tdtomato reporter mice as previously described (Nobis et al., 2011; Silberman, et al., 2013; Flavin, et al., 2014). Briefly, mice were allowed to acclimate in their home cage for one hour in a sound- and light-attenuating box (Med Associates Inc.). Following acclimation, mice were anesthetized with isoflurane and brains were quickly removed and submerged in ice-cold, oxygenated low sodium sucrose dissecting solution (in mM: 194 sucrose, 20 NaCl, 4.4 KCl, 2 $CaCl_2$, 1 $MgCl_2$, 1.2 NaH_2PO_4, 10 glucose, 26 $NaHCO_3$). A vibratome (Leica) was used to

prepare coronal brain slices (300 μm). Slices were transferred to a holding chamber containing oxygenated ACSF and allowed to recover for one hour.

Whole-cell, voltage clamp recordings - All electrophysiology recordings were made using Clampex 9.2-10.3 and analyzed using Clampfit 10.2-10.7 (Molecular Devices). Whole-cell, voltage-clamp recordings of AMPA receptor-mediated excitatory postsynaptic currents (EPSCs) were made at -70 mV and pharmacologically isolated by the addition of 25 mM picrotoxin (Tocris) to the ACSF (described above). Recording electrodes for electrical stimulation experiments were filled with (in mM) : 118 CsOH, 117 D-gluconic acid, 5 NaCl, 10 HEPES, 0.4 EGTA, 2 $MgCl_2$, 5 tetraethylammonium chloride, 4 ATP, 0.3 GTP; pH 7.2-7.3; 280-290 mOsmol. Recording electrodes for optical stimulation experiments were filled with (in mM): 135 K^+-gluconate, 5 NaCl, 2 $MgCl_2$, 10 HEPES, 0.6 EGTA, 4 ATP, 0.4 GTP; pH 7.2-7.3; 280-290 mOsmol. Electrical stimulation occurred for 1 ms every 30 s and a 50 ms inter-event interval was used to assess paired-pulse ratio (PPR). Optical stimulation was under the control of a T-Cube LED Driver (LEDD1B, Thorlabs) and passed through an EN-GFP filter cube (Olympus) to produce blue wavelength light. Stimulation occurred for 5 ms every 20 s. The presence of ChR2 in each slice was confirmed via fluorescence, but viral expression was not quantified. Instead, initial optical EPSCs (oEPSCs) were adjusted so that all baseline oEPSCs were between 100-300 pA. Neutral density filters and microscope apertures were adjusted to achieve this baseline amplitude. Data are represented as average amplitude of three sweeps, with amplitudes normalized to baseline oEPSC amplitude. For both electrical and optical stimulation, experiments in which the access resistance changed by >20% were not included in the data analyses. Access resistance was monitored continuously throughout experiments.

Statistical Analysis

All data are represented as mean ± SEM except for when SD is used to address within cell variability of latency to respond to optical stimulation. For the immunohistochemistry

experiments a two-way ANOVA was used to assess stress and guanfacine effects. *Post hoc* analysis was performed using Tukey's multiple comparisons test. For all RNA *in situ* experiments (except insula DREADD experiment), two-way ANOVAs were used to assess effect of both treatment and sex. When both factors (or an interaction) were found to have a significant effect, Tukey's multiple comparison test was used to make multiple comparisons. When there was no significant effect of sex, Sidak's multiple comparisons test was used to make comparisons within treatment groups for each sex. For the insula DREADD experiment, paired t-tests were used to directly compare one BNST (hM4Di injected side) with the contralateral BNST (GFP control injected side) for each animal. For electrophysiological experiments, paired t-tests were used to assess drug effects on amplitude and paired pulse ratio. Unpaired t-tests were used to compare oEPSC kinetics between insula and PBN inputs as well as to compare the effects of CNO on EPSC amplitude in control and hM4Di-expressing animals. Statistical analyses were performed using Graphpad Prism 7.

Reagents

All reagents used were purchased from Millipore Sigma unless otherwise noted in the text. For *in vivo* experiments, all drugs were diluted in sterile saline (0.9% sodium chloride; Hospira). For electrophysiological experiments, all drugs were diluted in diH_2O to make stock solution (10 mM) except for picrotoxin (diluted in DMSO) and norepinephrine (added directly to ACSF).

Results

cFos expression in BNST CRF neurons is increased by restraint stress and decreased by systemic administration of the α_{2A}-AR agonist guanfacine

As an index of neuronal activity in the dorsal BNST (dBNST) we used immunohistochemistry to identify neurons expressing cFos following an acute restraint stress (Figure 3a). We found that cFos expression is significantly increased after restraint stress when

compared to the control no-stress condition (Figure 3b-c). Analysis via one-way ANOVA shows a significant effect of time after restraint stress ($F(4,10) = 19.57$, $p < 0.001$). *Post hoc* analysis with Dunnett's multiple comparison test reveals that cFos is significantly increased relative to the no stress control (12.9±4.3 cells/dBNST) at 30 min (39.8±1.3 cells/dBNST, $p < 0.001$), 1 hr (37.1±2.3 cells/dBNST, $p < 0.001$), and 2 hr (25.1±2 cells/dBNST, $p = 0.028$) after restraint stress, but is no longer significantly increased after 4 hr (17.8±2.4 cells, $p = 0.53$).

To look specifically at restraint stress activation of CRF cells, we used both a fluorescent *in situ* hybridization assay (Figure 3e) and a well-validated previously utilized CRF-tdtomato reporter mouse (Silberman, et al., 2013; Chen, et al., 2015) to quantify co-localization of cFos with dBNST CRF neurons using immunohistochemistry (Figure 3f). We found similar increases in the percentage of cFos+ CRF neurons following restraint stress in both assays (Figure 3d-g). For the RNA *in situ* assay (Figure 3d), a 2-way ANOVA shows a significant effect of stress on the percentage of *Crh* cells that express *Fos* ($F(1,15) = 27.18$, $p < 0.001$), but no effect of sex ($F(1,15) = 0.57$, $p = 0.462$) and no interaction between the variables ($F(1,15) = 0.57$, $p = 0.46$). Sidak's multiple comparisons test shows a significant increase in *Fos+ Crh* neurons in both males (no stress: 13.7±2.4%; stress: 28.1±3.6%; $p = 0.011$) and females (no stress: 13.7±2.1%; stress: 33.0±4.8%; $p = 0.002$).

Previous work has shown that administration of α_{2A}-AR agonists systemically, or directly into the BNST, can inhibit CRF-dependent behaviors such as drug withdrawal-related phenotypes and stress-induced reinstatement of drug seeking behavior (Shaham et al., 2000; Wang, et al., 2001; Mantsch et al., 2010). Further, α_{2A}-AR activation in the BNST is able to decrease excitatory drive (Shields, et al., 2009; Flavin, et al., 2014). Thus, we wanted to assess the impact the α_{2A}-AR agonist guanfacine (1 mg/kg) on the activity of CRF neurons (Figure 3f-g). A 2-way ANOVA showed a significant effect of guanfacine ($F(1,28) = 17.71$, $p = 0.0002$) and stress ($F(1,28) = 22.94$, $p < 0.0001$), but no significant interaction ($F(1,28) = 0.20$, $p = 0.657$). A *post hoc* analysis using Tukey's multiple comparisons test shows a significant increase in cFos+

CRF neurons following restraint stress (no stress, saline: 10.5±3.2%; stress, saline: 24.1±2.8%; $p = 0.003$). Treatment with guanfacine prior to restraint stress results in a significantly lower percentage of cFos+ CRF neurons as compared to saline treated stress animals (stress, guanfacine: 12.0±1.9%; $p = 0.009$). Additionally, treatment with guanfacine in the no stress condition significantly decreased cFos+ CRF neurons as compared to the guanfacine/stress condition (no stress, guanfacine: 0.7±0.3%; $p = 0.030$). Together these data show that acute restraint stress results in transient cFos activation in CRF neurons, and that cFos expression in CRF neurons can be reduced by treatment with guanfacine.

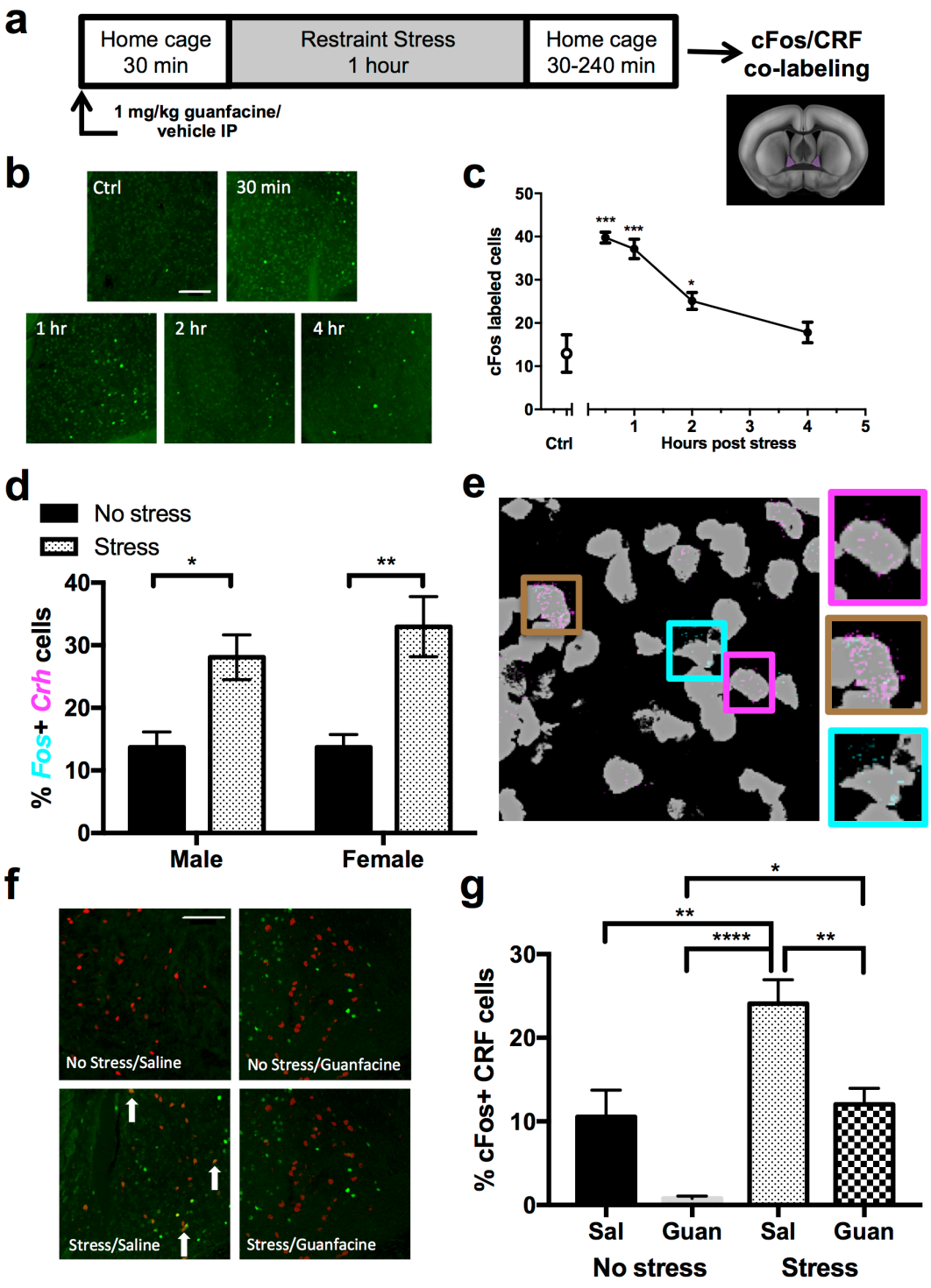

Figure 3. Restraint stress induces transient cFos expression in BNST CRF neurons in an α_{2A}-AR sensitive manner. a) Schematic showing timeline of animal injection, restraint stress, and *in situ* hybridization/immunohistochemistry assays, along with image of coronal section with the dBNST highlighted (purple) to denote region used for analysis throughout. b) Representative images of cFos labeling in the dBNST showing control, 30 min, 1 hr, 2 hr, and 4 hr time points

after restraint stress. Scale bar = 100 μm. c) Summary data showing the mean±SEM number of cFos labeled cells in dBNST sections from control conditions or at various time-points following a 1-hr restraint stress. n=3 male mice/group. *indicates significant difference from control conditions (***p<0.001, *p<0.05). d) Summary bar graph showing the percentage of *Crh* neurons that express *Fos* 30 min after restraint stress in male and female mice. Males: no stress n=5, stress n=5; Females: no stress n=5, stress n=4. *indicates significant difference between stress conditions (*p<0.05; **p<0.01). e) Example image of RNA *in situ* assay (gray: DAPI-labeled nuclei, magenta: *Crh* transcripts, cyan: *Fos* transcripts). Boxes provide magnified examples of cells expressing one or both transcripts (magenta: *Crh*, brown: *Crh/Fos*, cyan: *Fos*). f) Representative fluorescent immunohistochemical images of merged cFos (green) and CRF (red) labeling in the dBNST 30 min after restraint stress for no stress/saline, no stress/guanfacine, stress/saline, and stress/guanfacine conditions. Scale bar = 100 μm. g) Summary bar graph showing the mean±SEM percentage of cFos+ CRF neurons 30 min after restraint stress for the following conditions: No stress/saline (n=9; 6 male/3 female), no stress/guanfacine (n=6; 4 male/2 female), stress/saline (n=8; 5 male/3 female), stress/guanfacine (n=9; 4 male/5 female). *indicates significant difference compared to each

Norepinephrine inhibits glutamatergic transmission onto CRF neurons via α-AR activation

In previous studies, we and others have found that activation of noradrenergic receptors can regulate excitatory drive in unidentified neuronal populations in the dorsal BNST (Krawczyk et al., 2011; Nobis, et al., 2011; Flavin, et al., 2014). In order to better understand the interaction between NE signaling and BNST CRF neuron activation, we examined the actions of NE and agonists for both α- and β-ARs in modulating excitatory drive onto CRF neurons. We recorded from tdtomato+ neurons in the BNST of CRF reporter mice and evoked glutamatergic excitatory postsynaptic currents (EPSCs) by electrical stimulation in the presence of picrotoxin. A paired t-test shows that 10 min bath application of 1 μM NE significantly inhibited EPSC amplitude (-42.5±8.7% change from baseline, p = 0.008, Figure 4a) without significantly altering the paired pulse ratio (PPR) of the EPSCs (+8.3±9.8% change from baseline, p = 0.44). To further dissect NE signaling, we then repeated the electrical stimulation experiment using agonists for α_1-, α_{2A}-, and β-ARs (Figure 4b-d). A paired t-test shows that, similar to NE, bath application of 100 μM methoxamine (α_1-AR agonist) significantly inhibits EPSC amplitude (-26.0±7.3% change from baseline, p = 0.10, Figure 4b) without significantly altering PPR (-1.5±5.3% change from baseline, p = 0.56). A paired t-test shows that bath application of 1 μM guanfacine (α_{2A}-AR agonist) also significantly inhibited EPSC amplitude (-60.5±4.7% change from baseline, p <

0.0001, Figure 4c), while also significantly increasing PPR (+32.7±5.7% change from baseline, $p < 0.001$). Finally, a paired t-test shows that bath application of 3 μM isoproterenol (β-AR agonist) significantly increases EPSC amplitude (+28.8±7.2% change from baseline, $p = 0.007$, Figure 4d) without altering PPR (-6.7±5.0% change from baseline, $p = 0.15$).

Based on the ability of systemic guanfacine to decrease stress-induced cFos in CRF cells in our previous experiments, we further focused on the actions of α_{2A}-AR signaling using the antagonist atipamezole (1 μM). *Ex vivo* slices were pretreated with atipamezole before bath application of 1 μM NE, with the antagonist remaining in the bath for the duration of the experiment. The time course shown in Figure 4f demonstrates that atipamezole is able to block the effects of NE on excitatory drive. A paired t-test shows that in the presence of atipamezole, bath application of 1 μM NE no longer significantly inhibits EPSC amplitude (+21.3±11.7% change from baseline, $p = 0.143$, Figure 4g) and PPR remains unaltered (-1.1±6.4% change from baseline, $p = 0.940$).

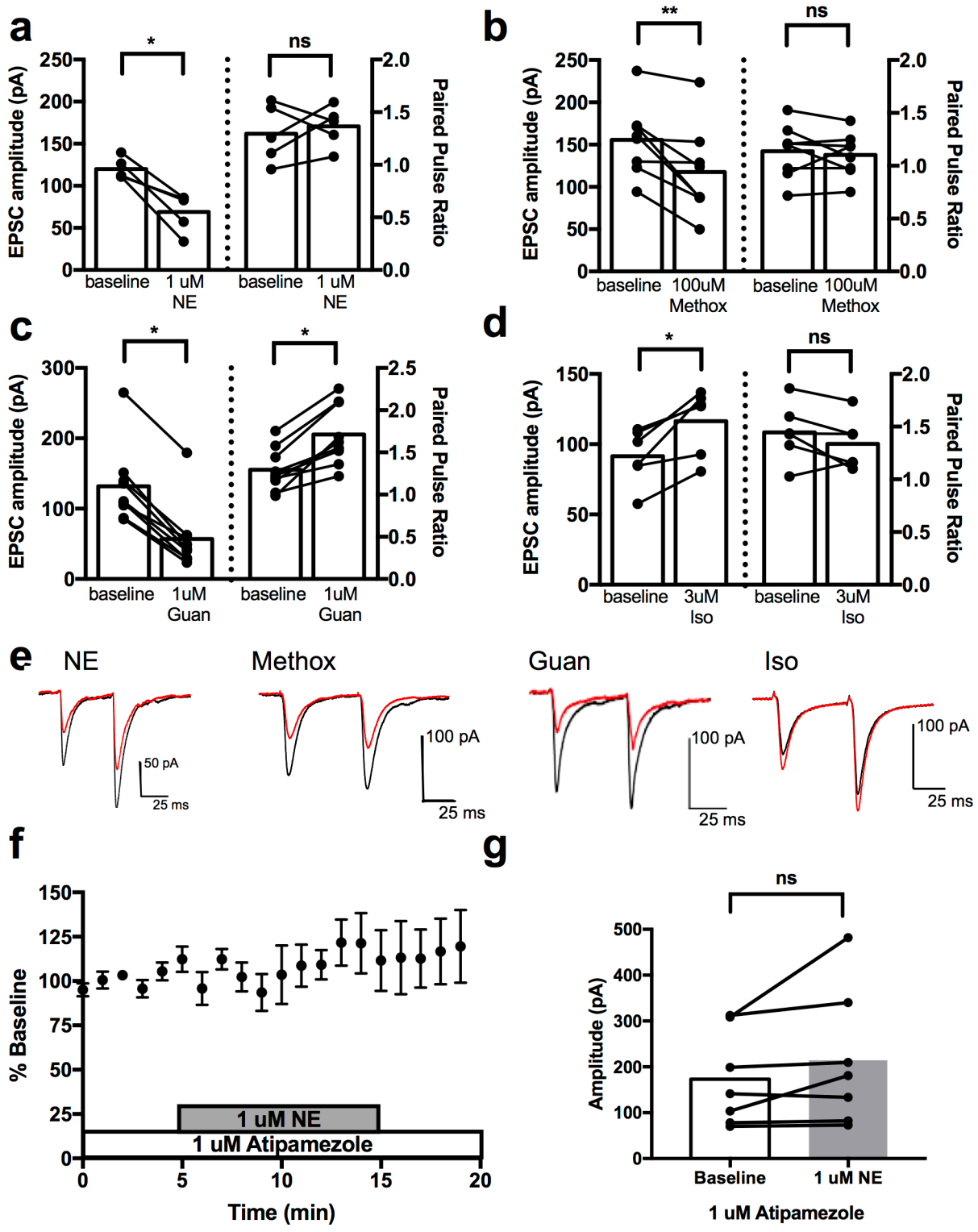

Figure 4. NE regulation of excitatory drive onto CRF neurons is mediated by α-AR signaling and can be blocked by the of α_{2A}-AR antagonist atipamezole. a-d) Bar graphs summarizing the effects of adrenergic receptor (AR) agonists on EPSC amplitude (left) and paired pulse ratio (PPR, right) in BNST CRF neurons. a) Effects of norepinephrine (NE) (n=5

cells, 3 male mice) b) Effects of α_1-AR agonist methoxamine (Methox) (n=8 cells, 4 male mice) c) Effects of α_{2A}-AR agonist guanfacine (Guan) (n=5 cells, 3 male mice) d) Effects of β-AR agonist isoproterenol (Iso) (n=6 cells, 3 male mice) *indicates significant difference compared to baseline (*$p<0.05$). e) Representative EPSC traces before (black) and after (red) AR agonist application. f) Timecourse showing effects of pretreatment with α_{2A}-AR antagonist atipamezole on NE modulation of EPSC amplitude in BNST CRF neurons, graphed as a percentage of baseline. g) Bar graph comparing EPSC amplitude during atipamezole pretreatment before and after NE application (n=7 cells, 1 male mouse, 3 female mice).

Input-specific NE action on excitatory control of BNST CRF neurons

We next utilized *ex vivo* channelrhodopsin assisted circuit mapping to begin to determine regions that provide excitatory input to BNST CRF neurons, examining the parabrachial nucleus (PBN) and insular cortex (McDonald, et al., 1999; Dobolyi, et al., 2005). AAV5-CamKIIα-ChR2-YFP was stereotaxically injected into the region of interest in CRF reporter mice (Figure 5a) and allowed to express for at minimum six weeks before preparing slices for electrophysiology. After verifying ChR2 expression in terminals in the BNST via visual inspection, we recorded from tdtomato+ neurons in the BNST and used full-field blue-light stimulation to evoke optical EPSCs (oEPSCs) in the presence of picrotoxin. For each cell recorded from, we noted the presence or absence of an oEPSC, and in the case of cells that responded, continued to stimulate every 20 s for 10 min to allow for response kinetics analysis. The PBN and insula exhibited different response profiles (Figure 5b): insular cortex afferent stimulation led to a reliable response in CRF neurons (87% of cells responded, 20/23 cells), while PBN afferent stimulation resulted in an intermediate phenotype (50% of cells responded, 14/28 cells). Immunohistochemistry staining of calcitonin gene-related peptide (CGRP) in the BNST as a marker for the PBN input (Shimada, et al., 1989) provides further anatomical support of this intermediate phenotype, as some but not all CRF cell somas are surrounded by CGRP+ terminals (Figure 5c).

Having identified the insular cortex and PBN as providing excitatory input to BNST CRF neurons, we next analyzed the response kinetics of recorded oEPSCs from these inputs (Figure 5d). Unpaired t-tests show that oEPSCs resulting from insula terminal stimulation as compared to PBN terminal stimulation have a significantly greater latency to peak following optical

stimulation (PBN: 11.51±0.96 ms; insula: 15.25±1.04 ms; p = 0.03), while showing less variability in latency to respond between sweeps within a cell (PBN: SD = 1.84 ms; insula: SD = 1.03 ms). Additionally, the decay time of insular input oEPSCs was significantly longer (PBN: 11.63±1.99 ms; insula: 18.73±1.79 ms; p = 0.023). Rise time was not significantly different between the two (PBN: 3.8±0.7 ms; insula: 4.57±0.43 ms; p=0.342).

Next, we determined whether NE could modulate these inputs as seen in the electrical stimulation experiments. The same optical stimulation set-up was used as described for the mapping experiments, but now AR agonists were bath applied during stimulation (Figure 5e-f). A paired t-test (Figure 5h) shows that 20 min bath application of 1 μM NE significantly inhibits oEPSC amplitude when stimulating PBN afferents (-44.3±9.4% change from baseline, p = 0.018), while not altering oEPSC amplitude during insular stimulation (-4.2±3.7% change from baseline, p = 0.341). This demonstrates that while both regions send glutamatergic inputs to BNST CRF neurons, only the PBN input is sensitive to regulation by NE. Having shown the effects of NE in the electrical stimulation experiments to be mediated by α_{2A}-AR signaling, we also tested the effect of guanfacine on PBN afferent stimulation-evoked oEPSCs (Figure 5g). A paired t-test (Figure 5h) shows that 20 min bath application of 1 μM guanfacine significantly reduces oEPSC amplitude similar to NE application (-40.0±11.5% change from baseline, p = 0.026). This provides further support for the role of α_{2A}-AR signaling in mediating CRF neuronal activity in the BNST.

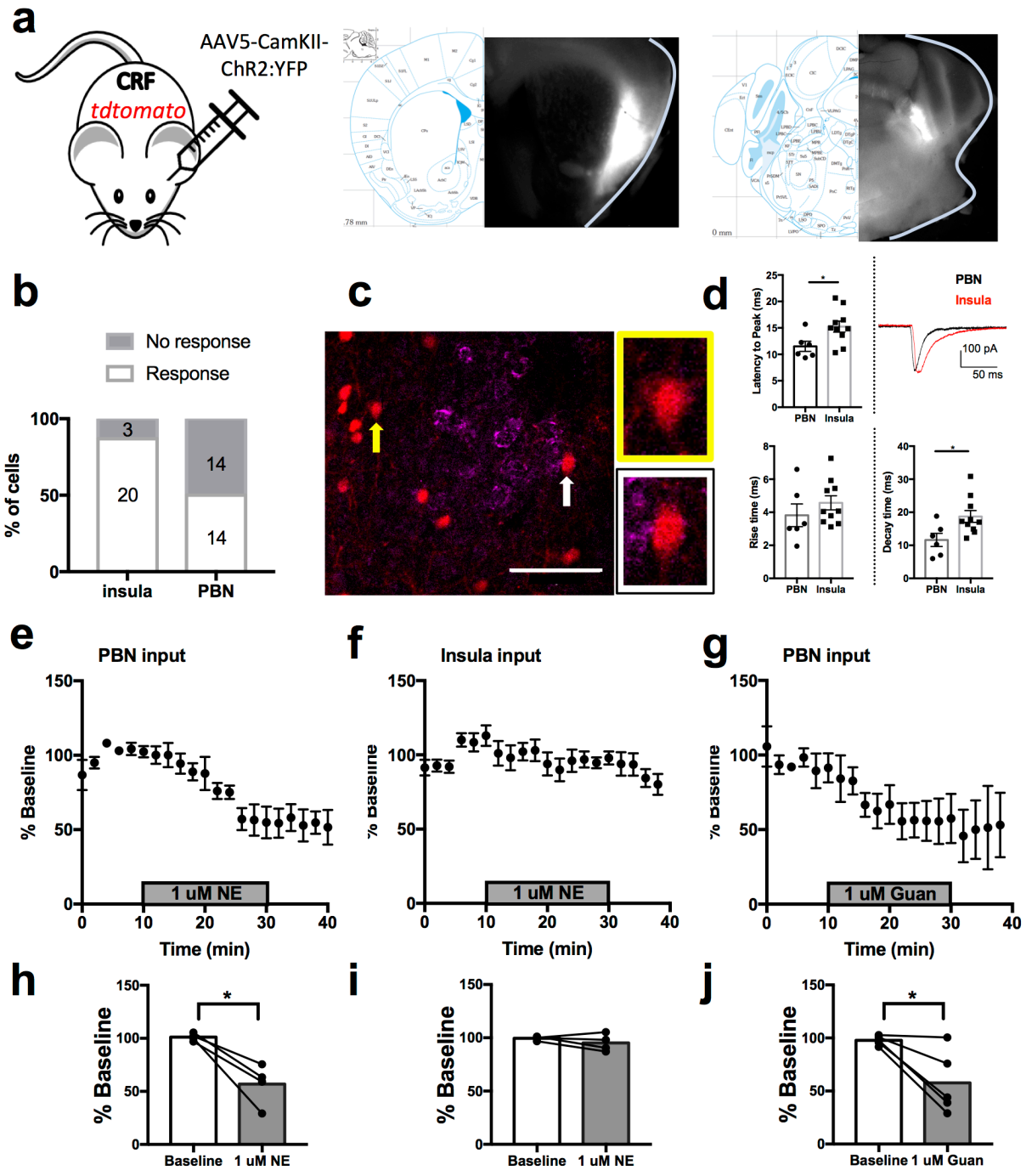

Figure 5. BNST CRF neurons receive kinetically distinct excitatory input from both the insular cortex and PBN, but the PBN input can be regulated by both NE and guanfacine. a) Illustrated mouse indicating that for Figure 3, CRF-tdtomato reporter mice were stereotaxically injected with AAV5-CamKIIα-ChR2:YFP, along with example stereo microscope images of injection sites for insular cortex and parabrachial nucleus (PBN). b) Summary of percentage of BNST CRF cells that respond to insula (male: n=7 cells, 3 mice; female: n=16 cells, 11 mice) or PBN (male: n=10 cells, 2 mice; female: n=18 cells, 6 mice). c) Representative image of CGRP labeling (purple; marking PBN input) around BNST CRF neurons (red)

demonstrating CRF cells surrounded by CGRP (white arrow; white box: magnified image of cell) and CRF cells without PBN input (yellow arrow; yellow box: magnified image of cell). Scale bar = 50 μm. d) Bar graphs comparing oEPSC kinetics between PBN (n=6 cells, female mice) and insula (n=10 cells, female mice) stimulation. Top left: Latency to oEPSC peak (ms). Top right: Representative oEPSC traces from insula (red) and PBN (black). Bottom left: Rise time (10-90%) of oEPSC (ms). Bottom right: Decay time (90-10%) of oEPSC (ms). *indicates significant difference using unpaired t-test (*$p<0.05$). e-f) Summary graphs showing effect of NE on oEPSC amplitude, graphed as percentage of baseline, for PBN stimulation (d; n=4, 3 female mice) and insula stimulation (e; n=4, 4 female mice). g) Summary graph showing effect of guanfacine on oEPSC amplitude, graphed as percentage of baseline, for PBN stimulation (n=5, 2 male mice, 2 female mice). h-j) Bar graphs comparing average oEPSC amplitude, graphed as % of baseline, 5 min before and after drug wash-on. *indicates significant difference using paired t-test (*$p<0.05$). All data are represented as mean±SEM.

Activation of PBN hM4Di blunts stress-induced Fos specifically in females

Having identified the PBN as a guanfacine-sensitive glutamatergic input to BNST CRF neurons, we next wanted to determine if manipulating the activity of this input could alter the restraint stress-induced *Fos* response in a manner similar to systemic guanfacine administration. To do this we utilized a chemogenetic strategy through the use of the hM4Di DREADD, which couples to Gi-signaling as the α_{2A}-AR does to mimic activation of the α_{2A}-AR by guanfacine. AAV5-hSyn-HA-hM4D(Gi)-mCherry was stereotaxically injected bilaterally into the PBN and given at least three weeks for expression to occur (Figure 6c). To verify activity, we recorded from tdtomato+ neurons in *ex* vivo slices containing the BNST while using electrical stimulation in the presence of picrotoxin to evoke EPSCs. We found that 10 min bath application of 10 μM CNO was able to reduce EPSC amplitude only in hM4Di injected animals (Figure 6e). An unpaired t-test comparing cells from control animals to cells from hM4Di-injected animals showed a significant decrease in EPSC amplitude in hM4Di animals during the last 5 min of CNO application (-25.5±7.3% change from baseline, $p = 0.007$). A separate cohort of hM4Di injected mice then underwent the same restraint stress paradigm as before, receiving an IP injection of CNO (3 mg/kg) 30 min prior to the stressor (Figure 6a). Using fluorescent *in situ* hybridization, we found that activation of the hM4Di DREADD significantly alters stress-induced *Fos* in females but not in males (Figure 6b). A 2-way ANOVA shows a significant effect of

treatment ($F(2,23) = 11.76$, $p < 0.001$), but no effect of sex ($F(1,23) = 0.73$, $p = 0.401$) and no interaction ($F(2,23) = 1.01$, $p = 0.380$). *Post hoc* analysis using Tukey's multiple comparisons test reveals a significant difference in percentage of *Fos+ Crh* cells between the stress/saline and stress/CNO mice in females (stress/saline: 32.5±3.6%; stress/CNO: 18.4±5.2%; $p = 0.047$), but not in males (stress/saline: 23.4±5.1%; stress/CNO: 20.0±3.4%; $p = 0.820$).

To rule out potential off-target actions of CNO, in a control experiment we assessed the effects of CNO alone without expression of the hM4Di DREADD on restraint stress-induced cFos expression in BNST CRF neurons (Figure 6d). An unpaired t-test found no change in the percentage of cFos+ CRF neurons across stress/saline and stress/CNO treatment (stress/saline: 28.3±3.6%; stress/CNO: 27.4±4.9%; $p = 0.878$). Together, these data show that activation of PBN-expressed hM4Di DREADD can mimic actions of guanfacine by decreasing stress-induced *Fos* activation in *Crh* cells in female, but not male mice.

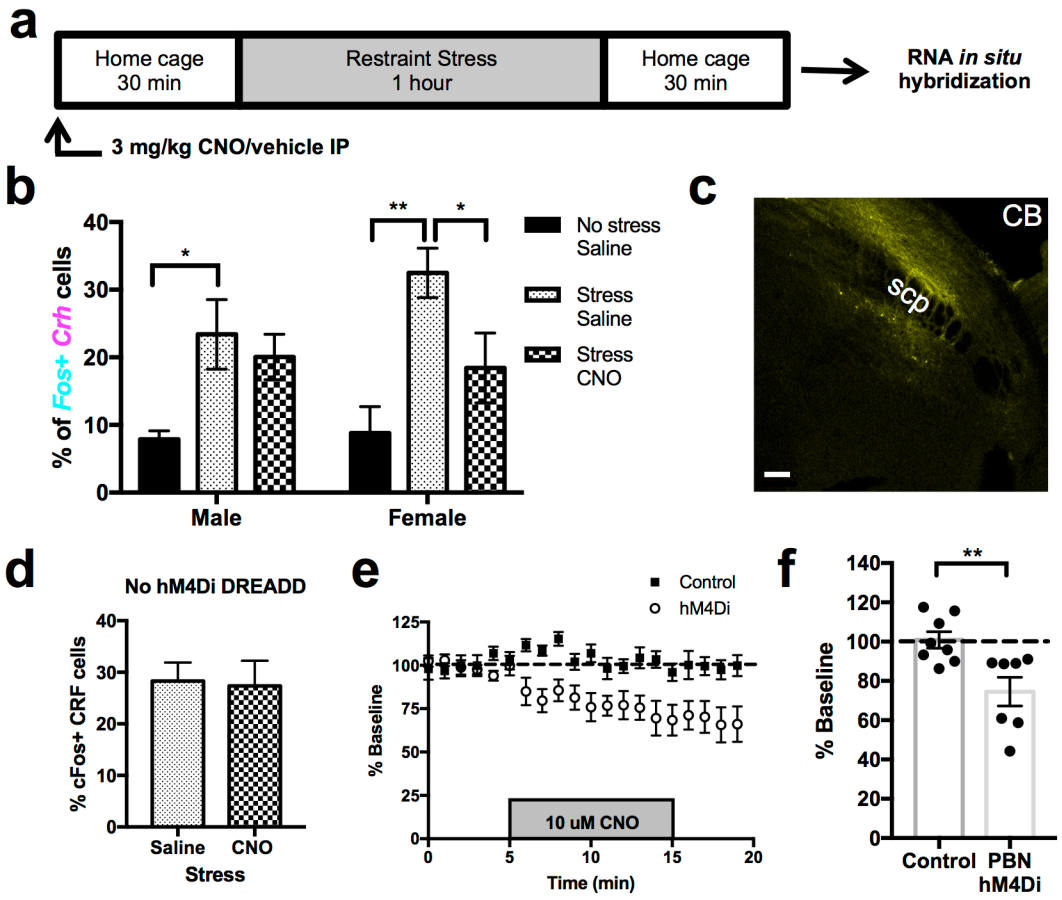

Figure 6. Activation of PBN-expressed Gi-coupled DREADD hM4Di blunts *Fos* activation only in female mice. a) Schematic showing timeline of animal injection, restraint stress, and RNA *in situ* hybridization assay. b) Summary bar graph showing effect of CNO injection on percentage of *Crh* cells that express *Fos* 30 min after restraint stress in male and female mice (n=5/mice per group; exception: female, no stress/saline n=4). *indicates significant difference between treatment groups within each sex (*p<0.05, **p<0.01). c) Example confocal image showing AAV5-hSyn-hM4D(Gi)-mCherry PBN injection site. Scale bar = 100 μm; scp = superior cerebellar peduncle; CB = cerebellum. d) Bar graph summarizing results of control immunohistochemistry experiment showing effect of CNO injection on male C57 mice (saline: n=4; CNO: n=3) with no hM4Di DREADD expression. e) Timecourse of CNO application on EPSC amplitude in BNST CRF cells, graphed as percentage of baseline, comparing control mice (n=8 cells, 2 male mice, 2 female mice) and PBN hM4Di-expressing mice (n=7 cells, 1 male mouse, 1 female mouse). f) Summary bar graph showing average EPSC amplitude as a percentage of baseline during last 5 min of CNO application. *indicates significant difference between control and hM4Di groups using unpaired t-test (**p<0.01). All data are represented as mean±SEM.

Activation of insular cortex hM4Di blunts stress-induced Fos in males and females

In Figure 5, we found a high prevalence of excitatory connections between the insular cortex and CRF cells, with almost all CRF cells assessed responding to stimulation of insula terminals in the BNST. Based on this robust response rate, we wanted to determine if manipulating insular activity would alter the stress activation of BNST CRF neurons as observed with the PBN input. To do this, we once again utilized DREADDs. Here, we stereotaxically injected the hM4Di virus into the insula in one hemisphere of the brain and then injected a control AAV5-hSyn-GFP virus into the contralateral hemisphere, allowing for direct comparison between hemispheres within a given mouse. As before, CNO was given 30 min prior to restraint stress and tissue was taken for processing 30 min after the termination of the stressor (Figure 7a). Fluorescent *in situ* hybridization assays revealed that an acute injection of CNO prior to the stress significantly reduces the percentage of *Fos*+ *Crh* cells in the hM4Di-injected hemisphere as compared to the control GFP-injected hemisphere (GFP: 41.8±5.1%; hM4Di: 29.5±4.2%; $p < 0.001$; Figure 5b). Thus, similar to the PBN DREADD experiment, activating insula-expressed hM4Di DREADD decreases stress-induced *Fos* activation in *Crh* neurons; however, unlike with the PBN, this effect occurred in both male and female mice.

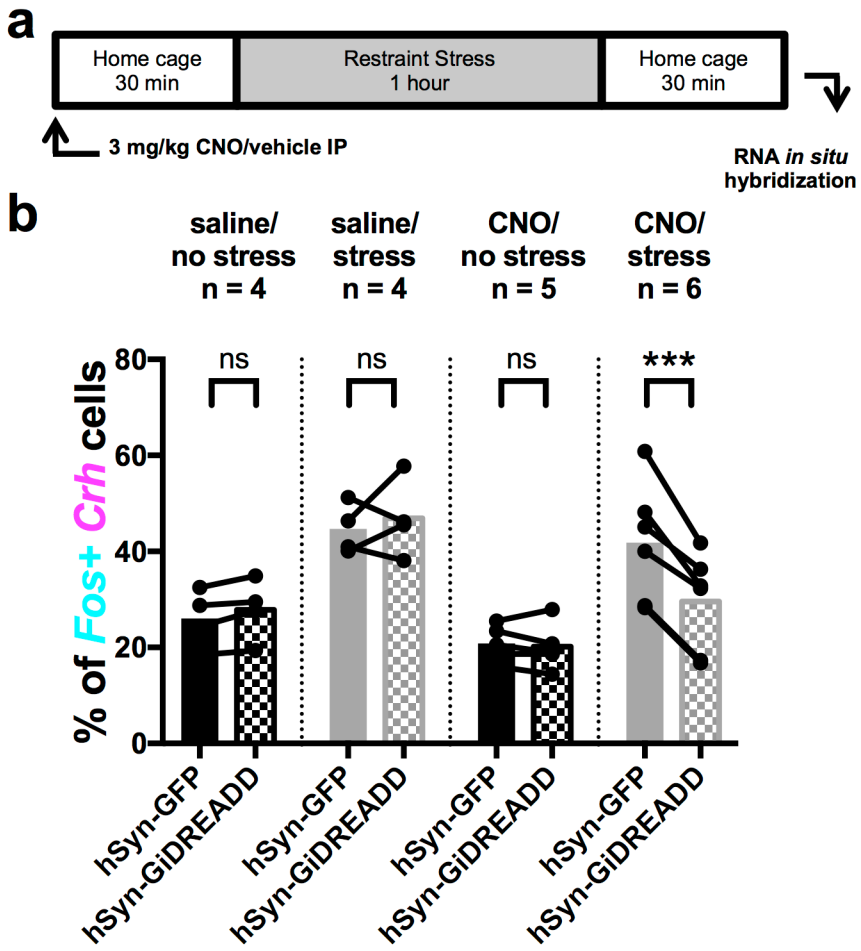

Figure 7. Activation of insula-expressed Gi-coupled hM4Di DREADD blunts *Fos* activation in both males and females. a) Schematic showing timeline of animal injection, restraint stress, and RNA *in situ* hybridization assay. b) Percent of all BNST *Crh* neurons that express the *Fos* transcript 30 min after restraint stress. Solid bars represent neurons in the ipsilateral BNST of insula control virus (hSyn-GFP)-injected hemisphere. Checkered bars represent neurons in the ipsilateral BNST of the insula hM4Di-injected hemisphere. (saline/no stress: n=4; saline/stress: n=4; CNO/no stress: n=5; CNO/stress: n=6) *indicates significant difference between GFP-injected and hM4Di DREADD-injected hemispheres using a paired t-test (***p<0.001). All data presented as the mean with individual data points for each animal.

Increasing endogenous 2-AG prevents stress-induced increases in Fos in BNST Crh cells

Although the modulation of insular activity can alter the stress activation of BNST CRF neurons, the insula input to these cells is not sensitive to regulation by NE (Figure 5f). In an attempt to better understand this modulation that is separate from NE signaling, we explored another neuromodulatory system, the eCB system. Data from our lab has demonstrated that the

insula input to BNST CRF cells is sensitive to regulation by the eCB system (S. Centanni, unpublished data). Similar to the action of guanfacine at α_{2A}-ARs, the endogenous ligands of the eCB system also act on Gi-coupled GPCRs (CB1R and CB2R). These ligands, including 2-AG, are produced post-synaptically and then travel in a retrograde manner to bind receptors located on pre-synaptic terminals (Kano, et al., 2009; Ohno-Shosaku and Kano, 2014). In order to investigate the role of eCB activated Gi-signaling in the BNST stress response, we utilized the monoacylglycerol (MAG) lipase inhibitor JZL184 to increase 2-AG levels. JZL184 was administered systemically 2 hours prior to acute restraint stress and once again *in situ* hybridization assays were used to measure *Fos* expression in BNST *Crh* neurons (Figure 8a). We found that the percentage of *Crh* cells expressing *Fos* after stress is significantly blunted in female mice that received systemic JZL184 (Figure 8b). A 2-way ANOVA reveals a significant effect of drug treatment ($F(2,22) = 27.21$, $p < 0.0001$) and a trending interaction between the variables ($F(2,22) = 2.82$, $p = 0.082$), but no effect of sex alone ($F(1,21) = 0.13$, $p = 0.724$). *Post hoc* analysis using Tukey's multiple comparisons test reveals a significant increase in the percentage of *Crh* cells expressing *Fos* following stress in both saline-treated males (no stress/saline: 13.0±3.2%; stress/saline: 28.9±3.0%; $p = 0.004$) and females (no stress/saline: 9.1±2.4%; stress/saline: 38.0±2.7%; $p < 0.0001$). However, JZL184 administration only had a significant effect in females (stress/JZL: 21.0±3.0%; $p = 0.001$), blunting the stress induced *Fos* increase. This experiment demonstrates that the eCB system can modulate the stress-induced upregulation of *Fos* in BNST *Crh* cells, in a sex-specific manner.

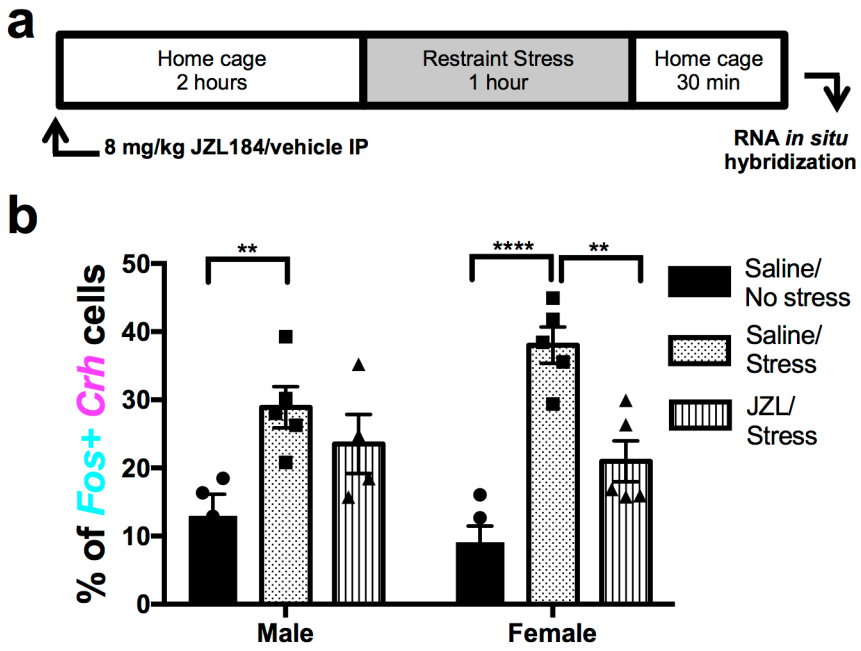

Figure 8. The MAG lipase inhibitor JZL184 blunts restraint stress-induced increase in *Fos*+ BNST *Crh* cells. a) Schematic showing timeline of animal injection, restraint stress, and RNA *in situ* hybridization assay. b) Summary bar graph showing effect of JZL184 injection on percentage of *Crh* cells that express *Fos* 30 min after restraint stress in male and female mice (n=5/mice per group; exception: male, no stress/saline and stress/JZL n=4). *indicates significant difference between treatment groups within each sex (**p<0.01, ****p<0.0001). All data are represented as mean±SEM.

Discussion

We find that restraint stress increases cFos expression in BNST CRF neurons, and that systemic administration of the clinically well-tolerated drug guanfacine, an α_{2A}-AR agonist, reduces their activity. Using *ex vivo* electrophysiology, we demonstrated that NE inhibits excitatory input to these cells via α_2-ARs activation, but that agonists for each class of AR produces modulation of excitatory drive, suggesting likely state-dependent actions *in vivo*. *Ex vivo* channelrhodopsin-assisted mapping identified the insular cortex and PBN as glutamatergic inputs to CRF cells, but only the PBN was sensitive to NE and guanfacine modulation. CNO activation of PBN-expressed Gi-coupled DREADDs (hM4Di) was able to mimic actions of guanfacine by decreasing stress-induced *Fos* in *Crh* neurons in female mice. However, activation of insula-expressed hM4Di was also able to decrease stress-induced *Fos*, suggesting

additional effects beyond the NE system. Indeed, increasing eCB signaling through the use of the MAG lipase inhibitor JZL184 also led to decreases in *Fos* expression in *Crh* cells following acute restraint stress.

Stress-induced activation of BNST CRF neurons

Anxiogenic stimuli have been shown to induce cFos expression in CRF neurons throughout the BNST in both mice and rats (Butler et al., 2016; Lin et al., 2018) suggesting that, despite known anatomical differences in the CRF systems of rodents (Daniel, et al., 2017), increased CRF activation in the BNST following aversive stimuli may be an important conserved signal. We found both males and females exhibited increased cFos+ CRF neurons in response to stress and both were sensitive to regulation by systemic guanfacine administration. Interestingly, guanfacine was able to alter cFos expression in the no stress condition, showing that guanfacine actions do not require stress activation of these neurons. Substantial evidence has demonstrated sex differences within the CRF system, both at the level of the HPA axis and at extrahypothalamic sites (Bangasser and Valentino, 2014). In rats, females have been shown to have higher numbers of CRF cells in the vBNST, as well as increased colocalization with *Fos* following stress (Babb, et al., 2013). However, our work in mice in the dBNST did not exhibit any sex differences when only looking at the co-expression of *Fos/Crh*. Beyond the differences between species and BNST subregions, it is also difficult to compare levels of stress achieved, as our restraint stress period was longer.

Norepinephrine modulation of excitatory drive onto CRF neurons

Our experiments provide insight into the specific mechanisms underlying systemic guanfacine regulation of stress-induced cFos expression in BNST CRF neurons. Stress has been shown to increase NE signaling within the BNST (Pacak, et al., 1995) and previous work has shown that isoproterenol, a β-AR agonist, can increase glutamatergic transmission in the

BNST via a CRF receptor dependent mechanism and can depolarize BNST CRF neurons (Nobis, et al., 2011; Silberman, et al., 2013). We showed that isoproterenol can increase glutamatergic drive onto CRF neurons, likely through post-synaptic actions. Conversely, the stimulation of α-ARs works in opposition to regulate CRF neuron activity. While NE and methoxamine did not alter PPR, guanfacine was able to alter this ratio, suggesting that NE can potentially regulate excitatory input postsynaptically by actions of α_1-ARs as well as presynaptically by α_{2a}-ARs located on glutamatergic terminals pre-synaptic to CRF cells. Specifically blocking α_2-ARs with atipamezole completely inhibited the actions of NE and in some cells uncovered possible NE actions at β-ARs. A trend toward a similar phenomenon was recently reported in a population of vBNST neurons as well (Gungor et al., 2018). These results, in combination with the systemic effects of guanfacine administration, suggest that the balance between NE activation of β- and α-ARs may be key in controlling the response of CRF neurons to stress. These results led us to focus on α_2-AR signaling, but future studies are needed to tease apart the contribution of α_1-AR and β-AR signaling in regulating CRF neurons.
We identified two excitatory inputs to CRF neurons using optogenetic stimulation: the insula and the PBN. We observed differential oEPSC kinetics from the insula and PBN stimulations. The slower kinetics of the insular input could suggest an axo-dendritic synapse, while the faster PBN kinetics and CGRP immunohistochemistry findings agree with known axo-somatic connections in the BNST (Shimada, et al., 1989; Dobolyi, et al., 2005). While overall the kinetics observed are slower than those seen with electrical stimulation, the same optical stimulation protocol was used for both inputs, allowing for direct comparison.

We found that NE and guanfacine could inhibit the PBN input, while the insula input was insensitive. This finding is similar to previous work showing that the PBN input to unidentified BNST neurons can be inhibited by guanfacine, while the basolateral amygdala input was insensitive (Flavin, et al., 2014). This suggests that the actions of NE on CRF cells are at least in part working through α_{2A}-ARs on PBN terminals pre-synaptic to CRF cells. Previous studies in

the CeA have suggested that α_{2A}-ARs decrease PBN release probability by directly interacting with the release machinery (Delaney et al., 2007). The input selectivity of NE regulation demonstrates that targeting this system produces highly specific tailoring of excitatory drive to the BNST.

Modulation of PBN activity using the Gi-coupled DREADD hM4Di

Having identified the PBN as a guanfacine-sensitive input to BNST CRF neurons, we further explored the regulation of this input in BNST stress responses, particularly given recent findings that the PBN encodes danger signals (Campos, et al., 2018). We showed that activation of the Gi-coupled DREADD hM4Di in PBN neurons could mimic actions of guanfacine by decreasing stress-induced *Fos* in *Crh* neurons. Interestingly, while guanfacine was effective in blocking the CRF neuron stress response in both males and females, our PBN manipulation investigating *Fos* responses after restraint was female-specific. The ineffectiveness of PBN hM4Di activation in males suggests that guanfacine inhibition at PBN terminals is only one mechanism altering cFos activation in CRF neurons. Of note, α_{2A}-ARs are expressed in multiple compartments throughout the BNST and not just at PBN terminals (Flavin, et al., 2014). While we have shown the insular input to be insensitive to NE, guanfacine could be inhibiting other glutamatergic inputs to the BNST. For example, the paraventricular thalamus has been implicated in extended amygdala fear circuitry (Myers et al., 2014; Penzo, et al., 2015). Additionally, there are other modulatory systems recruited by stress that may contribute to activation. Serotonin is known to play a role in promoting anxiety and can activate CRF neurons (Marcinkiewcz et al., 2016). Dynorphin actions at kappa opioid receptors have been shown to inhibit anxiolytic circuitry in the BNST (Crowley et al., 2016). Alternatively, decreases in neuropeptide Y signaling following stress could increase CRF neuron activation (Pleil et al., 2015). Another reason for the observed difference could be sex-specific distinctions in the PBN innervation of the BNST. Previous work has shown that optical stimulation of PBN terminals can

result in either PBN-activated cells or PBN-inhibited cells (Flavin, et al., 2014). The balance between these two types of cells in the BNST could be sex-specific and potentially lead to the female-specific result we observed. Indeed, female rats have shown greater PBN activation following visceral noxious stimuli, providing evidence of regional sex differences (Wang et al., 2009). Future studies addressing sex differences in the PBN input will be important to better understand this result.

Modulation of both insula signaling and the eCB system can alter stress-induced activation of BNST CRF neurons

While the insula input to BNST CRF cells was insensitive to NE regulation, its high fidelity connectivity to CRF cells in both males and females warranted further investigation. Furthermore, the role of the insula in sensing the internal state of the body, suggests that it may be an important player in regulating the body's response to stress (Craig, 2002; Gogolla, 2017). We found that activation of the Gi-coupled DREADD hM4Di in the insula could decrease the stress-induced increase in BNST *Crh* cells expressing *Fos*, similar to what was seen in the PBN. Notably, unlike with the female-specific PBN manipulation, stress activation was decreased in both males and females. This suggests that stress may lead to increased insula activity in neurons that project to the BNST. In human studies, increased insula activity has been reported in individuals with high-trait anxiety (Alvarez, et al., 2015), supporting a role for insula signaling in stress-related phenotypes. Knowing that the insula input is insensitive to NE, we investigated activation of another Gi-linked GPCR in the BNST (CB1R) by the eCB system. Increasing 2-AG levels, an endogenous CB1R ligand, using systemic administration of JZL184 resulted in a blunted stress activation of BNST CRF cells, with fewer *Crh* neurons expressing *Fos* transcripts. However, this occurred specifically in female mice. This sex-specific effect of eCB signaling is not unprecedented, as differences in depressive-like behavior in male and female mice have been observed in a mouse model that genetically disrupts 2-AG synthesis

(Shonesy, et al., 2014). One site of action for eCB signaling in the BNST is indeed at insular terminals (S. Centanni, unpublished data), suggesting that our insula-expressed hM4Di experiment may be mimicking effects of endogenous CB1R signaling. However, CB1 receptors are expressed throughout the entirety of the CNS (Herkenham, et al., 1990), and thus effects at other inputs to the BNST, as well as multi-synaptic effects cannot be ruled out.

Together, our results have led us to propose a model by which activation of Gi-coupled GPCR signaling located on afferents in the BNST can decrease activation of BNST CRF neurons. While stress increases NE release that can act at many different receptor subclasses throughout the BNST, specifically targeting α_{2A}-ARs located on PBN terminals pre-synaptic to CRF cells can decrease activation of these cells. Furthermore, increasing eCB signaling also decreases stress activation of BNST CRF neurons, potentially through activation of CB1Rs located on insula terminals. In conclusion, these findings provide a framework for understanding how the interaction between stress and glutamatergic signaling can modulate stress responsivity of BNST CRF neurons through multiple mechanisms. We have identified both molecular and circuit specific targets for addressing the pathophysiology underlying stress-related psychiatric disorders. Additionally, we have identified multiple female-specific effects in Gi-coupled GPCR regulation of BNST CRF cells, providing further evidence of mechanistic differences in the stress response between males and females. Future studies will further dissect the input specificity of this stress response, while continuing to focus on sex differences within the system in order to better identify targets for manipulating this stress circuitry.

Chapter 3

Examining the regulation of the female-specific increase in co-expressing *Crh/Prkcd* BNST neurons following stress

Adapted from: *Fetterly et al., α_{2A}-adrenergic receptor activation decreases parabrachial nucleus excitatory drive onto BNST CRF neurons and reduces their activity in vivo*

Introduction

In Chapter 2, the PBN-expressed hM4Di experiment revealed a sex-specific alteration in regulation of restraint stress activation of BNST CRF neurons. Interestingly, females have a higher reported prevalence of stress-related psychiatric illnesses (Breslau, 2002; Kessler, et al., 2012; Bangasser and Valentino, 2014). Furthermore, the BNST is known to be highly sexually dimorphic (Gu et al., 2003; Han and De Vries, 2003). Specifically, the vBNST CRF system may be more stress reactive in females (Sterrenburg, et al., 2012; Babb, et al., 2013). Understanding the mechanism underlying sex-specific differences is important for developing targeted treatments best suited for men and women.

One of the biggest obstacles in studying the BNST is overcoming the heterogeneity of the region. In addition to using input specificity as done in Chapter 2, post-synaptic markers can help to subdivide this complex region. In the central amygdala (CeA), CRF signaling has been shown to play a facilitating role in fear (Fadok et al., 2017; Sanford et al., 2017; Asok et al., 2018). Another CeA population is defined by the expression of Protein Kinase C δ (PKCδ); when activated, these cells can regulate the fear response, although their precise role is complicated, as studies have shown that they play a role in both decreasing the fear response and in conveying aversive signals (Ciocchi, et al., 2010; Yu, et al., 2017). Notably, there is relatively little cellular overlap between PKCδ and CRF in the CeA (Haubensak, et al., 2010). Similarly, the BNST contains a population of PKCδ-expressing neurons. Although the role of these BNST neurons is unknown, PKCδ can be used as an additional marker of specific cell populations in the BNST. Additionally, the gene for PKCδ (*Prkcd*) is known to have an estrogen

response element (Shanmugam et al., 1999), making this a potentially relevant protein for studying sex differences.

This study utilizes PKCδ to sub-divide the BNST in the experiments from Chapter 2, in an attempt to further dissect the heterogeneous stress responsive cell populations in the BNST. Interestingly, the use of this marker uncovered a stress-induced increase in the co-expression of *Crh/Prkcd* transcripts in the dBNST specifically in females. Here, we describe this female-specific stress response and investigate the regulation of this response by modulating the systems shown to decrease stress activation (*Fos*) of BNST CRF neurons. Furthermore, we compare and contrast the sex differences observed in modulating the *Fos* recruitment and *Prkcd* recruitment in *Crh* cells.

Methods

Animals

Adult male and female C57BL/6J mice (>7 weeks of age; The Jackson Laboratory; RRID: IMSR_JAX:000664) were used for all fluorescence *in situ* hybridization studies. Ovariectomy and sham surgeries were performed by Jax Surgical Services (The Jackson Laboratory) at 6 weeks of age. All mice were group housed (2-5 animals per cage) and maintained on a 12 hour light/dark cycle (lights on 0600-1800) under controlled temperature (20-25 °C) and humidity (30-50%) levels. Food and water were available *ad libitum*. All procedures were approved by the Institutional Animal Care and Use Committee at Vanderbilt University (Nashville, TN).

Restraint Stress Exposure

Mice were restrained during the light cycle (0600-1800) using 50 mL conical tubes (Fisher Scientific) altered to have holes throughout the tube and cap to allow for airflow (McElligott, et al., 2010). Order of restraint was counterbalanced within experimental groups, to account for differences in time of day. Prior to undergoing restraint, mice were handled for five

days as described previously (Olsen and Winder, 2010). Mice were allowed to acclimate to the test location in their home cage for one hour in a sound- and light-attenuating box (Med Associates Inc.). During restraint, mice were placed inside separate sound- and light-attenuating boxes for one hour before being returned to their home cage for 30 minutes. In some experiments, mice were treated with guanfacine (1mg/kg IP; Fisher Scientific) or Clozapine-N-oxide (CNO; 3mg/kg IP) 30 min prior to restraint stress. For the eCB system manipulaiton, mice were treated with JZL184 (8 mg/kg IP; Cayman Chemical) 2 hr prior to restraint stress).

RNA in situ hybridization

Fluorescence *in situ* hybridization assays were performed using the RNAScope Fluorescent Multiplex Reagent Kit (Advanced Cell Diagnostics) to visualize RNA transcripts in BNST coronal sections. Probes used include Mm-Crh-C1, Mm-Fos-C2, and Mm-Prkcd-C3. Mice were put under isoflurane anesthesia and brains were quickly extracted, submerged in ice-cold, oxygenated (95% O_2/5% CO_2) artificial cerebrospinal fluid (ACSF; in mM: 124 NaCl, 4.4 KCl, 2.5 $CaCl_2$, 1.3 $MgSO_4$, 1 NaH_2PO_4, 10 glucose, 26 $NaHCO_3$), and flash-frozen in Optimal Cutting Temperature Solution (VWR) using Super Friendly Freeze-It Spray (Fisher Scientific). Embedded brains were stored at -80 °C prior to being cut on a cryostat (Leica, CM3050S). Slices (16 µm) were adhered to charged slides (Denville Scientific) and immediately frozen with dry ice and stored at -80 °C until staining. Fixation, dehydration, hybridization, and staining protocols for fresh frozen tissue were carried out according to ACD's online specifications. Z-stack BNST images were obtained with a 63x/1.4 NA oil lens on a Zeiss 710 scanning confocal microscope. Three images were taken to cover the dorsal, medial, and lateral areas of the dorsal BNST (Bregma +0.14). Negative control images (negative control probe: DapB) were used to determine brightness and contrast parameters for experimental images. Max intensity projections were used for analysis with ImageJ software (NIH). Counts were combined for the three BNST regions and then averaged with the counts for the contralateral BNST in the slice. Transcripts were identified as individual dots within a cell, using DAPI-labeled nuclei to identify

individual cells. A blinded reviewer identified cells as positive for zero, one, two, or three of the following transcripts: *Crh*, *Prkcd, Fos*. Negative control images obtained from slices incubated with the control prob DapB were used to determine thresholding parameters that excluded non-specific fluorescence.

Microinjection Surgeries

Mice that were >6 weeks of age were used for viral injections studies. Mice were anesthetized with isoflurane and injected intracranially with AAV constructs expressing DREADD as described below. For the PBN DREADD experiment, 200-300 nL of AAV5-hSyn-hM4D(Gi)-mCherry (Addgene) was injected at 40 nL/min into the PBN (AP: -5.34, ML: ±1.31, DV: -4.30; 15.03° angle). For the insula DREADD experiment, 200-300 nL of AAV5-hSyn-hM4D(Gi)-YFP (University of North Carolina Viral Vector Core) was injected into the insula (AP: 0.02, ML: ±3.66, DV: -4.30) of one hemisphere, with the control virus AAV5-hSyn-GFP (University of North Carolina Viral Vector Core) injected into the contralateral hemisphere. Mice were treated with 5 mg/kg of ketoprofen 24 hours and 48 hours following surgery. Virally injected mice were killed 6 –12 weeks after surgery for anatomical and electrophysiological analysis.

Statistical Analysis

All data are represented as mean ± SEM except for when SD is used to address within cell variability of latency to respond to optical stimulation. For all RNA *in situ* experiments, two-way ANOVAs were used to assess effect of both treatment and sex. When both factors (or an interaction) were found to have a significant effect, Tukey's multiple comparison test was used to make multiple comparisons. When there was no significant effect of sex, Sidak's multiple comparisons test was used to make comparisons within treatment groups for each sex. Statistical analyses were performed using Graphpad Prism 7.

Reagents

All reagents used were purchased from Millipore Sigma unless otherwise noted in the text. For *in vivo* experiments, all drugs were diluted in sterile saline (0.9% sodium chloride; Hospira).

Results

Further definition of post-synaptic cell identity using Prkcd reveals a stress-sensitive increase in Prkcd/Crh co-expression in female mice.

Based on knowledge of PKCδ neurons opposing actions to CRF cells in the fear response in the CeA (Haubensak, et al., 2010; Asok, et al., 2018), we hypothesized that PKCδ could similarly be an important marker in the BNST, and included *Prkcd* transcript analysis in our *in situ* hybridization assays from Chapter 2 (Figure 9a-b). These studies revealed an interesting stress-sensitive sex difference. Following restraint stress, we observe a female-specific increase in the percentage of *Crh* neurons co-expressing *Prkcd* (Figure 9c). Analysis by 2-way ANOVA results in a significant effect of both stress ($F(1,15) = 18.07$, $p = 0.001$) and sex ($F(1,15) = 6.89$, $p = 0.019$), as well as a significant interaction ($F(1,15) = 16.43$, $p = 0.001$). *Post hoc* analysis using Tukey's multiple comparisons test shows a significant increase in the percentage of *Crh* cells expressing *Prkcd* following stress in females (no stress: 22.3±2.5%; stress: 49.3±3.7%; $p < 0.001$), but no difference in males (no stress: 27±4.4%; stress: 27.6±1.8%; $p = 0.99$). This results in a significant difference between males and females following restraint stress ($p = 0.002$). To determine if the co-expression of *Crh* and *Prkcd* in females after stress was due to an increase in *Crh* neurons or an increase in *Prkcd* neurons we looked at the overall number of neurons expressing these transcripts in the dBNST (Figure 9d-e). A 2-way ANOVA shows that *Crh* cell number remained unchanged throughout the experiment with no main effect of either stress ($F(1,15) = 0.24$, $p = 0.629$) or sex ($F(1,15) = 0.13$, $p = 0.724$), and no interaction ($F(1,15) = 0.30$, $p = 0.589$). Conversely, total *Prkcd* cell number did not remain constant, as a 2-way ANOVA reveals a significant interaction between stress and sex ($F(1,15 = 6.68$, $p = 0.021$), but no main effect of either alone (sex: $F(1,15) =$

0.01, p = 0.920; stress: F(1,15) = 3.70, p = 0.073). *Post hoc* analysis with Tukey's multiple comparisons test shows a significant increase in the number of *Prkcd* expressing cells in females following stress (no stress: 204±19.2 cells; stress 405±55.7 cells; p = 0.033), but not in males (no stress: 314.6±61.0 cells; stress 285.2±32.6 cells; p = 0.962). This suggests that *Prkcd* is being upregulated in *Crh* expressing neurons and not vice versa.

In order to examine restraint stress activation of this newly identified neuronal population co-expressing *Crh*/*Prkcd,* we also looked at the presence of *Fos* transcripts in these neurons (Figure 9f). When analyzing the percentage of *Crh*/*Prkcd* cells that contain *Fos*, a 2-way ANOVA reveals a significant effect of stress (F(1,15) = 7.41, p = 0.016), but no effect of sex (F(1,15) = 0.02, p = 0.889) and no interaction (F(1,15) = 0.93, p = 0.353). Sidak's multiple comparisons test shows a significant increase in *Fos+ Crh/Prkcd* cells following stress in females (no stress: 17.7±2.9%; stress: 34.7±6.0%; p = 0.046), with no change in males (no stress: 21.5±3.5%; stress: 29.6±5.8%; p = 0.389). However, this *Crh/Prkcd* population in females only accounts for approximately half of the *Crh* cells, thus we also quantified *Fos* transcripts in *Crh* neurons that do not co-express *Prkcd* (Figure 9g). A 2-way ANOVA shows a significant effect of stress (F(1,15) = 39.99, p < 0.0001) on the percentage of *Fos+ Crh (Prkcd-)* cells, but no effect of sex (F(1,15) = 0.69, p = 0.418) and no interaction (F(1,15) = 0.18, p = 0.675). *Post hoc* analysis using Sidak's multiple comparisons tests show a significant increase in *Fos+ Crh (Prkcd-)* cells following stress in both males (no stress: 11.1±1.6%; stress: 27.8±3.1%; p = 0.001) and females (no stress: 12.3±2.3%; stress: 31.4±4.2%; p = 0.001).

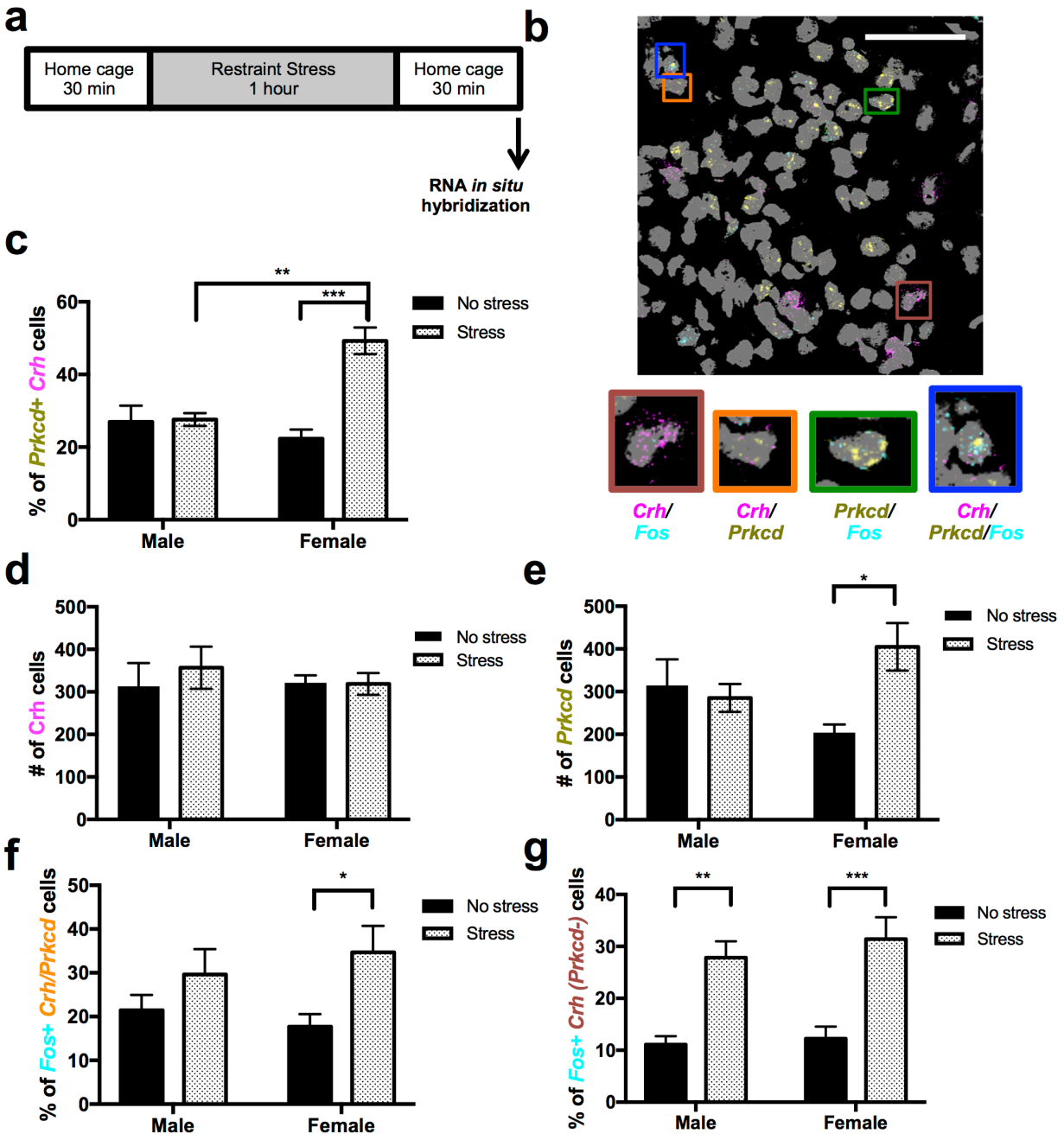

Figure 9. RNA *in situ* assay reveals a female-specific stress-induced increase in *Prkcd/Crh* co-expression. a) Schematic showing timeline of restraint stress and RNA *in situ* hybridization assay. b) Example image of RNA *in situ* assay (gray: DAPI-labeled nuclei, magenta: *Crh* transcripts, yellow: *Prkcd* transcripts, cyan: *Fos* transcripts). Boxes provide magnified examples of cells expressing multiple transcripts (maroon: *Crh/Fos*, orange: *Crh/Prkcd*, green: *Prkcd/Fos*, blue: *Crh/Prkcd/Fos*). c) Summary bar graph showing the percentage of *Crh* neurons that express *Fos* 30 min after restraint stress in male and female mice. * indicates significant difference compared to each other group (**p<0.01; ***p<0.001). d) Summary bar graph showing the number of *Crh* expressing cells 30 min after restraint stress in male and female mice. d) Summary bar graph showing the number of *Prkcd* expressing cells 30

min after restraint stress in male and female mice. *indicates significant difference between stress conditions (*p<0.05). f) Summary bar graph showing the percentage of co-localized *Crh/Prkcd* cells that express *Fos* 30 min after restraint stress in male and female mice. * indicates significant difference between stress conditions (*p<0.05). g) Summary bar graph showing the percentage of *Crh* cells (lacking *Prkcd*) that express *Fos* 30 min after restraint stress in male and female mice * indicates significant difference between stress conditions (**p<0.01, ***p<0.001). c-g) Males: no stress n=5, stress n=5; Females: no stress n=5, stress n=4. All data are represented as mean±SEM.

Increase in Crh/Prkcd co-localization following stress is mechanistically distinct from Gi-coupled GPCR suppression of BNST CRF neuron Fos response

We next wanted to determine if the stress-related increase in *Prkcd/Crh* in females could be blocked by any of the Gi-coupled GPCR manipulations shown to decrease *Fos* in Chapter 2. PBN-expressed hM4Di DREADD activation did not change the increase in co-expression of *Prkcd/Crh* in female mice after stress (Figure 10a). A 2-way ANOVA shows a significant effect of sex ($F(1,23) = 5.60$, $p = 0.027$), but no effect of treatment ($F(2,23) = 0.69$, $p = 0.512$) and no interaction ($F(2,23) = 2.87$, $p = 0.077$). Tukey's multiple comparisons test shows that there is no significant difference in percentage of *Prkcd+ Crh* cells between the stress/saline and stress/CNO mice in females (stress/saline: 37.1±4.6%; stress/CNO: 35.8±6.3%; $p = 0.973$). Similarly, systemic JZL administration also does not effect the stress-induced increase in *Crh/Prkcd* cells (Figure 10b). Analysis using a 2-way ANOVA reveals a significant effect of sex ($F(1,22) = 7.71$, $p = 0.011$), but no significant effect of treatment ($F(2,22) = 2.53$, $p = 0.103$) and no interaction between these variables ($F(2,22) = 1.47$, $p = 0.251$). *Post hoc* analysis using Tukey's multiple comparisons test confirms a female-specific significant increase co-expression of *Crh/Prkcd* following stress (no stress/saline: 22.9±3.8%; stress/saline: 37.9±6.5%; $p = 0.049$). However, JZL administration does not significantly alter this co-expression as compared to the stress/saline group (stress/JZL: 33.4±3.6%; $p = 0.732$). Finally, the effect of insula-expressed hM4Di on *Crh/Prkcd* co-expression was also evaluated (Figure 10c). In Chapter 2, male and female data is combined, as both sexes are equally affected by activation of hM4Di in the insula. Therefore, we have had to separate this data here to evaluate the female-specific

increase co-localized transcripts. Additionally, in order to isolate the effect of DREADD activation, only the data from hemispheres injected with the hM4Di DREADD have been included. As with the PBN-expressed DREADD, activation of insula hM4Di does not suppress the upregulation of *Crh/Prkcd* co-expressing cells. A 2-way ANOVA demonstrates a significant interaction between the variables ($F(1,7) = 6.56$, $p = 0.037$), as well as a significant effect of treatment ($F(1,7) = 6.48$, $p = 0.038$), despite being underpowered after separating the data by sex. However, there is not a significant effect of sex alone ($F(1,7) = 2.117$, $p = 0.189$). Sidak's multiple comparisons test shows that, even with systemic CNO administration to activate the insula DREADD, acute restraint stress still significantly increases *Crh/Prkcd* co-expression in females (no stress/CNO: 14.0±7.0%; stress/CNO: 53.4±9.3%; $p = 0.013$). This suggests that while the increase in *Crh/Prkcd* colocalization in females is an interesting observation, it is mechanistically separate from sex differences observed following PBN hM4Di activation and JZL activation. Furthermore, activation of insula-expressed hM4Di also does not alter *Crh/Prkcd* co-expression, showing that this sex-difference cannot be modulated by the same neuromodulatory systems shown to regulate stress-induced *Fos* in Chapter 2.

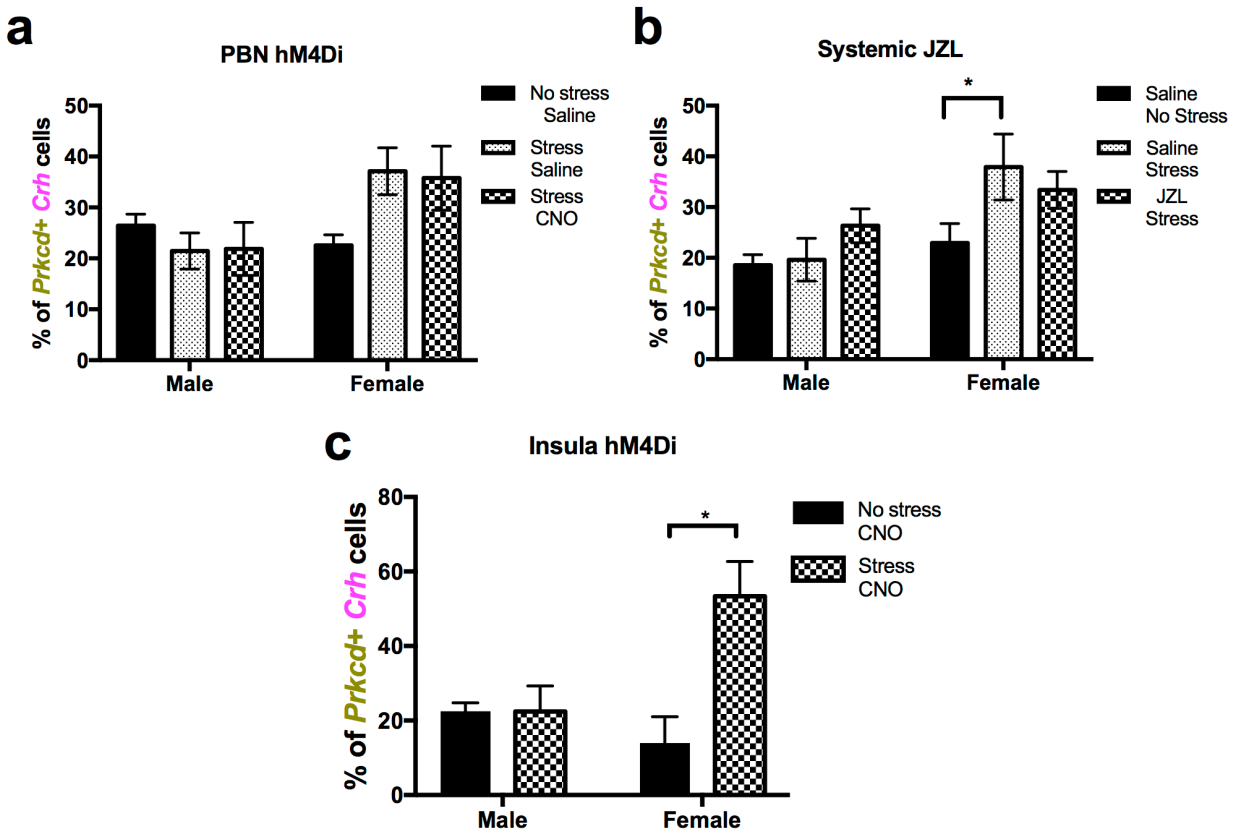

Figure 10. Activation of Gi-coupled GPCR signaling does not alter stress-induced increase in *Crh/Prkcd* in female mice. a) Summary bar graph showing effect of CNO injection in mice with PBN-expressed hM4Di on percentage of BNST *Crh* cells that express *Prkcd* 30 min after restraint stress in male and female mice (n=5 mice/group; exception: female, no stress/saline n=4). b) Summary bar graph showing effect of systemic JZL administration on percentage of BNST *Crh* cells that express *Prkcd* 30 min after restraint stress in male and female mice (n=5 mice/group; excecption: male, no stress/saline and stress/JZL n=4 mice). *indicates significant difference between stress control groups in female mice (*p<0.05). c) Summary bar graph showing effect of stress and CNO injection in male and female mice with insula-expressed hM4Di on percentage of BNST *Crh* cells that express *Prkcd* 30 min after restraint stress (n=3 mice/group; exception: male, no stress/CNO n=2 mice). *indicates significant difference between treatment groups in female mice (*p<0.05). All data are represented as mean±SEM.

Stress-induced Fos activation of Crh cells and upregulation of Crh/Prkcd co-expression are both altered in ovariectomized mice

Finally, in order to begin to investigate a potential role for hormonal signaling related to the estrous cycle in observed sex-differences in BNST CRF neuron stress responsivity, we utilized ovariectomized (ovx) mice in our restraint stress paradigm. Ovx surgery was performed

at 6 weeks of age at The Jackson Laboratory before being sent to Vanderbilt. Mice were then allowed to acclimate for one week at Vanderbilt before handling and restraint stress beginning at 8 weeks of age. RNA *in situ* hybridization analysis shows that ovariectomy substantially reduces stress-induced *Fos* expression in dBNST *Crh* cells (Figure 11a). A 2-way ANOVA reveals a significant effect of both ovx surgery ($F(1,16) = 5.53$, $p = 0.032$) and stress ($F(1,16) = 10.53$, $p = 0.005$), but no significant interaction ($F(1,16) = 3.41$, $p = 0.083$). Tukey's multiple comparison test shows that while stress still increases the percentage of *Fos+ Crh* cells in mice receiving a control sham surgery (no stress: 7.2±1.8%; stress: 27.3±6.8%; $p = 0.012$), those that underwent ovx surgery no longer show a stress-induced *Fos* response in *Crh* cells (no stress: 5.2±1.6%; stress 10.7±3.1%; $p = 0.758$). Additionally, when analyzing *Prkcd*, we see that the stress-induced increase in *Crh/Prkcd* co-expression is also blocked in ovariectomized mice (Figure 11b). Statistical analysis using 2-way ANOVA shows a significant effect of ovx surgery ($F(1,16) = 11.71$, $p = 0.003$), but no significant effect of stress ($F(1,16) = 1.86$, $p = 0.192$). However, there is a significant interaction between the variables ($F(1,16) = 7.93$, $p = 0.012$). *Post hoc*, Tukey's multiple comparisons show that mice that underwent sham surgery have a significant increase in *Crh/Prkcd* co-expression following stress (no stress: 21.6±5.2%; stress: 37.6±3.9%; $p = 0.042$). Conversely, ovariectomized mice no longer show a significant increase in *Crh/Prkcd* co-expressing cells (no stress: 19.3±3.6%; stress: 13.7±1.8%; $p = 0.736$). These results provide evidence for the involvement of sex hormones in the signaling pathways involved in the stress response of BNST CRF neurons.

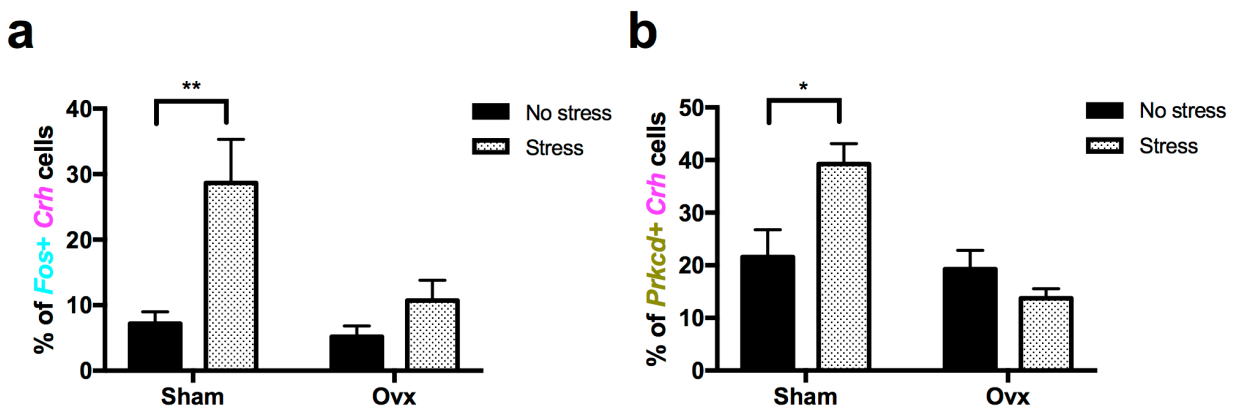

Figure 11. Ovariectomoy alters both stress-induced increase in *Fos* expression in *Crh* cells and increases in *Crh/Prkcd* co-expression in female mice. a-b) Summary bar graphs showing effect of oavariectomy on percentage of *Crh* cells that express *Fos* (a) or *Prkcd* (b) 30 min after restraint stress in female mice (n= 5 mice/group). *indicates significant difference between stress conditions (**p<0.01, *p<0.05). All data are represented as mean±SEM.

Discussion

Stress-induced increase in co-expression of Crh/Prkcd in female mice

While using PKCδ as a marker to further dissect the heterogeneous BNST, we uncovered an additional sex difference in the BNST stress response. We found that expression of *Crh* and *Prkcd* desegregated after stress, resulting in increased co-expression of the two transcripts specifically in females. As this co-expressing population of neurons also show a stress-induced *Fos* response, it is possible that this population marks a uniquely stress-sensitive population of neurons in the female. Additionally, as the number of cells expressing *Crh* transcript remained stable, this increase in co-expression is likely driven by changes in *Prkcd* expression regulation. The ovariectomy experiment demonstrated that ovarian hormones are necessary for this co-expression phenotype. Notably, *Prkcd* has an estrogen response element and can be increased by estrogen signaling in other systems (Shanmugam, et al., 1999). Furthermore, PKCδ signaling has been linked to neuroinflammatory responses, which can be activated by stress (Ghayur et al., 1996; Anantharam et al., 2002), making this newfound population of neurons in the female BNST an interesting target for future studies.

Gi-coupled GPCR regulation of *Crh/Prkcd* co-expression

In Chapter 2, several female-specific effects were observed in the Gi-coupled GPCR regulation of *Fos* expression in BNST *Crh* neurons. Specifically, both activation of CB1 receptors (via increased eCB signaling) and activation of PBN-expressed hM4Di DREADD led to decreased stress-induced *Fos* in *Crh* cells, but only in female mice. Interestingly, these same manipulations did not change the upregulation of *Prkcd*. This suggests that these observed sex differences are mechanistically distinct. Activation of inusla-expressed hM4Di DREADD was also seen to modulate the *Fos* expression in BNST *Crh* cells, however, this effect was sex-independent and was similarly unable to modulate the stress-induced sex difference in *Crh/Prkcd* co-expression.

Effects of ovariectomy on sex differences in BNST CRF neuron stress responsivity

In addition to abolishing the stress-induced increase in *Crh/Prkcd* co-expression, ovariectomy also significantly blunted the *Fos* response in *Crh* cells following stress. While the regulation of *Prkcd* expression by ovarian hormones is unsurprising considering the known estrogen response element discussed above, the regulation of the *Fos* response was unexpected. First, we see an increase in *Fos* in *Crh* cells in both males and females, with no significant difference in magnitude of response between the groups. Furthermore, while sex differences have been reported in restraint stress-induced *Fos* in another region of the BNST, the anteroventral portion, these effects were independent of estrous cycle stages (Babb, et al., 2013). This provides additional evidence of differences in *Fos* recruitment in dBNST neurons as compared to other regions of the BNST. Future studies will need to investigate the mechanism of action for ovarian hormone signaling in regulating *Fos* and determine how these actions are altered by the various stages of the estrous cycle.

Taken together, these experiments uncover an additional sex difference underlying the BNST response to stress and suggest that multiple mechanisms are responsible for regulating

these sex-specific effects. As the mechanistic underpinnings of increased stress-related psychiatric disorders in women are not well understood, the co-expressing *Crh/Prkcd* population of cells in females will be interesting to focus in future studies. A better understanding of what sets this neuronal population apart from other BNST cells, as well as further exploration of the mechanistic control of these cells will provide additional insight into female-specific stress signaling in the brain.

Chapter 4

Conclusions and Future Directions

Overall, these studies represent an effort to detail mechanisms underlying the stress activation of BNST neurons. The heterogeneity of the BNST was examined through a combination of techniques, including using genetic markers of cell identity, investigating specific glutamatergic inputs to these cells, and exploring the signaling role of multiple Gi-coupled GPCRs. In the end, this approach led to the identification of two separate glutamatergic circuits involved in the stress-recruitment of CRF neurons in the BNST, which could be differentially modulated by activation of Gi-coupled GPCRs. While these studies provide a framework for targeting pathways involved in controlling the BNST stress response, there remain many questions about the precise function and mechanistic control of these circuits.

Measuring *in vivo* activity of BNST CRF neurons during restraint stress

Throughout these studies, the presence of *Fos* mRNA transcripts was used as a marker for neuronal activation. As an immediate early gene, *Fos* expression has been shown to reliably increase in depolarized neurons and has proven to be a very useful tool in neuroscience (Hoffman et al., 1993; McReynolds et al., 2018). This approach was very useful in that it allowed for *post hoc* identification of BNST neurons activated by restraint stress and could be combined with investigation of other transcripts co-expressed with *Fos*. These co-expression studies allow us to study stress activation in a specific subset of BNST neurons, helping to dissect BNST heterogeneity. While the use of *Fos* as a marker of activation provided interesting insights, it does not allow for real-time observation of neuronal activity during a stressor. For instance, *Fos* expression indicates that a neuron was activated at some point during the stress paradigm, but the precise time-course of this activation and correlations with behavior are unclear.

One way to address the real-time aspect of CRF cell activation during stress would be to utilize *in vivo* calcium imaging approaches. Fiber photometry is a method for detecting calcium transients in specific brain regions in awake and behaving animals. Using genetically encoded calcium indicators (such as GCaMP), which provide a fluorescent readout of changes in calcium signaling, it is possible to study defined populations of cells (Cui et al., 2013). In order to follow up on the *Fos* experiments, I would stereotaxically inject a Cre-dependent GCaMP virus into the BNST of CRF-tomato reporter mice and then implant the optic fiber in the BNST as well. This would allow for isolation of calcium signals occurring in specifically BNST CRF neurons. Changes in calcium signal could then be measured before restraint stress, during restraint stress, and following the termination of stress. This would provide insight as to if CRF neurons are active throughout restraint stress or within a specific period of the stress. For instance, while being restrained mice exhibit two distinct behaviors, passive coping (with little to no movement of the body) and actively struggling. I predict that CRF neurons would be more active during active bouts of struggling, which could be determined by time-locking the calcium signal to this behavioral occurrence. Once the real-time activation pattern of CRF neurons during restraint stress has been determined, the various manipulations (PBN and insula Gi-DREADD, guanfacine, JZL184) shown to decrease *Fos* in Chapter 2 could be utilized to confirm their real-time manipulation of CRF activity.

This fiber photometry approach could also be used to specifically assess activity at terminal fields. To do this, the GCaMP virus would be stereotaxically injected into the input region of interest (PBN or insula) and then the fiber optic would still be implanted in the BNST. As calcium is a necessary component of neurotransmitter release, the measurement of calcium transients in these terminals relays information about synaptic activity at this terminal. This approach would be helpful in both determining the mechanistic outcome of activating the Gi-coupled hM4Di DREADD, as well as testing the actions of systemic guanfacine and JZL184 administration. For both the insula and the PBN experiments, we hypothesize that CNO

administration results in Gi-coupled DREADD activation, leading to neuronal silencing of this input to the BNST (Armbruster et al., 2007). Indeed, the electrophysiological validation of the DREADD supports this hypothesis, as decreased glutamatergic drive onto BNST CRF neurons was observed when washing on CNO in an *ex vivo* slice prep of PBN hM4Di-injected mice. However, GPCR signaling is quite complex and there are many different downstream targets of Gi signaling. For example, activation of a Gi-coupled GPCR has actually been shown to lead to have excitatory actions both in prefrontal cortex neurons (Wang et al., 2007) and in the BNST (N. Harris, unpublished data). Therefore, fiber photometry would allow us to test this hypothesis *in vivo*, showing that activating either the insula- or PBN-expressed hM4Di leads to decreased activity at the terminal fields in the BNST. Similarly, using this set-up would also provide *in vivo* evidence of the actions of systemic guanfacine and JZL184 administration. Once again, our conclusions about where these drugs are acting come from *ex vivo* slice electrophysiology experiments. Using fiber photometry, we could measure changes in input-specific terminal activity to more conclusively link the systemic administration with direct actions on BNST inputs.

There are several caveats that come with using this approach. First, measuring changes in calcium signal does not equate to measuring actual neuronal firing. Calcium mobilization is an important consequence of neuronal action potential firing, but these transients are still only a proxy for action potentials (Miyawaki et al., 1997; Broussard et al., 2014). Second, some technical challenges could occur in filtering out background noise from actual signals. This is particularly true for experiments looking at calcium signals in terminals, as these signals will be smaller than the calcium dynamics observed in cell bodies. Keeping these caveats in mind, fiber photometry presents a unique opportunity for real-time exploration of BNST CRF cell activity during stress.

DREADD effects: direct actions vs. multi-synaptic circuit

Using *ex vivo* whole-cell electrophysiology we identified direct synaptic inputs to BNST CRF cells, including inputs from both the insula and PBN. We then used the Gi-coupled DREADD hM4Di to manipulate neuronal activity in these input regions and observed changes in *Fos* expression in the BNST. This supports the hypothesis that manipulating the input, via DREADD activation, to BNST CRF cells directly leads to a decrease in stress-induced *Fos* expression in these cells. However, this experimental set-up does not exclude a potential multi-synaptic circuit effect, in which PBN or insula projections first synapse in another brain region, which then sends a projection to the BNST, altering *Fos* expression in *Crh* cells. To begin to test the importance of the direct synaptic connection, a retrograde Cre-expressing virus (rAAV2-Cre; Tervo et al., 2016) injected into the BNST could be used in combination with a Cre-dependent hM4Di-expressing virus in the PBN/insula. This would result in the Gi DREADD only being expressed in insula or PBN cells that project to the BNST. If systemic CNO administration still results in a decrease in stress-induced *Fos* expression in *Crh* cells, this would further support the importance of a direct monosynaptic input to BNST CRF cells from the insula/PBN. While this design largely eliminates the effect of inputs from brain regions not expressing the DREADD virus, the same neurons that project to the BNST could send collateral projections to other brain regions that could ultimately be influencing the BNST response. Additionally, the retrograde virus in the BNST would not be specific to CRF cells, so the PBN/insula input being evaluated would be to unidentified BNST neurons. As a large portion of BNST neurons are interneurons, this leaves the potential for a local multi-synaptic circuit effect within the BNST itself. However, this manipulation using the retrograde Cre virus would be the first step in demonstrating the sufficiency of insula or PBN BNST-projecting neurons in modulating *Fos* in BNST *Crh* cells.

Role of insula/PBN inputs in modulating other stress-related behaviors

As detailed in Chapter 1, the stress response is a complex system and influences a wide-variety of behaviors. While restraint stress is a simple paradigm that allows for evaluation of the effects of an acute stressor on BNST physiology, the question remains of how this physiology relates back to other types of stress, as well as to stress-related behaviors. First, other types of stressors could be evaluated. Studies in both mice and rats have shown that stressors such as electric foot-shock, predator odor exposure, multimodal stress, and exposure to the elevated plus maze (EPM) all result in increases in *Fos* expression in the BNST in CRF cells (Butler, et al., 2016; Lin, et al., 2018), providing evidence that the *Fos* response we are studying generalizes to multiple types of stress, although these studies varied in the sub-region of the BNST being investigated. Repeating the DREADD experiments using alternative stressors such as these would provide insight into the importance of both the PBN and insula inputs in generalized stress responding. Additionally, the development of stress-related psychiatric disorders is often associated with prolonged stress/disturbances to homeostasis (Chrousos, 2009) and the BNST plays a role in sustained fear responses (Davis, et al., 2010). While acute restraint stress provides a simple model, understanding how BNST CRF cells respond to chronic stress (both homotypic and variable stressors) will be important to further understanding the role of these neurons in stress-related psychopathology.

Evidence from our lab suggests that BNST CRF cells are important in other stress-related phenotypes, including the circuitry underlying withdrawal/prolonged abstinence from alcohol. Our lab has demonstrated a *Fos* response in the BNST *Crh* neurons 15 days into forced abstinence following a chronic alcohol-drinking model (S. Centanni, unpublished data). This *Fos* response can be blocked by activation of insula-expressed hM4Di (S. Centanni, unpublished data). Additionally, activating the insula-expressed hM4Di prevents negative affective symptoms normally observed in mice following forced abstinence from alcohol (Holleran et al., 2016; S. Centanni, unpublished data), suggesting that the insula is an important

regulator of stress-related behaviors. Following up on this, I would first investigate the insula to BNST connection specifically, as suggested above for the restraint stress-experiments. Additionally, I would look into the role of the PBN in modulating these same abstinence-induced phenotypes. Furthermore, the importance of these inputs in other stress-related behaviors could be investigated. For instance, activation of either the insula- or PBN-expressed hM4Di may alter stress-induced reinstatement to drug-seeking behaviors, which could be tested in mice using a conditioned place preference assay. Additionally, these inputs may be involved in anxiety-like behaviors observed in the EPM or open-field tasks. Both of these tasks rely on the aversion of mice to exposed and brightly lit areas and have been validated pharmacologically using anxiolytic drugs (Cryan and Holmes, 2005). Future studies should address the role of the insula and PBN inputs to the BNST in regulating anxiety behaviors observed in these paradigms. Furthermore, I would predict that while these inputs may not influence basal responses in these tasks, activation of hM4Di expressed in insula or PBN might dampen stress-induced increases in anxiety-like behaviors. Overall, having identified these inputs in regulating BNST CRF neuron stress responses, it will be important to gain an understanding of the behavioral relevance of these regulatory circuits.

Evaluating relative contributions of insula and PBN inputs to CRF neuron *Fos* response

As both the insula and PBN were implicated in regulating BNST CRF responses, I have so far discussed continuing to study these inputs in parallel. However, I am interested in beginning to understand the relative contributions of these two inputs to the observed BNST CRF neuron *Fos* response, as this may have implications for the potential of these inputs in influencing behaviors. In Chapter 2, the various oEPSC kinetics of these inputs to BNST CRF neurons were analyzed, with the insula input showing increased latency to respond, as well as slower decay time. As discussed, the fast PBN connection may result from known axo-somatic synapses (Shimada, et al., 1989; Dobolyi, et al., 2005), while the slower insula input kinetics

suggest an axo-dendritic connection. I predict that these axo-somatic synapses from the PBN input may allow for greater influence of BNST CRF neuron activity. However, the *ex vivo* mapping data demonstrates that a larger percentage of CRF neurons respond to insula stimulation as compared to PBN stimulation.

The experiments using hM4Di in either the insula or PBN reveal that altering activity in only one of these regions is able to influence the BNST *Fos* response, but these experiments do not provide any information about the relative contributions of these two regions. A potential way to test for relative contribution would be to utilize Gq-coupled DREADDs (hM3Dq) in combination with the Gi-coupled hM4Di. Using a similar Cre-dependent experimental set-up as described in the first section of this chapter, hM3Dq could be stereotaxically injected in either the insula or PBN while hM4Di was injected into the other region (Zhu et al., 2016). Systemic CNO administration prior to restraint stress would then activate both the Gq-coupled DREADD in one region and the Gi-coupled DREADD in the other region. The BNST *Fos* response could then be evaluated following the termination of stress as done previously. In the hM4Di alone experiments, activation of the DREADD was able to decrease stress-induced *Fos* in *Crh* neurons, therefore, activation of hM3Dq may be able to negate the effects of the hM4Di in the other region, resulting in unaltered stress-induced *Fos*. As an alternative, the hM3Dq DREADD could also be used in combination with the kappa-opiod receptor based DREADD (KORD; Vardy et al., 2015), allowing for independent activation of these DREADDs using two different ligands (CNO and salvinorin B). One interesting caveat to this experimental set-up is that currently the out come of activation of hM3Dq signaling in both the PBN and insula is unknown. Prior to attempting this complicated set-up, I would test the ability of PBN- or insula-expressed hM3Dq activation alone to induce a *Fos* response in the BNST, potentially mimicking the actions of restraint stress. A positive result here would provide further support for investigating the competing DREADD experiment.

Investigating PBN-input sex differences

Based on the ability of guanfacine to regulate the PBN input to BNST CRF cells in both males and females, the PBN Gi-DREADD experiment was designed to mimic the effects of guanfacine activation of α_{2A}-ARs located on PBN terminals. Interestingly, this DREADD experiment uncovered a sex-specific effect, where activation of the PBN-expressed hM4Di only altered *Fos* expression in BNST *Crh* cells in females, despite guanfacine altering this phenotype in both males and females. The discussion in Chapter 2 provides a description of potential actions for guanfacine outside of activating receptors on PBN terminals, but also brings up the potential for inherent differences in the PBN input to the BNST in males and females (Wang, et al., 2009). A first step to studying these potential sex differences would be to more thoroughly characterize electrophysiological differences in the PBN input to the BNST. The *ex vivo* mapping experiment demonstrates that 50% of CRF neurons respond to PBN-terminal stimulation, however, the majority of the cells recoded came from BNST slices prepared from female mice. Continuing to add to the number of cells recorded from in slices from male mice will help to determine if this response rate of 50% holds true for both sexes or if the response rate is actually higher in females. Similarly, the effects of guanfacine on regulating the PBN input to BNST cells combined data from male and female mice, but did not include enough cells to evaluate this effect separately in males and females. Adding data to this experiment may uncover differential sensitivity to guanfacine in males and females. Beyond continuing to add data to current experiments, electrophysiology could also be used to begin to evaluate differences in the strength of the PBN input. For example, AMPA/NMDA ratio measurements could be made by recording EPSCs at when holding the cell at both -70mV and +40 mV, providing information about synaptic strength. In addition to electrophysiology, staining for the CGRP receptor in both males and females, would also provide information about potential sex differences as this receptor has is marker from the PBN input (Shimada, et al., 1989). Additionally, as suggested in Chapter 2, current clamp recordings could be utilized to determine

the balance between PBN-activated and PBN-inhibited neurons in the BNST (Flavin, et al., 2014). Patch-clamp recordings of non-specific BNST neurons in male mice showed that ~50% of neurons were PBN-activated and ~50% were PBN inhibited (Flavin, et al., 2014). However, this ratio has not been evaluated in female mice. Additionally, it is unknown how specifically CRF cells respond. While it is possible that CRF cells fall into one of the two categories, activated or inhibited, the heterogeneity of CRF cells, as well as the 50% response rate observed during the *ex vivo* mapping experiment, suggests this may not be the case. Evaluating CRF cells specifically in both males and females could provide additional insight into sex-specific synaptic differences in the PBN input to the BNST.

Contribution of NE signaling at α_1- and β-AR subclasses

While Chapter 2 largely focuses on the regulation of BNST physiology via signaling at the α_2-AR, NE signaling also occurs through α_1- and β-ARs. Figure 4 demonstrates the differential effects of signaling at α- and β-ARs, where activation of both α_1- and α_2-ARs decreases excitatory drive onto BNST CRF neurons, activation of β-ARs actually increases excitatory drive onto these cells. NE application alone decreases excitatory drive onto CRF cells, suggesting that the physiological effects of NE in the BNST may be driven by α-AR signaling. As atipamezole is able to block the effects of NE (and even potentially uncover actions at β-ARs), signaling through α_2-ARs proved to be a potent pathway by which to regulate gluatamatergic drive onto CRF cells. However, the contributions of α_1-AR signaling still need to be explored. Previous work in the lab has shown that NE signaling through α_1-ARs in the BNST requires extended application of NE (McElligott and Winder, 2008). This suggests the contributions of the two classes of α-AR could depend on the timecourse of NE release, such that early actions of NE may largely depend on α_2-AR signaling, while prolonged actions of NE may additionally recruit α_1-AR. Examining the effect of prolonged application of NE on the regulation of excitatory drive in the BNST, as well as the effects of prazosin (α_1-AR antagonist)

would provide further insight into differences between these classes of α-ARs. In addition to the electrophysiology, it would also be interesting to evaluate the systemic effects of methoxamine (α_1-AR agonist) on stress-induced *Fos* recruitment of BNST CRF neurons.

The contribution of β-AR signaling in the BNST appears to be in direct opposition to α-AR signaling (Figure 4). This suggests that blocking β-AR signaling and thus biasing NE signaling towards the α-ARs may also be an effective way to manipulate BNST CRF neuron activity. Indeed, our lab has shown using immunohistochemistry that the systemic administration of propranolol (β-AR antagonist) is able to block the restraint stress-induced increase in cFos+ CRF cells (Y. Silberman, unpublished data). However, while guanfacine also decreases basal cFos expression in BNST CRF cells in the unstressed control condition, propranolol has no effect in this control condition (Y. Silberman, unpublished data). This suggests that the stress activation of CRF cells is necessary to have an effect of β-AR blockade. In a basal state, NE signaling on BNST CRF cells may be biased towards α-AR, however, stress related increases in NE (Pacak, et al., 1995) may additionally recruit β-AR signaling, altering the balance between α-β-AR signaling. This demonstrates the intricacies of NE signaling and emphasizes the state dependent effects of NE.

It is additionally important to consider that the actions of NE may be cell-type specific in the BNST, adding to the complexity of NE signaling in this region. For instance, while a systemic guanfacine injection decreases cFos in CRF cells, it actually increases cFos in non-CRF cells (Y. Silberman, unpublished data). Guanfacine induced cFos in the BNST has been shown to be driven by post-synaptic α_2-AR signaling, through intracellular interactions with HCN channels (N. Harris, unpublished data). These opposing actions of guanfacine suggest that differences in receptor localization, differences in cell type, and differences in stress activation can all alter the cellular effects of NE signaling.

Localizing effects of eCB signaling

The effects of systemic JZL184 administration implicated the eCB system in regulation of *Fos* recruitment in BNST CRF cells. Further evidence from our lab has shown that the insula input to BNST CRF cells is also regulated by the eCB system, suggesting a potential site of action for eCB signaling at insula terminals in the BNST. However, CB1Rs are widely expressed throughout the CNS (Herkenham, et al., 1990), leaving open many sites of eCB regulation in the BNST. A first step in testing the specificity of eCB regulation of the insula would be to test the regulation of other inputs to the BNST. This could be done using the same optogenetic *ex vivo* mapping experimental design used in Chapter 2, but instead of washing on AR ligands, a CB1R agonist (WIN55,212-2) could be used to assess the effect of activating CB1R on glutamatergic drive onto CRF cells from a specific input. As the PBN has been shown to similarly regulate *Fos* responses in BNST CRF cells, examining regulation of this input by the eCB system would be particularly interesting. As the insula input is insensitive to regulation by NE, finding that the PBN is insensitive to regulation by the eCB system would further demonstrate separate mechanisms of actions for these two inputs in regulating stress reactivity in the BNST.

Another way to assess the importance of eCB regulation of the insula input to the BNST would be to disrupt the connection between these two regions. Altering eCB signaling can be tricky due to the unique retrograde signaling mechanism. Our lab has recently crossed two mouse lines that contain floxed genes relating to two different components of the eCB system. One line has loxP sites flanking the gene for CB1R, while the other line has loxP sites flanking the gene for DAG lipase (the enzyme involved in synthesis of 2-AG). Therefore, when Cre is expressed, these genes will be knocked out. Knocking out DAG lipase in the BNST will affect eCB signaling at all inputs to the BNST and similarly, knocking out CB1Rs in the insula will affect signaling at all insula projection sites. One approach would therefore be to inject a Cre-expressing virus in the insula, to knock out CB1R signaling, in one hemisphere in the brain and then inject the same virus into the BNST, to knockout DAG lipase signaling, in the contralateral

hemisphere of the brain. This would result in a double dissociation of the insula to BNST connection and allow for testing of the relevance of eCB signaling at this specific input. Using this experimental design I could test for differences in baseline stress phenotypes in these animals, but I could also use this to assess the effects of systemic JZL184 on restraint stress-induced *Fos*. If this double dissociation design occludes the ability of JZL184 to decrease stress-induced *Fos* in *Crh* cells in females, this would specifically implicate the insula input to the BNST in controlling this response. However, a negative result in this case (JZL184 still decreases *Fos*), does not exclude the importance of the insula input as, even in a DAG lipase knockout mouse model, JZL184 administration was able to partially reverse some of the observed anxiety phenotypes (Shonesy, et al., 2014).

A final way to address the importance of the insula to BNST connection in eCB regulation of BNST *Fos* would be to once again utilize the fiber photometry setup. As discussed above, it is possible to record changes in calcium signal in the insula terminals in the BNST in awake-behaving mice. Therefore, using this set up, systemic JZL184 or saline could be given prior to restraint stress and then calcium transients in insula terminals in the BNST could be recorded both before and during restraint stress. If the eCB system is signaling at the insula input, I would expect to see decreased calcium transients in insular terminals in the JZL184 group as compared to the saline-injected group. Through the use of multiple techniques we can provide further support of the importance of a direct insula to BNST projection in regulating CRF neuron stress responsivity.

Exploring the upregulation of *Prkcd* in *Crh* cells

Chapter 3 describes an unexpected sex-specific effect of restraint stress, an upregulation of *Prkcd* in *Crh* neurons. Under basal conditions, these two populations of cells are largely separate. Additionally, the manipulations that regulate the *Fos* response often do not alter the *Prkcd* response, suggesting that this a mechanistically distinct stress-induced

phenotype. Currently, very little is known about this phenotype. One of the biggest questions remaining is if this upregulation is seen following other stressors or if it is a restraint stress-specific response. Evidence from our lab suggest that this *Prkcd* upregulation may be a more generalized stress response, as it is observed in mice that have undergone the chronic drinking forced abstinence paradigm (S. Centanni, unpublished data). Additional experiments need to be performed using other types of acute stressors, as well as looking at types of chronic stress.

In addition to determining how generalizable the *Prkcd* upregulation phenotype is, the time course of this response is also unknown. While we know *Prkcd/Crh* co-expression is increased 30 min after the end of restraint stress, the length of this phenotype is unclear. Based on the *Fos* response, it is possible that the *Prkcd* upregulation is also transient. However, as these two phenotypes seem to be mechanistically distinct, it is possible that this upregulation results in long-term changes in cells. Additionally, currently we have only assessed *Prkcd* mRNA transcripts, which does not necessarily translate to protein levels. Using immunohistochemistry and a PKCδ antibody in CRF-tomato reporter mice, it is possible to test for upregulations in PKCδ protein expression in CRF neurons following restraint stress. Determining if this upregulation is a long-lasting change will be an important factor in being able to determine the behavioral role of these cells in the future.

If the *Prkcd* upregulation is a transient change, it may be possible to find another marker that identifies which CRF cells are sensitive to this stress-induced upregulation. Future RNA *in situ* hybridization assays assessing *Crh* and *Prkcd* expression after restraint stress could be used to screen for a marker (e.g. Calbindin, Enkephalin, NPY) of this unique stress-sensitive population of *Crh* neurons. Alternatively, *in situ* assays could be combined with viral tracer studies to try to identify these unique *Crh* neurons based on differing circuitry connections (Grabinski et al., 2015). Being able to predict which cells will show an upregulation in *Prkcd* following stress would provide insight into potential mechanism underlying this phenotype, while also making this cell population easier to study.

Behavioral importance of BNST PKCδ cells

Before we can begin to understand a role for cells that co-express *Prkcd/Crh* following stress, we first need to gain a better understanding of the function of PKCδ cells in the BNST in general. Evidence from the CeA suggests that PKCδ cells play a complex role in fear responses and aversion learning (Ciocchi, et al., 2010; Haubensak, et al., 2010; Yu, et al., 2017). Similarly, PKCδ cells in the BNST may play a role in anxiety responses. To begin to assess a general role of PKCδ cells in behavior, I would utilize a PKCδ-Cre mouse line (Haubensak, et al., 2010) to gain genetic access specifically to these cells. First, I would assess the *in vivo* activity of these neurons during stress and negative affect-related behavioral tasks (e.g. open field test and EPM). This could be done using a Cre-dependent GCaMP virus stereotaxically injected into the BNST of PKCδ-Cre mice. Additionally, a fiber optic probe would be implanted in the BNST, allowing for the recording of calcium transients using fiber photometry. These experiments would allow for assessment of neuronal activity during specific behavioral tasks. Alternatively, an optogenetics strategy could be used to assess the effect of activating these neurons during behavioral tasks, including the open field test and EPM. Once again the PKCδ-Cre mouse could be utilized, as a Cre-dependent ChR2 virus could be stereotaxically injected into the BNST along with an optic fiber to allow for *in vivo* stimulation of ChR2 during behavioral tasks (Sidor et al., 2015). Using this approach, changes in anxiety like-behavior as a result of PKCδ neuronal activation could be assessed. The fiber photometry approach would provide insight into normal patterns of activity for these cells during these behavioral tasks, which could then be used to guide stimulation patterns in the optogenetic experiment.

While these experiments would provide information about the behavioral relevance of PKCδ neurons in the BNST in general, they do not provide any insight as to the role of the *Crh/Prkcd* co-expressing cells that increase following restraint stress. Studying this population of cells will largely depend on determining the specifics of the time course of *Prkcd* upregulation, as discussed above. If *Prkcd* levels do not remain elevated, the identification of an additional

genetic marker of these cells would be important for attempting to study this specific population. However, if the *Prkcd* upregulation remains increased on a longer time scale, there are several options for studying these cells. First, a viral vector expressing an shRNA directed against *Prkcd* could be utilized to knockdown levels of *Prkcd*. Ideally this could be done using a Cre-dependent virus that could then be stereotaxically injected into the BNST of CRF-cre mice, resulting in knockdown of *Prkcd* specifically in CRF neurons. Alternatively, these cells could be accessed using a cross of two mouse lines: PKCδ-Cre and CRF-Flp. Similar to Cre-recombinase and loxP sites, Flp-recombinase can be used to remove a gene flanked by FRT sites. Recently, a viral approach known as INTRSECT has led to the development of viral constructs that depend on the expression of both Cre and Flp (Fenno et al., 2014; Fenno et al., 2017). Utilizing this strategy in the PKCδ-Cre and CRF-Flp cross, we could target CRF cells alone with a Flp-dependent virus, PKCδ cells alone with a Cre-dependent virus, or the co-expressing CRF/PKCδ with a the INTRSECT construct that is Cre and Flp dependent. For instance, if these viral constructs expressed GCaMP, this approach could be used to compare the activity of CRF cells, PKCδ cells, and co-expressing CRF/PKCδ cells during restraint stress. This would provide further insight as to the role of this subpopulation of CRF cells during stress.

Estrous cycle-dependent manipulation of the BNST stress response

In Chapter 3, using ovariectomized mice, we showed that both the stress-induced increase in *Fos* in *Crh* neurons and the upregulation of *Prkcd* in *Crh* neurons were dependent on ovarian hormones. As discuess earlier, the regulation of the *Prkcd* response by estrogens is potentially due to the estrogen response element on *Prkcd* (Shanmugam, et al., 1999); however, the regulation of the *Fos* response by ovarian hormones was surprising, as this *Fos* increase is observed in both males and females. Additionally, stress-induced *Fos* increases in the vBNST are not dependent on estrous cycle stages (Babb, et al., 2013). While these ovariectomy results demonstrate the importance of ovarian hormones in these signaling

processes, this does not rely any information about the actual stages of the estrous cycle. The estrous cycle is divided into four stages (proestrus, estrus, metestrus, and diestrus). In order to determine the effect of estrous cycle stage on *Fos* expression and *Prkcd* expression, we would need to determine the stage of the cycle each mouse was in on the day of restraint stress. As the various stages in the estrous cycle correspond to surges in different hormones, understanding how the stages affect the stress-induced phenotype in the BNST could help lead towards potential mechanisms underlying this regulation. Furthermore, ovariectomy results in the removal of the whole organ, which involves more that just estrogen. To further confirm the role of estrogen signaling in these phenotypes, estradiol could be given to ovariectomized mice to determine if this rescues the phenotypes that were blocked by ovariectomy. Additionally, differences in estrogen receptor (alpha and beta) immunoreactivity could be assessed in the BNST before and after exposure to stress. Beyond direct signaling in the BNST, estrogen signaling in other portions of the stress response (e.g. brainstem NE nuclei, HPA axis), could be influencing circuitry within the BNST. While the increase in *Fos* occurred in both males and females, understanding the role of estrogen in regulating this response may provide insight as to key mechanistic differences influencing the response of the BNST to stress. These insights may help in developing therapies that are differentially targeted for males and females.

Overall Conclusions

Overall, this dissertation aimed to dissect the circuitry underlying stress responsivity of CRF cells in the BNST, while also providing insights into the regulatory mechanisms controlling this response. This was achieved by combining techniques addressing specific inputs to CRF cells with studies exploring regulatory control be various neurmodulatory systems in the BNST. While CRF in the BNST has been implicated in stress-related behaviors in many studies, the precise control of these neurons is less well understood. As the BNST is often found to have opposing behavioral actions depending on the precise region or population of cells being

studied, continuing to delve into specific mechanisms modulating BNST activity will be very important for future studies.

Identifying input-specific neuromodulatory mechanisms regulating the stress response may help in translating pre-clinical research to clinical trials. Often, overwhelmingly positive pre-clinical results in animal models fail to find success in human studies. For instance, despite the focus on the role of CRF signaling in addiction, CRFR1 antagonists have not been successful in treating alcohol dependence and craving in clinical trials (Kwako, et al., 2015; Schwandt, et al., 2016). While there are many possible explanations for the negative results in these trials (Pomrenze, et al., 2017), it is also possible that targeting the CRF system directly is too broad of a target, as CRF and CRF receptors are expressed in multiple regions throughout the CNS and CRF cells do not necessarily represent a homogenous population. Therefore, dissecting the mechanism underlying stress recruitment of CRF cells may provide new targets for developing successful treatments of stress-related disorders.

APPENDIX A

Evaluating Affective Behaviors Following Forced Abstinence From Sucrose Two-Bottle Choice Paradigm

The lab has previously demonstrated the development of depressive-like behaviors in mice that have undergone a chronic drinking paradigm followed by forced abstinence (Holleran, et al., 2016). In this model, mice undergo six weeks of a two-bottle choice setup where they can choose between a bottle containing water and a bottle containing ethanol. At the end of six weeks, the bottle with ethanol is replaced with a second water bottle. Affective behavior is the assessed following two weeks of this forced abstinence using the novelty suppressed feeding test (NSFT) and the forced swim test (FST; Bodnoff et al., 1988; Pang et al., 2013). Mice that underwent abstinence from ethanol exhibit increased latencies to feed in the NSFT and increased time spent immobile in the FST (Holleran, et al., 2016), suggesting increased depressive-like behavior. In the past few years, researchers have become increasingly interested in the overlap between circuitry underlying drugs of abuse and circuitry driving the consumption of highly palatable food (DiLeone et al., 2012). Therefore, we decided to compare a sucrose two-bottle choice paradigm to our ethanol-drinking model. Preliminary results suggested that forced abstinence from sucrose could similarly induce negative affective behaviors as observed in the ethanol model (K. Holleran, unpublished data).

To more thoroughly investigate this result, we replicated the finding comparing sucrose (10% w/v) to the ethanol ramp drinking paradigm (mice are started on low percentages of ethanol and this is incrementally increased until they reach 10% v/v). First, drinking behavior was directly compared for the sucrose, ethanol ramp, and a control water group by looking at the preference for sucrose/ethanol over water (Figure 12a). A 2-way ANOVA reveals a significant effect of treatment group ($F(2,42) = 138.8$, $p < 0.0001$) and time ($F(5,210) = 3.54$, $p = 0.004$), as well as a significant interaction between these variables ($F(10,210) = 1.92$, $p =$

0.043). *Post hoc* analysis using Tukey's multiple comparisons test shows that the sucrose group started out with a significantly higher preference for sucrose as compared to ethanol preference (Week 1: ethanol = 68.5±6.1%, sucrose = 98.6±0.3%, $p < 0.0001$; Week 2: ethanol = 78.7±4.6%, sucrose = 97.1±0.4%, $p = 0.003$; Week 3: ethanol = 82.1±4.3%, sucrose = 98.5±0.2%, $p = 0.01$). However, the preference of these two groups was no longer significantly different by Week 4 (ethanol = 87.6±2.2%, sucrose = 98.0±0.5%, $p = 0.154$). While preference rates became similar for ethanol and sucrose by the second half of the drinking paradigm, the sucrose group consumed significantly more sucrose (as compared to ethanol consumption) throughout the paradigm (Figure 12b). Analysis via a 2-way ANOVA shows a significant effect of treatment group ($F(1,28) = 194.7$, $p < 0.0001$) and time ($F(5,140) = 3.5$, $p = 0.005$) on grams consumed, as well as a significant interaction between these variables ($F(5,140) = 3.5$, $p = 0.005$). Sidak's multiple comparison reveals that the sucrose mice consumed significantly more grams/day of sucrose as compared to ethanol grams/day every week of the paradigm (ethanol: 2-3g/day; sucrose = 10-11g/day; $p < 0.0001$). Despite this significant difference in volume consumed, mice gained weight at the same rate in all treatment groups throughout the study (Figure 12c). A 2-way ANOVA reveals only a significant effect of time on weight ($F(7,294) = 273.4$, $p < 0.0001$), with no effect of treatment group ($F(2,42) = 0.60$, $p = 0.551$) and no interaction ($F(14,294) = 0.41$, $p = 0.971$).

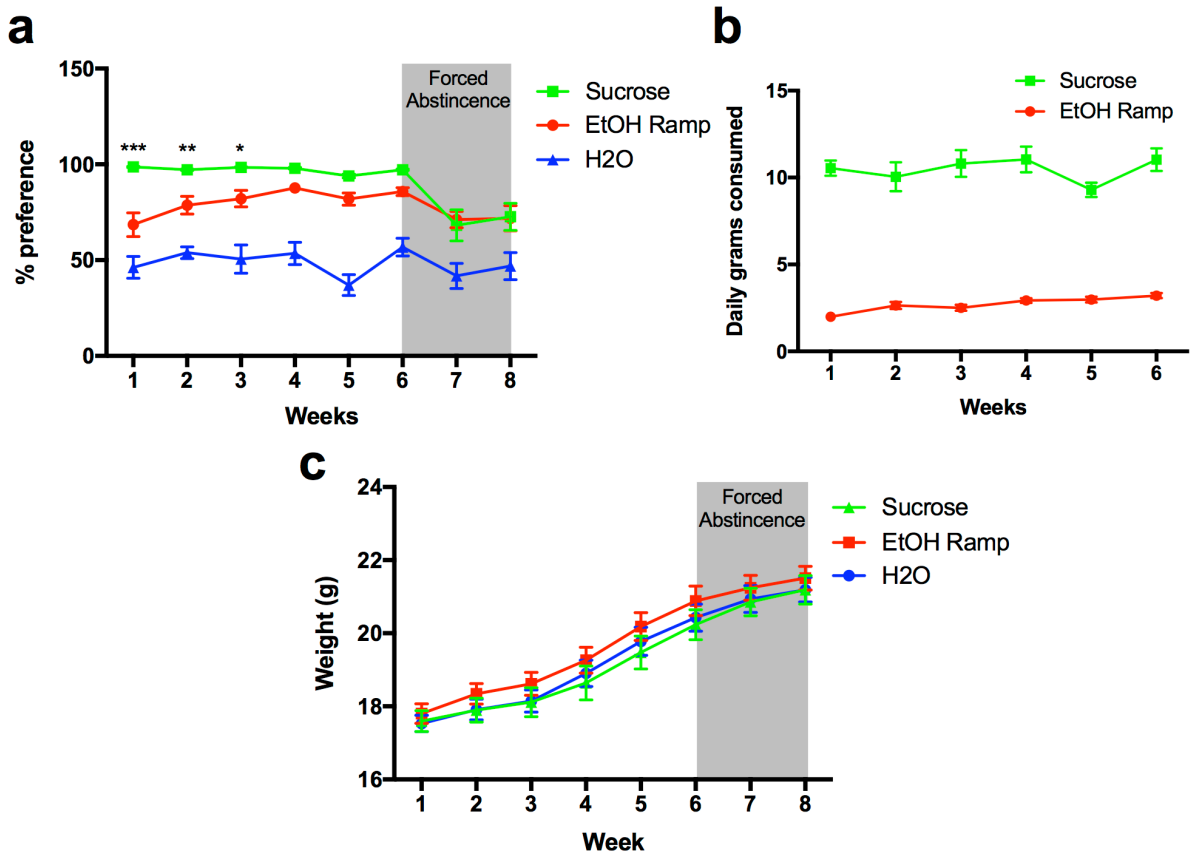

Figure 12. Sucrose two-bottle choice paradigm results in both high preference and high consumption sucrose without altering weight gain. a) Summary graph showing % preference for sucrose/ethanol each week of the drinking paradigm. b) Summary graph showing average daily grams of sucrose or ethanol solution consumed for each week of the paradigm. c) Summary graph showing weight gain throughout the experiment in each of the treatment groups. n = 15 female mice/treatment group. *indicates significant difference between sucrose and ethanol groups (***p<0.001, **p<0.01, *p<0.05).

After establishing high sucrose drinking preference, negative affective behavior was then evaluated using both the NSFT and FST as previously used in evaluating the effects of forced abstinence from alcohol (Holleran, et al., 2016). Mice from the sucrose paradigm were compared to mice that had undergone two versions of the ethanol drinking paradigm, the ethanol ramp as described earlier, as well as a group who underwent sucrose fade with initial ethanol solutions containing 10% sucrose, which is slowly removed until the solution is 10% ethanol alone. The NSFT replicated a depressive-like phenotype in both ethanol groups, as well as well as revealing this same phenotype in the sucrose group following 15 days of forced

abstinence (Figure 13a). A one-way ANOVA shows a significant effect of treatment ($F(3,50) = 3.08$, $p = 0.006$). Dunnett's multiple comparisons test shows a significant increase in latency to feed for all three treatment groups as compared to the control water group (water: 183.8±35.0s; ethanol, suc fade: 335.2±24.1s, $p = 0.019$; ethanol ramp: 420.5±79.1s, $p = 0.002$; sucrose: 342.4±34.4s, $p = 0.032$). However, the same depressive-like phenotypes were not replicated in the FST (Figure 13b). A one-way ANOVA demonstrates no significant overall effect ($F(2,42) = 1.01$, $p = 0.373$). To further assess negative affect, we also used the novelty induced hypophagia (NIH) test. This assay is similar to NSFT where increases in latency suggest increases in depressive-like behavior, but NIH utilizes a palatable substance instead of the regular food pellet used in NSFT (Louderback, et al., 2013). Interestingly, mice that had undergone forced abstinence from ethanol actually exhibited a decreased latency in the NIH test (Figure 13c). A one-way ANOVA shows a significant overall effect ($F(2,42) = 4.37$, $p = 0.019$). Dunnett's multiple comparisons test reveals a significant difference between the water group and the ethanol group (water: 393.1±46.3s; ethanol: 222.5±18.0s; $p = 0.017$), but no difference between the water and sucrose groups (sucrose: 369.5±58.3s; $p = 0.902$). However, when this assay was repeated with a second cohort of mice, these effects were no longer observed (Figure 13d). A one-way ANOVA is only trending towards significance ($F(2,42) = 2.65$, $p = 0.083$) and no significant multiple comparisons are observed (water: 356.2±63.0s; ethanol: 473.2±73.6s, $p = 0.452$; sucrose: 243.9±46.1s, $p = 0.557$). If anything, the ethanol group is now trending in the opposite direction, suggesting that there is no consistent phenotype observed using the NIH test.

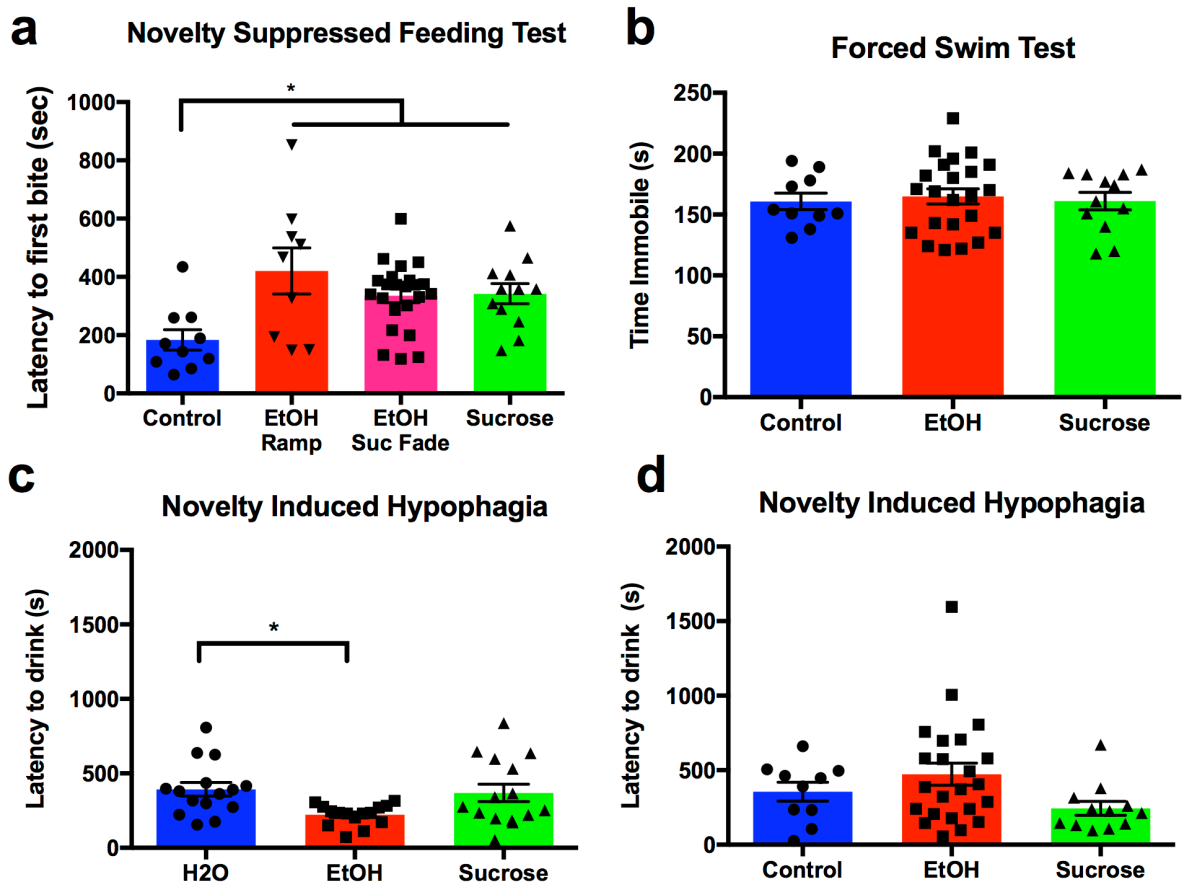

Figure 13. Evaluating negative affect following forced abstinence from sucrose.
a) Summary bar graph of latency to first bite in the NSFT following 15 days of forced abstinence from either ethanol or sucrose. Control: n = 10 female mice; ethanol ramp: n = 9 female mice; ethanol suc fade: n = 23 female mice; sucrose: n = 12 female mice. b) Summary bar graph of time spent immobile in the FST following 15 days of forced abstinence from either ethanol or sucrose. Control: n = 10 female mice; ethanol: n = 23 female mice; sucrose: n = 12 female mice. c-d) Summary bar graph of latency to drink in the NIH assay following 15 days of forced abstinence from ethanol or sucrose. c) n = 15 female mice/group d) control: n = 10 female mice; ethanol: n = 23 female mice; sucrose: n = 12 female mice. *indicates significant difference as compared to control water group (*p<0.05).

Having observed negative affective behavior in the NSFT, we next wanted to determine how long mice needed to drink sucrose before forced abstinence would result in an affective phenotype. We evaluated this time course by using a 2-week, 4-week, and 6-week sucrose-drinking paradigm followed by 15 days of forced abstinence from sucrose. All mice developed a preference for sucrose regardless of the length of the paradigm (Figure 14a). Analysis using a 2-way ANOVA shows a significant effect of both treatment ($F(3,36) = 37.53$, $p < 0.0001$) and

time ($F(2,72) = 18.05$, $p < 0.0001$) on preference, but no interaction between the variables ($F(6,72) = 1.73$, $p = 0.126$). Tukey's multiple comparisons test reveals no difference in preference between the three sucrose groups. Next, affective behavior was assessed once again using the NSFT (Figure 14b). However, a one-way ANOVA was only trending towards a significant overall effect ($F(3,36) = 2.27$, $p = 0.097$), therefore the negative affect observed in Figure 13 was not replicated. Differences in experimental procedure on the day of the test may have led to increased variability, which is particularly visible in the control water group.

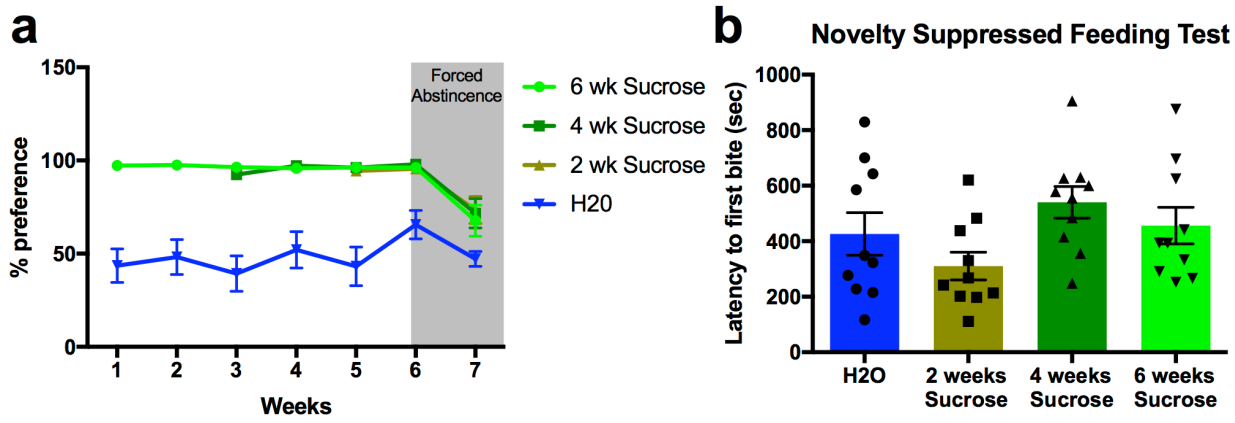

Figure 14. Evaluating effect of length of sucrose drinking paradigm on negative affective behaviors. a) Summary graph showing % preference for sucrose each week of the drinking paradigm in mice exposed to 2-, 4-, or 6-weeks of sucrose. b) Summary bar graph of latency to first bite in the NSFT following 15 days forced abstinence from sucrose. n = 10 female mice/group.

When evaluating negative affect in the ethanol drinking paradigm previously, we observed that the depressive-like phenotype could be blocked by treatment with either ketamine or JZL184 prior to the NSFT assay (Holleran, et al., 2016). We then tested the ability of these same drugs to modulate affective behavior following forced abstinence from sucrose (Figure 15). Once again, the sucrose mice developed a preference for sucrose throughout the drinking paradigm (Figure 15a). However, when negative affect was assessed, we were once again unable to replicate the results seen in Figure 13a (Figure 15b). Instead, a one-way ANOVA

showed no significant overall effect (F(3, 41) = 1.4, p = 0.257). Therefore, it was not possible to interpret any potential effects of ketamine or JZL184.

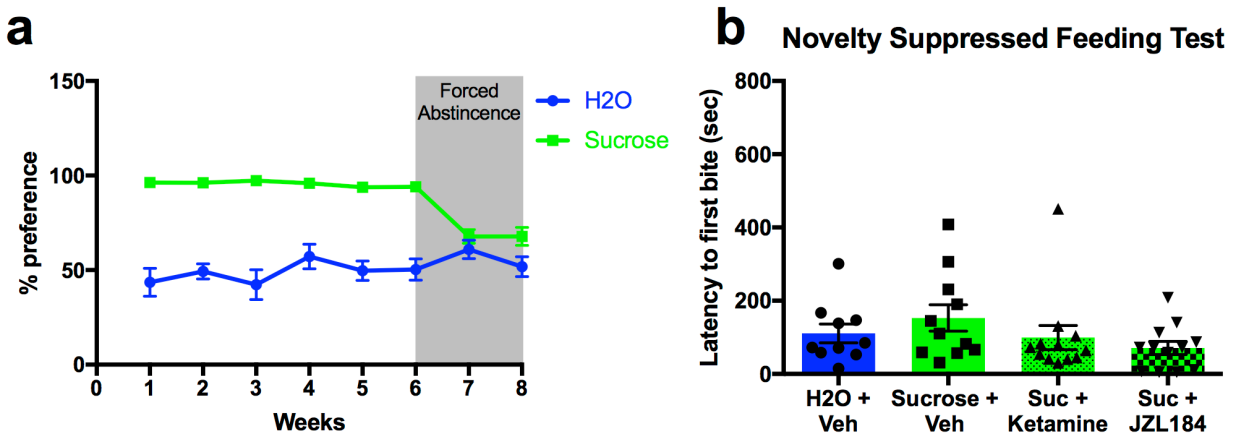

Figure 15. Evaluating Ketamine and JZL184 in the NSFT following forced abstinence from sucrose. a) Summary graph showing % preference for sucrose each week of the drinking paradigm**.** b) Summary bar graph showing effect of systemic ketamine and JZL184 on latency to first bite in the NSFT following 15 days forced abstinence from sucrose. Control: n = 10 female mice; sucrose/veh: n = 11 female mice; suc/ketamine and suc/JZL184: n = 12 female mice.

One final cohort of mice was used to determine if the negative affective behavior observed initially following forced abstinence from sucrose was a phenotype that could be replicated. Additionally, we wanted to compare the effects of sucrose to a non-caloric sweetener, saccharin. We found that saccharin two-bottle choice resulted in a preference level similar to that seen with sucrose (Figure 16a). A two-way ANOVA shows a significant effect of time ($F(7,294) = 25.69$, $p < 0.0001$) and treatment group ($F(2,42) = 296.4$, $p < 0.0001$) on preference, as well as a significant interaction between the variables ($F(14,294) = 5.05$, $p < 0.0001$). Tukey's multiple comparisons test shows that the saccharin and sucrose group did not differ in preference levels throughout the experiment. We next assessed weight gain as saccharin is non-caloric (Figure 16b). A 2-way ANOVA reveals a significant effect of time ($F(7,294) = 251.6$, $p < 0.0001$), but no effect of treatment group on weight ($F(2,42) = 0.65$, $p = 0.525$) and no interaction between the variables ($F(14,294) = 0.79$, $p = 0.681$). This demonstrates that the caloric difference between sucrose and saccharin/water does not have an

affect on overall weight gain. To then assess negative affective behavior, we once again utilized the NSFT (Figure 16c). In the sucrose group, we additionally wanted to assess the ability of ketamine to alter affective behavior as attempted previously. However, we were still not able to replicate the initial depressive-like phenotype observed in Figure 13. A one-way ANOVA shows no significant overall effect ($F(3,41) = 0.67$, $p = 0.575$) for the NSFT assay. We also utilized the FST to assess affect and similarly saw no effect of sucrose or saccharin on behaviors (Figure 16d). A one-way ANOVA of the FST assay also shows no significant overall effect ($F(3,41) = 0.41$, $p = 0.748$).

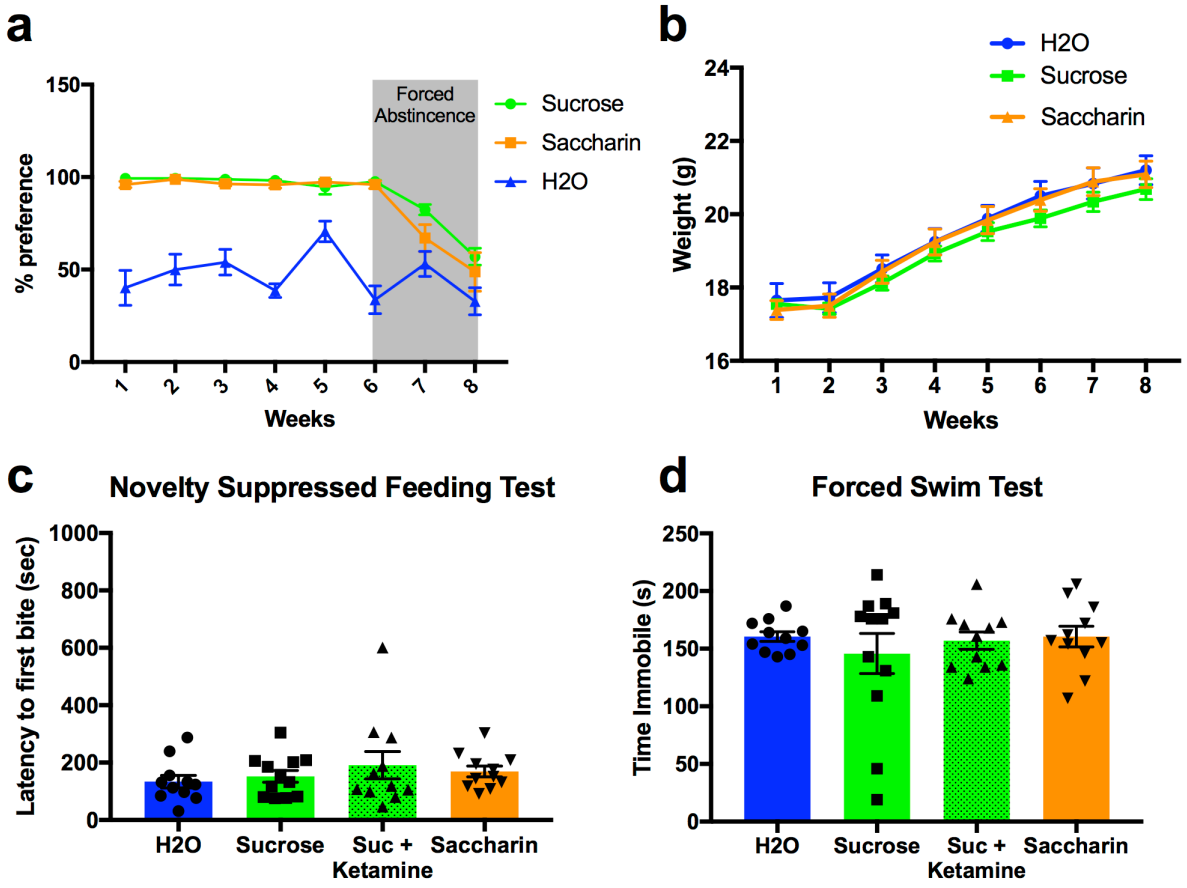

Figure 16. Comparing effects of forced abstinence from sucrose and non-caloric saccharin on negative affective behavior. a) Summary graph showing % preference for sucrose or saccharin each week of the drinking paradigm. b) Summary graph showing weight gain for each drinking group throughout the 8 weeks. c-d) Summary bar graph showing the latency to first bite in the NSFT (c) or immobility time during FST (d) following 15 day forced abstinence from sucrose or saccharine (a portion of sucrose mice were given systemic ketamine prior to the assay). n = 11 female mice/group (exception for sucrose: n = 12 mice).

Our inability to replicate the initial depressive-like phenotype observed following forced abstinence from sucrose suggests that this phenotype may be inherently more variable than the phenotype observed in ethanol drinking mice. This could be due to differences in the underlying circuitry controlling responding to sugar as compared to ethanol. While the initial results were promising, the difficulty in replicating the initial phenotype has led us to stop efforts to follow-up on this project.

APPENDIX B

Examining the Effects of Caloric Restriction on CRF mRNA Levels in the Extended Amygdala

Dieting has been shown to be an effective way to lose weight, but continuing to maintain this weight loss long-term has proven much more difficult. Research suggest that the failure rate for maintaining weight loss is >80% (Wing and Phelan, 2005). Stress has been hypothesized to be a contributing factor to difficulties in weight maintenance as stress has been associated with the consumption of calorically dense food (Teegarden and Bale, 2008). Indeed, the stress and reward pathways intersect and have long been studied in the addiction field (Erb and Stewart, 1999; Koob, 2009). Specifically, changes in the CRF system in following caloric restriction dieting models have been observed in male mice specifically in the extended amygdala (Pankevich et al., 2010). This suggests that dieting may alter stress responsivity and could underlie alterations in the drive for calorically dense food following stressful events.

To further explore the relationship between CRF in the extended amygdala and caloric restriction, we first wanted to extend these experiments to female mice. Additionally, we wanted to examine a potential role for guanfacine in regulating this response. In male mice, caloric restriction resulted in increased depressive-like behavior in the forced swim test and increased levels of corticosterone (Pankevich, et al., 2010). We hypothesized that guanfacine administration during caloric restriction would result in decreased NE levels, potentially counteracting the increased stress responsivity observed following caloric restriction. Individually-housed female mice first underwent a ten-day baseline period, where daily food intake was measured. After establishing this baseline, mice were individually restricted to 75% of their daily food intake for 3 weeks. During this restriction period, a subset of mice received daily IP injections of guanfacine (1mg/kg). Body weight was measured daily throughout the experiment. Following the end of the restriction period, brain punches from both the BNST and CeA were taken, and qRT-PCR was used to measure CRF mRNA levels in these regions.

Caloric restriction resulted in significant weight loss in the mice as compared to control *ad libitum* fed mice (Figure 17a). A 2-way ANOVA reveals a significant effect of both treatment group ($F(3,16) = 18.33$, $p < 0.0001$) and time ($F(21,336) = 3.96$, $p < 0.0001$), as well as a significant interaction between there variables ($F(63,336) = 9.14$, $p < 0.0001$). Post-hoc analysis using Tukey's multiple comparisons tests shows that daily guanfacine administration did not affect weight changes throughout the experiment in either the control mice or food restricted mice. We then measured CRF mRNA levels in both the BNST and CeA (Figure 17b-c). In contrast to the reported effects of caloric restriction in male mice (Pankevich, et al., 2010), we did not observe a significant effect of caloric restriction ($F(1,15) = 2.59$, $p = 0.129$) or guanfacine administration ($F(1,15) = 1.36$, $p = 0.262$) on BNST CRF mRNA levels (Figure 17b). Additionally, there was no interaction between these variables ($F(1,15) = 0.37$, $p = 0.554$). Similarly, the reported decrease in CeA CRF mRNA levels following caloric restriction in male mice was also not observed in female mice (Pankevich, et al., 2010; Figure 17c). Analysis via a 2-way ANOVA did reveal an overall significant effect of both food restriction ($F(1,16) = 4.64$, $p = 0.047$) and drug treatment ($F(1,16) = 13.37$, $p = 0.002$), but no interaction between these variables ($F(1,16) = 2.91$, $p = 0.107$). Tukey's multiple comparisons test shows that the calorically restricted mice that received daily guanfacine administration have significantly elevated CRF mRNA levels in the CeA as compared to both the saline control mice ($p = 0.004$) and the saline food restricted mice ($p = 0.008$). These results show that female mice may respond differently to caloric restriction as compared to male mice, as the same decrease in CRF mRNA levels in the BNST and CeA were not observed.

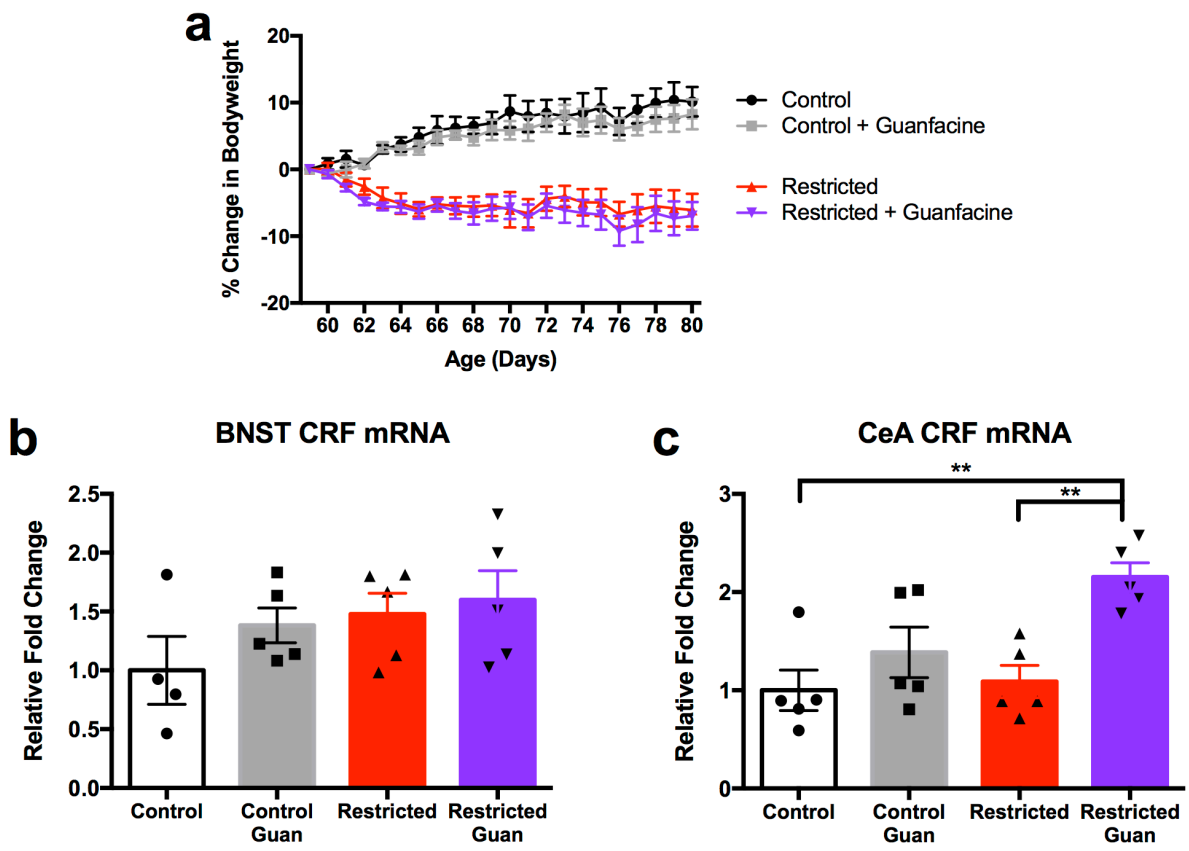

Figure 17. Examining the effects of caloric restriction and systemic guanfacine administration on changes in bodyweight and CRF mRNA levels in the extended amygdala. a) Graph showing the percent change in bodyweight daily during three weeks of food restriction in mice receiving daily IP injections of saline or guanfacine. b-c) Summary bar graphs comparing CRF mRNA levels in the BNST(b) and CeA(c) following food restriction and daily guanfacine administration. n =5 female mice/group (exception: control n =4 female mice) *indicates significant difference between groups (**p<0.01).

As the initial caloric restriction experiments done using female mice did not match results reported for male mice, we next wanted to directly compare male and female mice using the same caloric restriction paradigm. As observed previously, caloric restriction resulted in a decrease in bodyweight in mice as compared to control mice (Figure 18a). A 2-way ANOVA shows a significant effect of both treatment ($F(3,25) = 43.28$, $p < 0.0001$) and time ($F(21,525) = 6.75$, $p < 0.0001$), as well as a significant interaction between the variables ($F(63,525) = 21.32$, $p < 0.0001$). However, *post hoc* analysis using Tukey's multiple comparisons tests reveals no significant difference in percent weight change between male and female mice in the control

group (p = 0.948) or in the food restricted group (p = 0.207). Following the end of caloric restriction, we once again assessed CRF mRNA levels in the BNST using qRT-PCR and were unable to replicate previously published findings (Pankevich, et al., 2010; Figure 18b). Analysis via a 2-way ANOVA shows no significant overall effect of food restriction ($F(1,25) = 0.91$, $p = 0.350$) or sex ($F(1,25) = 0.469$), $p = 0.500$), as well as no interaction between the variables ($F(1,25) = 0.91$, $p = 0.350$).

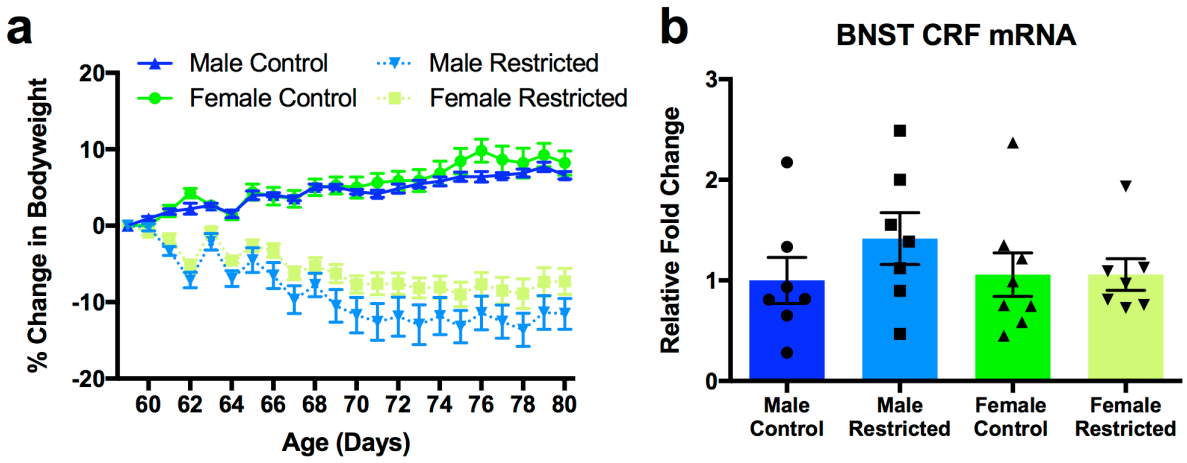

Figure 18. Comparing the effects of caloric restriction on BNST CRF mRNA levels in male and female mice. a) Graph showing the percent change in bodyweight daily during three weeks of food restriction in male and female mice. b) Summary bar graph comparing CRF mRNA levels in the BNST following caloric restriction in male and female mice. n = 7 mice/group (exception: female control n = 8 mice).

In our experiments, we did not observe any effects of caloric restriction alone on CRF mRNA levels in the extended amygdala in either male or female mice. Our inability to replicate previously published findings could be due to differences in experimental procedure, such as differences in mouse housing, mouse diet, brain punch technique, or RNA extraction techniques. Indeed, qRT-PCR was a new technique for the lab and some of the variability may have been due to inexperience. Based on our lack of a phenotype and inability to identify an obvious difference in experimental procedures, we have not followed up on these findings.

APPENDIX C

Evaluating the Effect of Restraint Stress on Bodyweight and Metabolic Phenotypes

Studies of humans diagnosed with anorexia nervosa have suggested that the HPA axis may be hyperactive in these individuals. After being exposed to a stressor, those suffering from anorexia have higher levels of salivary cortisol as compared to healthy controls (Gross et al., 1994). Similarly, rodent models have shown that exposure to stressors results in an anorectic phenotype with rodents consuming less food (Koob and Heinrichs, 1999). This phenotype also occurs with the injection of CRF-like peptides into the ventricles, implicating CRF-signaling specifically in driving anorectic behavior (Koob and Heinrichs, 1999).

Preliminary data from our lab suggests that exposure to chronic restraint stress can result in the development of a weight loss phenotype (Figure 19a). The restraint stress paradigm consisted of 10 days of restraint stress exposure (1 hour/day) followed by 5 days of no stress exposure. Male and female mice were weighed daily at the same time each day. A 2-way ANOVA reveals a significant effect of treatment ($F(3,34) = 27.53$, $p < 0.0001$) and time ($F(14, 476) = 62.71$, $p < 0.0001$), as well as a significant interaction between these variables ($F(42, 476) = 5.04$, $p < 0.0001$). Beginning on day 3 of the paradigm, the percent change in bodyweight becomes significantly different for the stress mice as compared to the unstressed mice as determined using Tukey's multiple comparisons (male: $p = 0.049$; female: $p < 0.0001$), with the unstressed mice continuing to gain weight while the stressed mice begin to lose weight. Furthermore, the stress resulted in a more severe phenotype in female mice. Tukey's multiple comparisons test shows a significant difference in weight loss between stressed male and female mice starting on day 5 of the paradigm ($p = 0.008$). However, later attempts to replicate these findings resulted in lower levels of weight loss, along with a greater effect in males (Figure 19b). A 2-way ANOVA still shows a significant effect of treatment ($F(3,26) = 4.29$, $p = 0.014$) and time ($F(14, 364) = 17.72$, $p < 0.0001$), as well as a significant interaction between these

variables ($F(42, 364) = 2.20$, $p < 0.0001$). During this run of the paradigm, the percent weight change of the stressed male mice did not become significantly different from the unstressed mice until day 4 of the paradigm ($p = 0.047$) and did not remain consistently different until day 7 ($p = 0.004$). Meanwhile, the percent weight change of stressed female mice never diverged from that of the control unstressed female mice. In this replication, the male mice develop a weight loss phenotype that was no longer observed in females, suggesting this phenotype may be inconsistent.

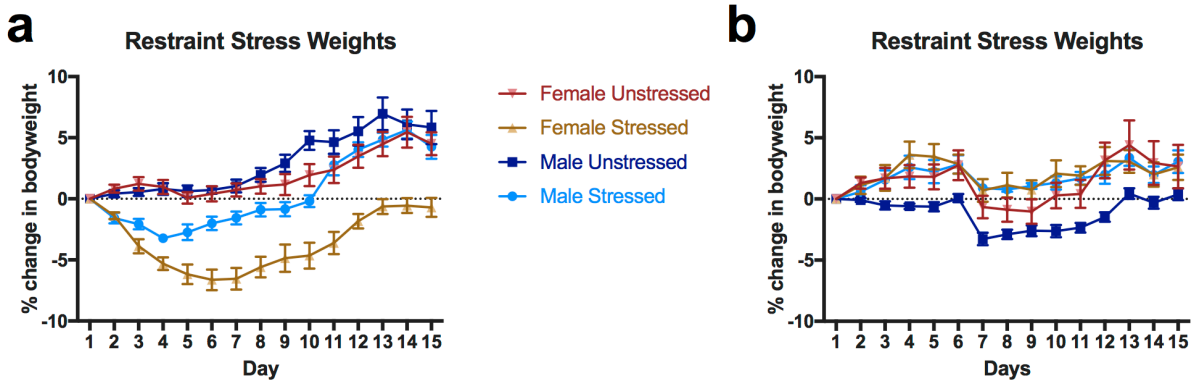

Figure 19. Evaluating the effect of daily restraint stress on changes in bodyweight in male and female mice. a-b) Graphs showing the percent change in bodyweight across 15 days with restraint stress occurring once daily for the first ten days. a) n = 10 mice/group (exception n = 8 mice for female stressed). b) n = 7 mice/unstressed group, n = 8 mice/stressed group.

Having initially observed a more severe phenotype in females, we chose to further investigate the mechanism of this phenotype specifically in female mice. As noted earlier, CRF has been shown to drive anorectic behavior; therefore, we investigated the role of CRF in our restraint stress-induced weight loss phenotype. We used two genetic strategies to selectively ablate CRF cells in female mice. First, we crossed our CRF-Cre mouse line with a ROSA-DTA line, resulting in diphtheria toxin expression in Cre-expressing CRF cells. This cross leads to the ablation of CRF cells throughout the mouse starting from birth. Additionally, we crossed our CRF-Cre mouse line with a ROSA-DTR line, resulting in diphtheria toxin receptor expression in Cre-expressing CRF cells. This line requires the injection of diphtheria toxin to initiate ablation of cells, allowing for control over the timeline of when cell ablation occurs. Using the same restraint

stress paradigm as before, we then evaluated the effect of ablating CRF cells from birth (DTA+ genotype) or during adulthood (DTR+ genotype) on restraint stress-induced weight loss. When combining the DTA/DTR genotypes, we observe no difference in change in bodyweight following restraint stress in mice with CRF cells ablated as compared to control mice (Figure 20a). A 2-way ANOVA reveals a significant effect of time ($F(14, 252) = 7.78$, $p < 0.0001$) but no effect of cell ablation on weight change ($F(1,18) = 0.012$, $p = 0.916$) and no significant interaction ($F(14,252) = 1.14$, $p = 0.325$). Analyzing the two genetic strategies separately, a 2-way ANOVA still shows no significant effect of DTA driven cell ablation (Figure 20b; $F(1,7) = 0.68$, $p = 0.438$) or DTR driven cell ablation (Figure 20c; $F(1,9) = 0.66$, $p = 0.4389$) on change in bodyweight. Interestingly, when comparing the control stressed group in the DTA experiment to the DTR experiment, the variability of restraint stress-induced weight loss becomes evident (Figure 20b-c).

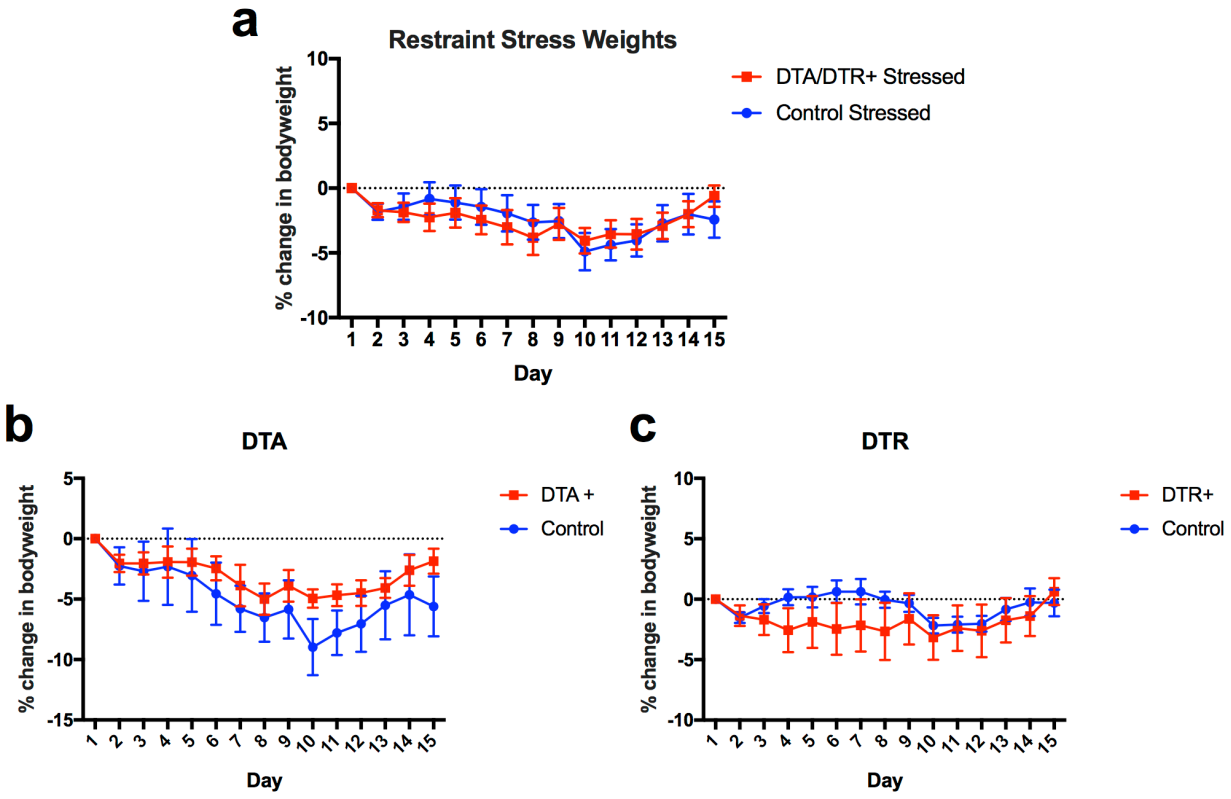

Figure 20. Evaluating the effect of CRF cell ablation of restraint stress-induced changes in weight. a-c) Graphs showing the effect of CRF cell ablation from birth (a,b) or in adulthood (a,c) on percent change in bodyweight across 15 days with restraint stress occurring once daily for the first ten days. n = 5 mice/DTA+ or DTR+ group; n = 4 mice/DTA control; n = 6 mice/DTR control.

Previous studies had shown that CRF administration could result in an anorectic phenotype (Koob and Heinrichs, 1999) and our stress studies did result in a decrease in bodyweight in mice, despite the variability in the phenotype. While we hypothesized that the stress was resulting in decreased feeding, and thus an anorectic phenotype, measuring bodyweight alone did not allow for this type of analysis. To gain a better understanding of what was driving the weight loss phenotype we utilized the Promethion Metabolic Screening system (Sable Systems International). Female mice underwent the same daily restraint stress paradigm for 10 days as described above before being placed in the Promethion system. Once again, the restraint stress paradigm resulted in variable weight loss, however the unstressed mice did gain significantly more weight than the stressed mice (Figure 21a). A 2-way ANOVA reveals a significant effect of time ($F(13,182) = 17.77$, $p < 0.0001$) and stress ($F(1,14) = 9.54$, $p = 0.008$), as well as a significant interaction between the variables ($F(13,182) = 2.66$, $p = 0.002$). Post hoc analysis using Sidak's multiple comparisons test shows that the two groups significantly diverge in weight change starting on day 9 of the paradigm ($p = 0.037$). Following the end of restraint stress, various metabolic factors were analyzed using the Promethion system. Surprisingly stress did not significantly alter several measures of food intake (Figure 21b-d). A 2-way ANOVA shows no significant effect of stress on summed food intake (Figure 21b; $F(1,14) = 0.36$, $p = 0.557$), average meal size (Figure 21c; $F(1,14) = 0.88$, $p = 0.364$), or number of meals (Figure 21c; $F(1,14) = 3.35$, $p = 0.088$). However, stress may have altered energy expenditure/respiration rate (Figure 21e-h). A 2-way ANOVA shows strong trends towards an effect of stress on average energy expenditure (Figure 21e; $F(1,14) = 3.30$, $p = 0.091$), total energy expenditure (Figure 21f; $F(1,14) = 3.18$, $p = 0.096$), average oxygen consumption (Figure 21g; $F(1,14) = 3.18$, $p = 0.096$), and average carbon dioxide production (Figure 21h;

F(1,14) = 3.26, p = 0.092). Together, these results suggest that it may be altered energy expenditure and not altered food intake that results in observed stress-induced weight changes.

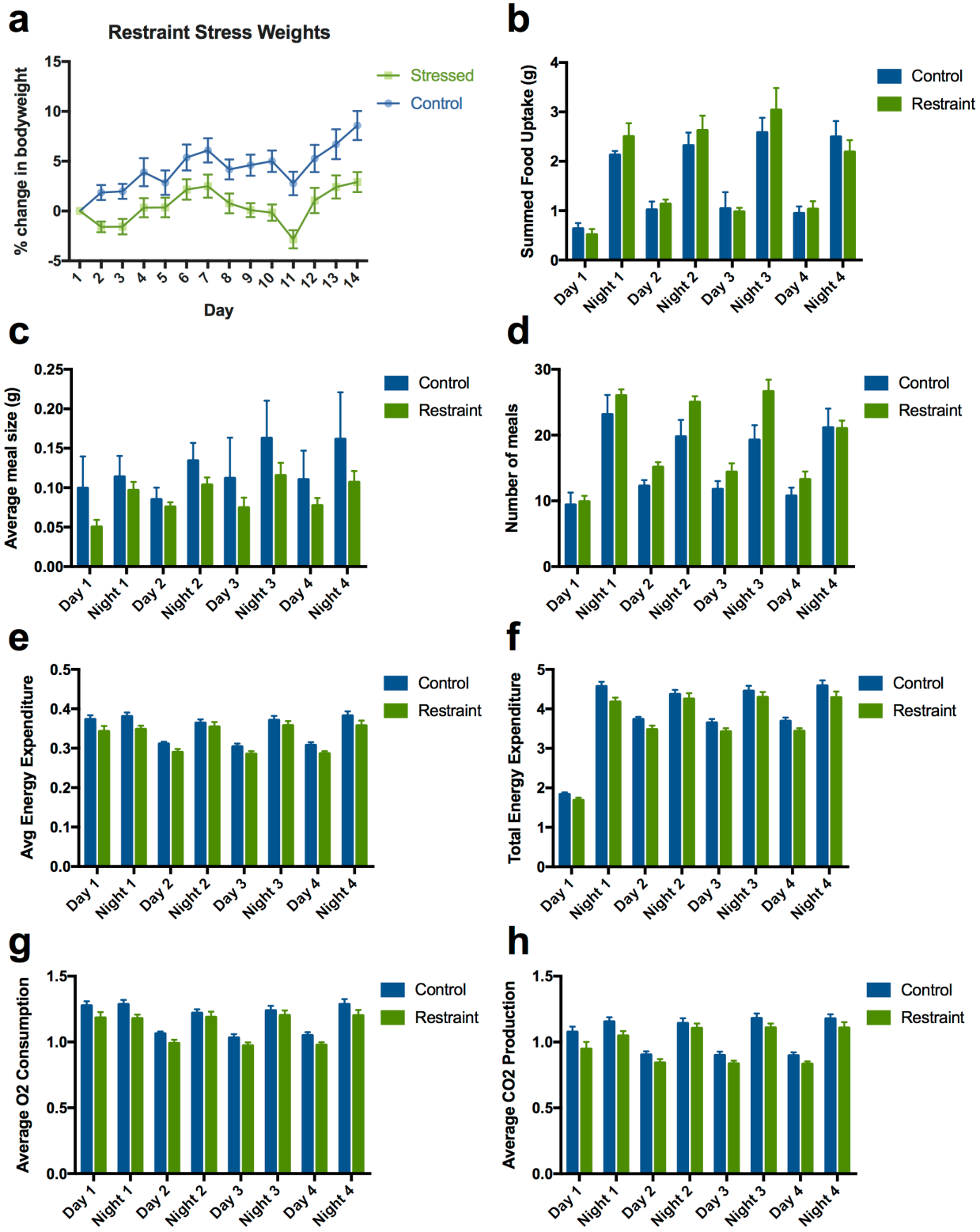

Figure 21. Examining the effect of restraint stress on changes in metabolic phenotypes. a) Graph showing the percent change in bodyweight across 14 days with restraint stress occurring once daily for the first ten days. b-d) Summary bar graphs showing daily/nightly Promethion measurements of feeding behavior, including summary food uptake (b), average meal size (c), and number of meals (d). e-h) Summary bar graphs showing daily/nightly Promethion measurements of average energy expenditure (e), total energy expenditure (f), average oxygen consumption (g), and average carbon dioxide production (h). n = 8 female mice/group.

To further explore differences between metabolic phenotypes in male and female mice, the same Promethion system measurements were made using a cohort of mice that contained both sexes. In general, male mice were seen to have greater energy expenditure (Figure 22a-b), including increased respiration rates (Figure 22c-d). These differences appear to be sex-based and not differences driven by stress. A 2-way ANOVA reveals a significant effect of treatment on both average energy expenditure (Figure 22a; $F(3,27) = 4.05$, $p = 0.017$) and total energy expenditure (Figure 22b; $F(3,27) = 4.05$, $p = 0.017$). However, post hoc analysis reveals that there is no significant difference between male and female control groups or male and female restraint groups for any of the days/nights tested. Similarly, a 2-way ANOVA reveals a significant effect of treatment on both average oxygen consumption (Figure 22c; $F(3,27) = 3.47$, $p = 0.030$) and average carbon dioxide production (Figure 22d; $F(3,27) = 6.65$, $p = 0.002$). Once again, there is no difference between control and restraint groups for either sex throughout the Promethion testing period. The lack of differences between control and restraint groups in this experiment once again highlights the variability observed between cohorts undergoing this restraint stress paradigm.

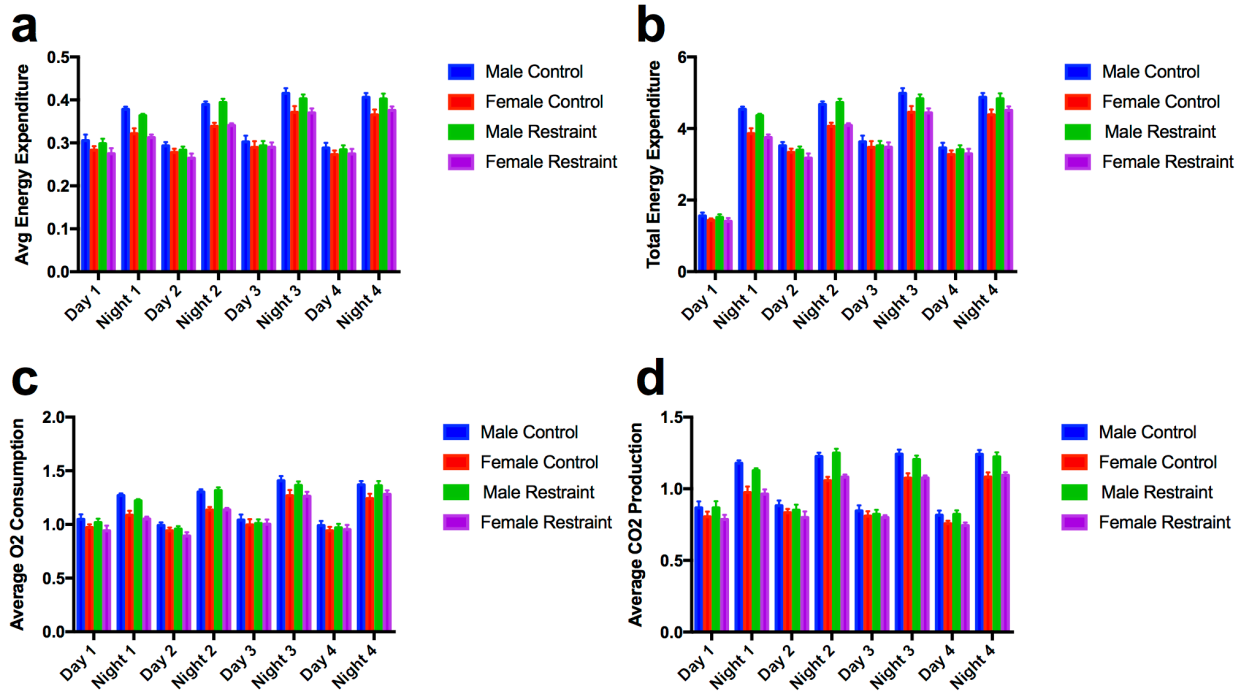

Figure 22. Comparing the effects of restraint stress on metabolic phenotypes in male and female mice. a-d) Summary bar graphs showing daily/nightly Promethion measurements of average energy expenditure (a), total energy expenditure (b), average oxygen consumption (c), and average carbon dioxide production (d) in male and female mice. n = 8 mice/group (exception: female/restraint n = 7 mice).

The variability in these experiments suggests that the observed weight loss and metabolic phenotypes are not easily reproducible. Several factors could be influencing this variability. For one, while the mice were weighed at the same time each day, the time of day may not have been consistent between cohorts. Similarly, the restraint stress may not have occurred at the same time each day for the various cohorts. Differences in circadian rhythm signaling could be affecting responses to both stress and alterations in bodyweight. The current inability to replicate the initial experimental findings has led us to no longer follow-up on these results.

APPENDIX D

Dissecting BNST Heterogeneity Using Calbindin as an Additional Neuronal Population Marker

Chapter 3 focuses on using *Prkcd* as an additional marker in RNA *in situ* hybridization assays to further divide the heterogeneous BNST into various cell populations. As we continue to dissect the neurons that are activated by stress in the BNST, we also ran assays assessing the expression of the transcript expression for Calbindin 2 (Calb2) in stressed and unstressed female mice. As observed in Figure 23a-b, the co-expression pattern of these three transcripts does change with exposure to acute restraint stress.

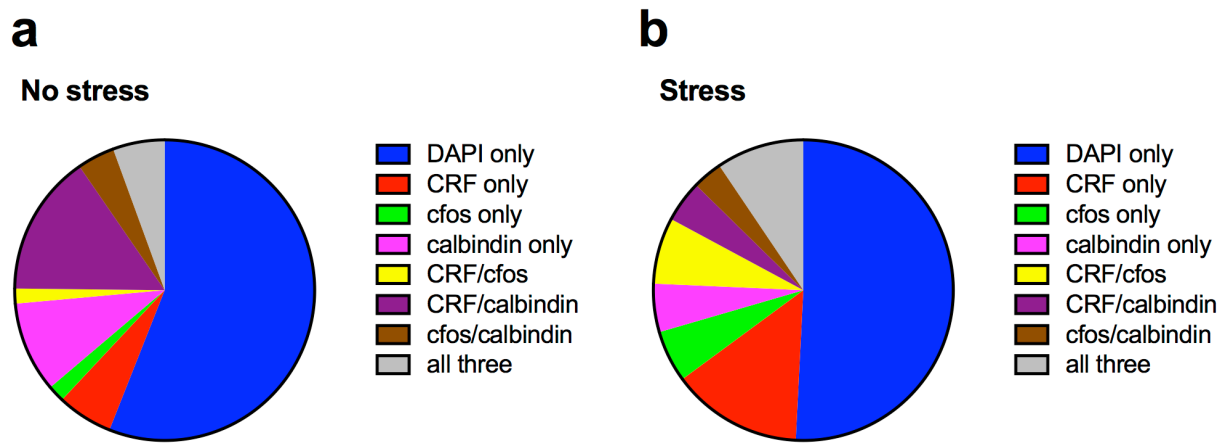

Figure 23. Examining the co-expression of mRNA transcripts for CRF, cFos, and Calbindin 2 in the dBNST of unstressed and stressed female mice. a-b) Pie charts showing co-expression pattern mRNA transcripts in control (a) and stressed (b) female mice. Graphed as a percentage of all cells.

With this cohort of mice we were able to replicate the stress-induced *Fos* observed in *Crh* cells discussed in Chapters 2 and 3 (Figure 24a-b). Comparing the *Calb2* expression in *Crh* cells shows that approximately half of CRF neurons express Calbindin in both the stress and control conditions, with potentially more CRF neurons expressing Calbindin in the control condition (Figure 24c-d). Finally, the majority of NON CRF neurons do not express Calbindin in both the control and stress conditions (Figure 24e-f).

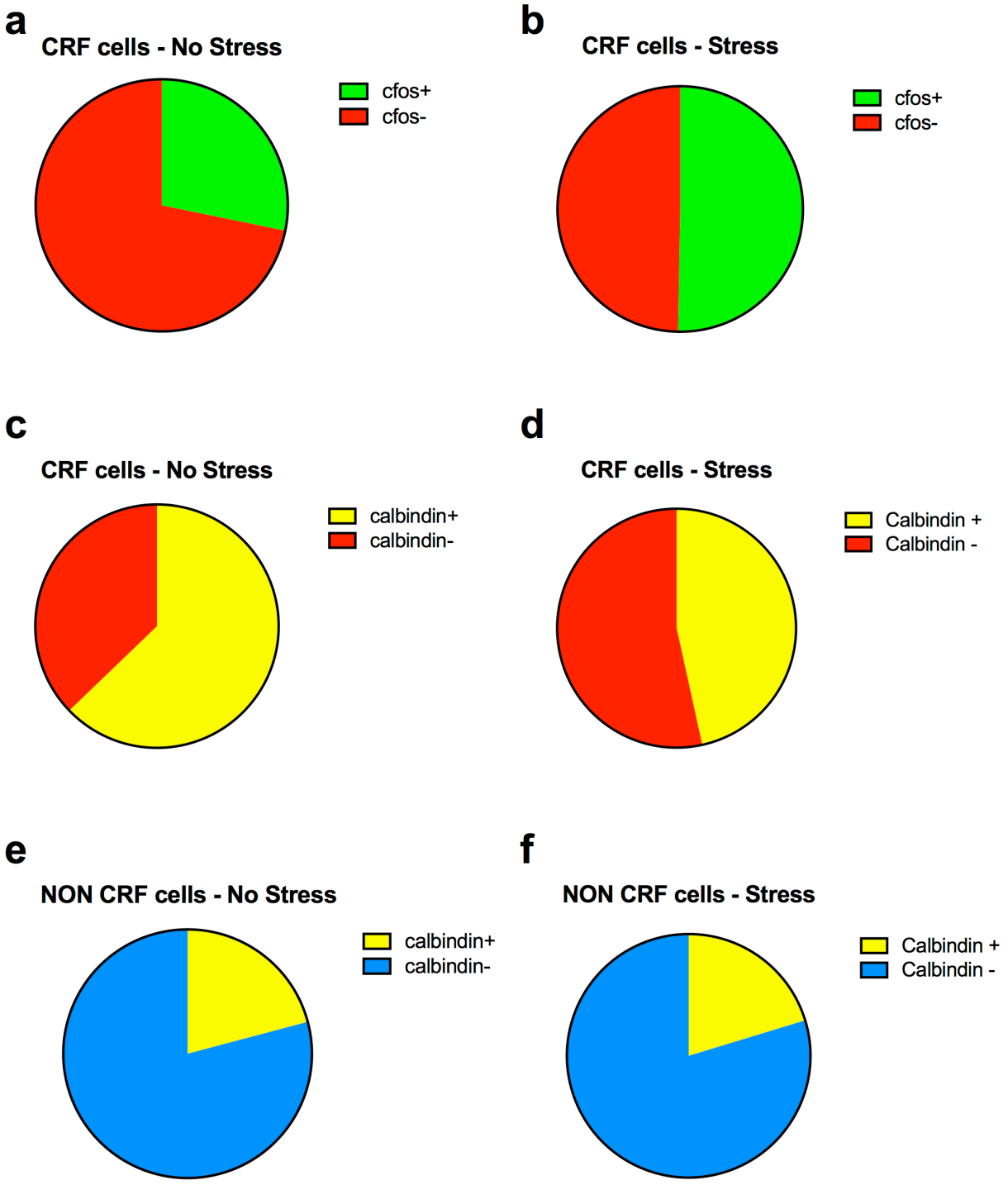

Figure 24. Visualizing stress-induced changes in co-expression of mRNA transcript markers in the dBNST. a-b) Pie charts showing the percentage of CRF cells that express cfos in control (a) and stressed (b) mice. c-d) Pie charts showing the percentage of CRF cells that express Calbindin in control (c) and stressed (d) mice. e-f) Pie charts showing the percentage of NON CRF cells that express Calbindin in control (e) and stressed (f) mice.

The co-expression of these transcripts needs to be further analyzed, looking at the variability in expression between mice and using statistical tests to verify significant stress-induced changes in co-expression of these transcripts. Of note, these experiments were all performed in female mice. Continuing to investigate potential sex differences in co-expression should also be a future avenue of research. As Calbindin has the potential to mark a subset of CRF neurons in the dBNST, looking at how this overlaps with *Prkcd* expression both with and without stress may lead to a better understanding of diverse BNST neuronal populations.

REFERENCES

Alfinito PD, Chen X, Mastroeni R, Pawlyk AC and Deecher DC (2009). Estradiol increases catecholamine levels in the hypothalamus of ovariectomized rats during the dark-phase. *Eur J Pharmacol*. **616** (1-3): 334-339.

Alheid GF and Heimer L (1988). New perspectives in basal forebrain organization of special relevance for neuropsychiatric disorders: the striatopallidal, amygdaloid, and corticopetal components of substantia innominata. *Neuroscience*. **27** (1): 1-39.

Allen LS and Gorski RA (1990). Sex difference in the bed nucleus of the stria terminalis of the human brain. *J Comp Neurol*. **302** (4): 697-706.

Aloisi AM, Ceccarelli I and Lupo C (1998). Behavioural and hormonal effects of restraint stress and formalin test in male and female rats. *Brain Res Bull*. **47** (1): 57-62.

Alvarez RP, Kirlic N, Misaki M, Bodurka J, Rhudy JL, Paulus MP and Drevets WC (2015). Increased anterior insula activity in anxious individuals is linked to diminished perceived control. *Transl Psychiatry*. **5**: e591.

Anantharam V, Kitazawa M, Wagner J, Kaul S and Kanthasamy AG (2002). Caspase-3-dependent proteolytic cleavage of protein kinase Cdelta is essential for oxidative stress-mediated dopaminergic cell death after exposure to methylcyclopentadienyl manganese tricarbonyl. *J Neurosci*. **22** (5): 1738-1751.

Arguello AA, Wang R, Lyons CM, Higginbotham JA, Hodges MA and Fuchs RA (2017). Role of the agranular insular cortex in contextual control over cocaine-seeking behavior in rats. *Psychopharmacology (Berl)*. **234** (16): 2431-2441.

Arluison M, Vankova M, Cesselin F and Leviel V (1990). Origin of some enkephalin-containing afferents to the ventro-medial region of the globus pallidus in the rat. *Brain Res Bull*. **25** (1): 25-34.

Armbruster BN, Li X, Pausch MH, Herlitze S and Roth BL (2007). Evolving the lock to fit the key to create a family of G protein-coupled receptors potently activated by an inert ligand. *Proc Natl Acad Sci U S A*. **104** (12): 5163-5168.

Asok A, Draper A, Hoffman AF, Schulkin J, Lupica CR and Rosen JB (2018). Optogenetic silencing of a corticotropin-releasing factor pathway from the central amygdala to the bed nucleus of the stria terminalis disrupts sustained fear. *Mol Psychiatry*. **23** (4): 914-922.

Aston-Jones G, Delfs JM, Druhan J and Zhu Y (1999). The bed nucleus of the stria terminalis. A target site for noradrenergic actions in opiate withdrawal. *Ann N Y Acad Sci*. **877**: 486-498.

Aston-Jones G, Ennis M, Pieribone VA, Nickell WT and Shipley MT (1986). The brain nucleus locus coeruleus: restricted afferent control of a broad efferent network. *Science*. **234** (4777): 734-737.

Aston-Jones G, Rajkowski J and Cohen J (2000). Locus coeruleus and regulation of behavioral flexibility and attention. *Prog Brain Res*. **126**: 165-182.

Atkinson HC and Waddell BJ (1997). Circadian variation in basal plasma corticosterone and adrenocorticotropin in the rat: sexual dimorphism and changes across the estrous cycle. *Endocrinology*. **138** (9): 3842-3848.

Avery SN, Clauss JA and Blackford JU (2016). The Human BNST: Functional Role in Anxiety and Addiction. *Neuropsychopharmacology*. **41** (1): 126-141.

Avery SN, Clauss JA, Winder DG, Woodward N, Heckers S and Blackford JU (2014). BNST neurocircuitry in humans. *Neuroimage*. **91**: 311-323.

Babb JA, Masini CV, Day HEW and Campeau S (2013). Sex differences in activated corticotropin-releasing factor neurons within stress-related neurocircuitry and hypothalamic–pituitary–adrenocortical axis hormones following restraint in rats. *Neuroscience*. **234** (0): 40-52.

Bangasser DA, Curtis A, Reyes BA, Bethea TT, Parastatidis I, Ischiropoulos H, Van Bockstaele EJ and Valentino RJ (2010). Sex differences in corticotropin-releasing factor receptor signaling and trafficking: potential role in female vulnerability to stress-related psychopathology. *Mol Psychiatry*. **15** (9): 877, 896-904.

Bangasser DA and Valentino RJ (2014). Sex differences in stress-related psychiatric disorders: neurobiological perspectives. *Front Neuroendocrinol*. **35** (3): 303-319.

Bangasser DA, Zhang X, Garachh V, Hanhauser E and Valentino RJ (2011). Sexual dimorphism in locus coeruleus dendritic morphology: a structural basis for sex differences in emotional arousal. *Physiol Behav*. **103** (3-4): 342-351.

Beaulieu S, Di Paolo T and Barden N (1986). Control of ACTH secretion by the central nucleus of the amygdala: implication of the serotoninergic system and its relevance to the glucocorticoid delayed negative feedback mechanism. *Neuroendocrinology*. **44** (2): 247-254.

Becker JB, Prendergast BJ and Liang JW (2016). Female rats are not more variable than male rats: a meta-analysis of neuroscience studies. *Biol Sex Differ*. **7**: 34.

Beery AK and Zucker I (2011). Sex bias in neuroscience and biomedical research. *Neurosci Biobehav Rev*. **35** (3): 565-572.

Bellocchio L, Soria-Gomez E, Quarta C, Metna-Laurent M, Cardinal P, Binder E, Cannich A, Delamarre A, Haring M, Martin-Fontecha M, Vega D, Leste-Lasserre T, Bartsch D, Monory K, Lutz B, Chaouloff F, Pagotto U, Guzman M, Cota D and Marsicano G (2013). Activation of the sympathetic nervous system mediates hypophagic and anxiety-like effects of CB(1) receptor blockade. *Proc Natl Acad Sci U S A*. **110** (12): 4786-4791.

Betley JN, Cao ZF, Ritola KD and Sternson SM (2013). Parallel, redundant circuit organization for homeostatic control of feeding behavior. *Cell*. **155** (6): 1337-1350.

Bodnoff SR, Suranyi-Cadotte B, Aitken DH, Quirion R and Meaney MJ (1988). The effects of chronic antidepressant treatment in an animal model of anxiety. *Psychopharmacology (Berl)*. **95** (3): 298-302.

Bonson KR, Grant SJ, Contoreggi CS, Links JM, Metcalfe J, Weyl HL, Kurian V, Ernst M and London ED (2002). Neural systems and cue-induced cocaine craving. *Neuropsychopharmacology*. **26** (3): 376-386.

Bota M, Sporns O and Swanson LW (2012). Neuroinformatics analysis of molecular expression patterns and neuron populations in gray matter regions: the rat BST as a rich exemplar. *Brain Res*. **1450**: 174-193.

Brady KT and Sinha R (2005). Co-occurring mental and substance use disorders: the neurobiological effects of chronic stress. *Am J Psychiatry*. **162** (8): 1483-1493.

Bremner JD, Randall P, Scott TM, Bronen RA, Seibyl JP, Southwick SM, Delaney RC, McCarthy G, Charney DS and Innis RB (1995). MRI-based measurement of hippocampal volume in patients with combat-related posttraumatic stress disorder. *Am J Psychiatry*. **152** (7): 973-981.

Breslau N (2002). Gender differences in trauma and posttraumatic stress disorder. *J Gend Specif Med*. **5** (1): 34-40.

Brinkmann L, Buff C, Neumeister P, Tupak SV, Becker MP, Herrmann MJ and Straube T (2017). Dissociation between amygdala and bed nucleus of the stria terminalis during threat anticipation in female post-traumatic stress disorder patients. *Hum Brain Mapp*.

Broussard GJ, Liang R and Tian L (2014). Monitoring activity in neural circuits with genetically encoded indicators. *Front Mol Neurosci*. **7**: 97.

Brown ZJ, Tribe E, D'Souza N A and Erb S (2009). Interaction between noradrenaline and corticotrophin-releasing factor in the reinstatement of cocaine seeking in the rat. *Psychopharmacology (Berl)*. **203** (1): 121-130.

Busch C, Bohl J and Ohm TG (1997). Spatial, temporal and numeric analysis of Alzheimer changes in the nucleus coeruleus. *Neurobiol Aging*. **18** (4): 401-406.

Butler RK, Oliver EM, Sharko AC, Parilla-Carrero J, Kaigler KF, Fadel JR and Wilson MA (2016). Activation of corticotropin releasing factor-containing neurons in the rat central amygdala and bed nucleus of the stria terminalis following exposure to two different anxiogenic stressors. *Behav Brain Res*. **304**: 92-101.

Bylund DB, Eikenberg DC, Hieble JP, Langer SZ, Lefkowitz RJ, Minneman KP, Molinoff PB, Ruffolo RR, Jr. and Trendelenburg U (1994). International Union of Pharmacology nomenclature of adrenoceptors. *Pharmacol Rev*. **46** (2): 121-136.

Bystritsky A and Kronemyer D (2014). Stress and anxiety: counterpart elements of the stress/anxiety complex. *Psychiatr Clin North Am*. **37** (4): 489-518.

Cahill L (2006). Why sex matters for neuroscience. *Nat Rev Neurosci*. **7** (6): 477-484.

Cai H, Haubensak W, Anthony TE and Anderson DJ (2014). Central amygdala PKC-delta(+) neurons mediate the influence of multiple anorexigenic signals. *Nat Neurosci*. **17** (9): 1240-1248.

Calogero AE, Gallucci WT, Gold PW and Chrousos GP (1988). Multiple feedback regulatory loops upon rat hypothalamic corticotropin-releasing hormone secretion. Potential clinical implications. *J Clin Invest*. **82** (3): 767-774.

Campos CA, Bowen AJ, Roman CW and Palmiter RD (2018). Encoding of danger by parabrachial CGRP neurons. *Nature*. **555** (7698): 617-622.

Campos CA, Bowen AJ, Schwartz MW and Palmiter RD (2016). Parabrachial CGRP Neurons Control Meal Termination. *Cell Metab*. **23** (5): 811-820.

Cannon WB (1915). Bodily changes in pain, hunger, fear and rage, an account of recent researches into the function of emotional excitement. New York: D. Appleton and Co.

Carter ME, Han S and Palmiter RD (2015). Parabrachial calcitonin gene-related Peptide neurons mediate conditioned taste aversion. *J Neurosci*. **35** (11): 4582-4586.

Carter ME, Soden ME, Zweifel LS and Palmiter RD (2013). Genetic identification of a neural circuit that suppresses appetite. *Nature*. **503** (7474): 111-114.

Carvalho-Netto EF, Myers B, Jones K, Solomon MB and Herman JP (2011). Sex differences in synaptic plasticity in stress-responsive brain regions following chronic variable stress. *Physiol Behav*. **104** (2): 242-247.

Casada JH and Dafny N (1991). Restraint and stimulation of bed nucleus of the stria terminalis produce similar stress-like behaviors. *Brain Res Bull*. **27** (2): 207-212.

Cecchi M, Khoshbouei H, Javors M and Morilak DA (2002). Modulatory effects of norepinephrine in the lateral bed nucleus of the stria terminalis on behavioral and neuroendocrine responses to acute stress. *Neuroscience*. **112** (1): 13-21.

Chen AC and Etkin A (2013). Hippocampal network connectivity and activation differentiates post-traumatic stress disorder from generalized anxiety disorder. *Neuropsychopharmacology*. **38** (10): 1889-1898.

Chen P, Fan Y, Li Y, Sun Z, Bissette G and Zhu MY (2012). Chronic social defeat up-regulates expression of norepinephrine transporter in rat brains. *Neurochem Int*. **60** (1): 9-20.

Chen Q, Roeder Z, Li MH, Zhang Y, Ingram SL and Heinricher MM (2017). Optogenetic evidence for a direct circuit linking nociceptive transmission through the parabrachial complex with pain-modulating neurons of the rostral ventromedial medulla (RVM). *eNeuro*. **4** (3).

Chen Y, Molet J, Gunn BG, Ressler K and Baram TZ (2015). Diversity of reporter expression patterns in transgenic mouse lines targeting corticotropin-releasing hormone-expressing neurons. *Endocrinology*. **156** (12): 4769-4780.

Choi DC, Furay AR, Evanson NK, Ostrander MM, Ulrich-Lai YM and Herman JP (2007). Bed nucleus of the stria terminalis subregions differentially regulate hypothalamic-pituitary-adrenal axis activity: implications for the integration of limbic inputs. *J Neurosci*. **27** (8): 2025-2034.

Choi DC, Nguyen MM, Tamashiro KL, Ma LY, Sakai RR and Herman JP (2006). Chronic social stress in the visible burrow system modulates stress-related gene expression in the bed nucleus of the stria terminalis. *Physiol Behav*. **89** (3): 301-310.

Chrousos GP (2009). Stress and disorders of the stress system. *Nat Rev Endocrinol*. **5** (7): 374-381.

Chrousos GP and Gold PW (1992). The concepts of stress and stress system disorders. Overview of physical and behavioral homeostasis. *JAMA*. **267** (9): 1244-1252.

Ciccocioppo R, Fedeli A, Economidou D, Policani F, Weiss F and Massi M (2003). The Bed Nucleus Is a Neuroanatomical Substrate for the Anorectic Effect of Corticotropin-Releasing Factor and for Its Reversal by Nociceptin/Orphanin FQ. *J Neurosci*. **23** (28): 9445-9451.

Ciccocioppo R, Martin-Fardon R, Weiss F and Massi M (2001). Nociceptin/orphanin FQ inhibits stress- and CRF-induced anorexia in rats. *Neuroreport*. **12** (6): 1145-1149.

Ciocchi S, Herry C, Grenier F, Wolff SB, Letzkus JJ, Vlachos I, Ehrlich I, Sprengel R, Deisseroth K, Stadler MB, Muller C and Luthi A (2010). Encoding of conditioned fear in central amygdala inhibitory circuits. *Nature*. **468** (7321): 277-282.

Cippitelli A, Damadzic R, Hansson AC, Singley E, Sommer WH, Eskay R, Thorsell A and Heilig M (2010). Neuropeptide Y (NPY) suppresses yohimbine-induced reinstatement of alcohol seeking. *Psychopharmacology (Berl)*. **208** (3): 417-426.

Cleck JN and Blendy JA (2008). Making a bad thing worse: adverse effects of stress on drug addiction. *J Clin Invest*. **118** (2): 454-461.

Cole RL and Sawchenko PE (2002). Neurotransmitter regulation of cellular activation and neuropeptide gene expression in the paraventricular nucleus of the hypothalamus. *J Neurosci*. **22** (3): 959-969.

Cottone P, Sabino V, Roberto M, Bajo M, Pockros L, Frihauf JB, Fekete EM, Steardo L, Rice KC, Grigoriadis DE, Conti B, Koob GF and Zorrilla EP (2009). CRF system recruitment mediates dark side of compulsive eating. *Proc Natl Acad Sci U S A*. **106** (47): 20016-20020.

Craig AD (2002). How do you feel? Interoception: the sense of the physiological condition of the body. *Nat Rev Neurosci*. **3** (8): 655-666.

Crestani CC, Alves FH, Gomes FV, Resstel LB, Correa FM and Herman JP (2013). Mechanisms in the bed nucleus of the stria terminalis involved in control of autonomic and neuroendocrine functions: a review. *Curr Neuropharmacol*. **11** (2): 141-159.

Crowley NA, Bloodgood DW, Hardaway JA, Kendra AM, McCall JG, Al-Hasani R, McCall NM, Yu W, Schools ZL, Krashes MJ, Lowell BB, Whistler JL, Bruchas MR and Kash TL (2016). Dynorphin Controls the Gain of an Amygdalar Anxiety Circuit. *Cell Rep*. **14** (12): 2774-2783.

Cryan JF and Holmes A (2005). The ascent of mouse: advances in modelling human depression and anxiety. *Nat Rev Drug Discov*. **4** (9): 775-790.

Cui G, Jun SB, Jin X, Pham MD, Vogel SS, Lovinger DM and Costa RM (2013). Concurrent activation of striatal direct and indirect pathways during action initiation. *Nature*. **494** (7436): 238-242.

Cullinan WE, Herman JP and Watson SJ (1993). Ventral subicular interaction with the hypothalamic paraventricular nucleus: evidence for a relay in the bed nucleus of the stria terminalis. *J Comp Neurol*. **332** (1): 1-20.

Cummings S, Elde R, Ells J and Lindall A (1983). Corticotropin-releasing factor immunoreactivity is widely distributed within the central nervous system of the rat: an immunohistochemical study. *J Neurosci*. **3** (7): 1355-1368.

Curtis AL, Bethea T and Valentino RJ (2006). Sexually dimorphic responses of the brain norepinephrine system to stress and corticotropin-releasing factor. *Neuropsychopharmacology*. **31** (3): 544-554.

Dabrowska J, Hazra R, Ahern TH, Guo JD, McDonald AJ, Mascagni F, Muller JF, Young LJ and Rainnie DG (2011). Neuroanatomical evidence for reciprocal regulation of the corticotrophin-releasing factor and oxytocin systems in the hypothalamus and the bed nucleus of the stria terminalis of the rat: Implications for balancing stress and affect. *Psychoneuroendocrinology*. **36** (9): 1312-1326.

Dabrowska J, Hazra R, Guo JD, Dewitt S and Rainnie DG (2013). Central CRF neurons are not created equal: phenotypic differences in CRF-containing neurons of the rat paraventricular hypothalamus and the bed nucleus of the stria terminalis. *Front Neurosci*. **7**: 156.

Daniel SE, Guo J and Rainnie DG (2017). A comparative analysis of the physiological properties of neurons in the anterolateral bed nucleus of the stria terminalis in the Mus musculus, Rattus norvegicus, and Macaca mulatta. *J Comp Neurol*. **525** (9): 2235-2248.

Dautzenberg FM and Hauger RL (2002). The CRF peptide family and their receptors: yet more partners discovered. *Trends Pharmacol Sci*. **23** (2): 71-77.

Davis M, Walker DL, Miles L and Grillon C (2010). Phasic vs sustained fear in rats and humans: role of the extended amygdala in fear vs anxiety. *Neuropsychopharmacology*. **35** (1): 105-135.

Day HE, Campeau S, Watson SJ, Jr. and Akil H (1997). Distribution of alpha 1a-, alpha 1b- and alpha 1d-adrenergic receptor mRNA in the rat brain and spinal cord. *J Chem Neuroanat*. **13** (2): 115-139.

de Kloet ER, Oitzl MS and Joels M (1999). Stress and cognition: are corticosteroids good or bad guys? *Trends Neurosci*. **22** (10): 422-426.

de Lacalle S and Saper CB (2000). Calcitonin gene-related peptide-like immunoreactivity marks putative visceral sensory pathways in human brain. *Neuroscience*. **100** (1): 115-130.

del Abril A, Segovia S and Guillamon A (1987). The bed nucleus of the stria terminalis in the rat: regional sex differences controlled by gonadal steroids early after birth. *Brain Res*. **429** (2): 295-300.

Delaney AJ, Crane JW and Sah P (2007). Noradrenaline modulates transmission at a central synapse by a presynaptic mechanism. *Neuron*. **56** (5): 880-892.

Delfs JM, Zhu Y, Druhan JP and Aston-Jones G (2000). Noradrenaline in the ventral forebrain is critical for opiate withdrawal-induced aversion. *Nature*. **403** (6768): 430-434.

Dhabhar FS (2014). Effects of stress on immune function: the good, the bad, and the beautiful. *Immunol Res*. **58** (2-3): 193-210.

Diamond DM, Bennett MC, Fleshner M and Rose GM (1992). Inverted-U relationship between the level of peripheral corticosterone and the magnitude of hippocampal primed burst potentiation. *Hippocampus*. **2** (4): 421-430.

DiLeone RJ, Taylor JR and Picciotto MR (2012). The drive to eat: comparisons and distinctions between mechanisms of food reward and drug addiction. *Nat Neurosci*. **15** (10): 1330-1335.

Dobolyi A, Irwin S, Makara G, Usdin TB and Palkovits M (2005). Calcitonin gene-related peptide-containing pathways in the rat forebrain. *J Comp Neurol*. **489** (1): 92-119.

Dong HW, Petrovich GD and Swanson LW (2001a). Topography of projections from amygdala to bed nuclei of the stria terminalis. *Brain Res Brain Res Rev*. **38** (1-2): 192-246.

Dong HW, Petrovich GD, Watts AG and Swanson LW (2001b). Basic organization of projections from the oval and fusiform nuclei of the bed nuclei of the stria terminalis in adult rat brain. *J Comp Neurol*. **436** (4): 430-455.

Dong HW and Swanson LW (2004). Organization of axonal projections from the anterolateral area of the bed nuclei of the stria terminalis. *J Comp Neurol*. **468** (2): 277-298.

Dong HW and Swanson LW (2006). Projections from bed nuclei of the stria terminalis, anteromedial area: cerebral hemisphere integration of neuroendocrine, autonomic, and behavioral aspects of energy balance. *J Comp Neurol*. **494** (1): 142-178.

Duncko R, Kiss A, Skultetyova I, Rusnak M and Jezova D (2001). Corticotropin-releasing hormone mRNA levels in response to chronic mild stress rise in male but not in female rats while tyrosine hydroxylase mRNA levels decrease in both sexes. *Psychoneuroendocrinology*. **26** (1): 77-89.

Dunn JD and Whitener J (1986). Plasma corticosterone responses to electrical stimulation of the amygdaloid complex: cytoarchitectural specificity. *Neuroendocrinology*. **42** (3): 211-217.

Egli RE, Kash TL, Choo K, Savchenko V, Matthews RT, Blakely RD and Winder DG (2005). Norepinephrine modulates glutamatergic transmission in the bed nucleus of the stria terminalis. *Neuropsychopharmacology*. **30** (4): 657-668.

Erb S, Shaham Y and Stewart J (2001). Stress-induced relapse to drug seeking in the rat: role of the bed nucleus of the stria terminalis and amygdala. *Stress*. **4** (4): 289-303.

Erb S and Stewart J (1999). A role for the bed nucleus of the stria terminalis, but not the amygdala, in the effects of corticotropin-releasing factor on stress-induced reinstatement of cocaine seeking. *J Neurosci*. **19** (20): Rc35.

Essner RA, Smith AG, Jamnik AA, Ryba AR, Trutner ZD and Carter ME (2017). AgRP Neurons Can Increase Food Intake during Conditions of Appetite Suppression and Inhibit Anorexigenic Parabrachial Neurons. *J Neurosci*. **37** (36): 8678-8687.

Fadok JP, Krabbe S, Markovic M, Courtin J, Xu C, Massi L, Botta P, Bylund K, Muller C, Kovacevic A, Tovote P and Luthi A (2017). A competitive inhibitory circuit for selection of active and passive fear responses. *Nature*. **542** (7639): 96-100.

Fenno LE, Mattis J, Ramakrishnan C and Deisseroth K (2017). A Guide to Creating and Testing New INTRSECT Constructs. *Curr Protoc Neurosci*. **80**: 4.39.31-34.39.24.

Fenno LE, Mattis J, Ramakrishnan C, Hyun M, Lee SY, He M, Tucciarone J, Selimbeyoglu A, Berndt A, Grosenick L, Zalocusky KA, Bernstein H, Swanson H, Perry C, Diester I, Boyce FM, Bass CE, Neve R, Huang ZJ and Deisseroth K (2014). Targeting cells with single vectors using multiple-feature Boolean logic. *Nat Methods*. **11** (7): 763-772.

Figueiredo HF, Bruestle A, Bodie B, Dolgas CM and Herman JP (2003). The medial prefrontal cortex differentially regulates stress-induced c-fos expression in the forebrain depending on type of stressor. *Eur J Neurosci*. **18** (8): 2357-2364.

Fitzgerald PB, Segrave R, Richardson KE, Knox LA, Herring S, Daskalakis ZJ and Bittar RG (2018). A pilot study of bed nucleus of the stria terminalis deep brain stimulation in treatment-resistant depression. *Brain Stimul*.

Flavin SA, Matthews RT, Wang Q, Muly EC and Winder DG (2014). alpha(2A)-adrenergic receptors filter parabrachial inputs to the bed nucleus of the stria terminalis. *J Neurosci*. **34** (28): 9319-9331.

Forray MI, Bustos G and Gysling K (1997). Regulation of norepinephrine release from the rat bed nucleus of the stria terminalis: in vivo microdialysis studies. *J Neurosci Res*. **50** (6): 1040-1046.

Forray MI and Gysling K (2004). Role of noradrenergic projections to the bed nucleus of the stria terminalis in the regulation of the hypothalamic-pituitary-adrenal axis. *Brain Res Brain Res Rev*. **47** (1-3): 145-160.

Forray MI, Gysling K, Andres ME, Bustos G and Araneda S (2000). Medullary noradrenergic neurons projecting to the bed nucleus of the stria terminalis express mRNA for the NMDA-NR1 receptor. *Brain Res Bull*. **52** (3): 163-169.

Fox HC, Morgan PT and Sinha R (2014). Sex differences in guanfacine effects on drug craving and stress arousal in cocaine-dependent individuals. *Neuropsychopharmacology*. **39** (6): 1527-1537.

Franklin KB and Paxinos G (2007). The mouse brain in stereotaxic coordinates. New York: Elsevier.

Funk CK, O'Dell LE, Crawford EF and Koob GF (2006). Corticotropin-releasing factor within the central nucleus of the amygdala mediates enhanced ethanol self-administration in withdrawn, ethanol-dependent rats. *J Neurosci*. **26** (44): 11324-11332.

Gallucci WT, Baum A, Laue L, Rabin DS, Chrousos GP, Gold PW and Kling MA (1993). Sex differences in sensitivity of the hypothalamic-pituitary-adrenal axis. *Health Psychol*. **12** (5): 420-425.

Garcia-Falgueras A, Pinos H, Collado P, Pasaro E, Fernandez R, Segovia S and Guillamon A (2005). The expression of brain sexual dimorphism in artificial selection of rat strains. *Brain Res*. **1052** (2): 130-138.

Garcia-Falgueras A, Pinos H, Fernandez R, Collado P, Pasaro E, Segovia S and Guillamon A (2006). Sexual dimorphism in hybrids rats. *Brain Res*. **1123** (1): 42-50.

George O, Ghozland S, Azar MR, Cottone P, Zorrilla EP, Parsons LH, O'Dell LE, Richardson HN and Koob GF (2007). CRF-CRF1 system activation mediates withdrawal-induced increases in nicotine self-administration in nicotine-dependent rats. *Proc Natl Acad Sci U S A*. **104** (43): 17198-17203.

Georges F and Aston-Jones G (2001). Potent regulation of midbrain dopamine neurons by the bed nucleus of the stria terminalis. *J Neurosci*. **21** (16): Rc160.

Gerra G, Volpi R, Delsignore R, Maninetti L, Caccavari R, Vourna S, Maestri D, Chiodera P, Ugolotti G and Coiro V (1992). Sex-related responses of beta-endorphin, ACTH, GH and PRL to cold exposure in humans. *Acta Endocrinol (Copenh)*. **126** (1): 24-28.

Ghayur T, Hugunin M, Talanian RV, Ratnofsky S, Quinlan C, Emoto Y, Pandey P, Datta R, Huang Y, Kharbanda S, Allen H, Kamen R, Wong W and Kufe D (1996). Proteolytic activation of protein kinase C delta by an ICE/CED 3-like protease induces characteristics of apoptosis. *J Exp Med*. **184** (6): 2399-2404.

Giardino WJ, Eban-Rothschild A, Christoffel DJ, Li SB, Malenka RC and de Lecea L (2018). Parallel circuits from the bed nuclei of stria terminalis to the lateral hypothalamus drive opposing emotional states. *Nat Neurosci*. **21** (8): 1084-1095.

Gogolla N (2017). The insular cortex. *Curr Biol*. **27** (12): R580-r586.

Gomes-de-Souza L, Oliveira LA, Benini R, Rodella P, Costa-Ferreira W and Crestani CC (2016). Involvement of endocannabinoid neurotransmission in the bed nucleus of stria terminalis in cardiovascular responses to acute restraint stress in rats. *Br J Pharmacol*. **173** (19): 2833-2844.

Grabinski TM, Kneynsberg A, Manfredsson FP and Kanaan NM (2015). A method for combining RNAscope in situ hybridization with immunohistochemistry in thick free-floating brain sections and primary neuronal cultures. *PLoS One*. **10** (3): e0120120.

Green B, Kavanagh D and Young R (2003). Being stoned: a review of self-reported cannabis effects. *Drug Alcohol Rev*. **22** (4): 453-460.

Gross MJ, Kahn JP, Laxenaire M, Nicolas JP and Burlet C (1994). [Corticotropin-releasing factor and anorexia nervosa: reactions of the hypothalamus-pituitary-adrenal axis to neurotropic stress]. *Ann Endocrinol (Paris)*. **55** (6): 221-228.

Grueter BA, Gosnell HB, Olsen CM, Schramm-Sapyta NL, Nekrasova T, Landreth GE and Winder DG (2006). Extracellular-signal regulated kinase 1-dependent metabotropic glutamate receptor 5-induced long-term depression in the bed nucleus of the stria terminalis is disrupted by cocaine administration. *J Neurosci*. **26** (12): 3210-3219.

Gu G, Cornea A and Simerly RB (2003). Sexual differentiation of projections from the principal nucleus of the bed nuclei of the stria terminalis. *J Comp Neurol*. **460** (4): 542-562.

Guarda AS, Schreyer CC, Boersma GJ, Tamashiro KL and Moran TH (2015). Anorexia nervosa as a motivated behavior: Relevance of anxiety, stress, fear and learning. *Physiol Behav*. **152** (Pt B): 466-472.

Guillemin R and Rosenberg B (1955). Humoral hypothalamic control of anterior pituitary: a study with combined tissue cultures. *Endocrinology*. **57** (5): 599-607.

Gungor NZ and Pare D (2014). CGRP inhibits neurons of the bed nucleus of the stria terminalis: implications for the regulation of fear and anxiety. *J Neurosci*. **34** (1): 60-65.

Gungor NZ, Yamamoto R and Pare D (2018). Glutamatergic and gabaergic ventral BNST neurons differ in their physiological properties and responsiveness to noradrenaline. *Neuropsychopharmacology*.

Gunn BG, Cunningham L, Mitchell SG, Swinny JD, Lambert JJ and Belelli D (2015). GABA(A) receptor-acting neurosteroids: A role in the development and regulation of the stress response. *Frontiers in Neuroendocrinology*. **36**: 28-48.

Guo JD, Hammack SE, Hazra R, Levita L and Rainnie DG (2009). Bi-directional modulation of bed nucleus of stria terminalis neurons by 5-HT: molecular expression and functional properties of excitatory 5-HT receptor subtypes. *Neuroscience*. **164** (4): 1776-1793.

Hammack SE, Mania I and Rainnie DG (2007). Differential expression of intrinsic membrane currents in defined cell types of the anterolateral bed nucleus of the stria terminalis. *J Neurophysiol*. **98** (2): 638-656.

Hammack SE and May V (2015). Pituitary adenylate cyclase activating polypeptide in stress-related disorders: data convergence from animal and human studies. *Biol Psychiatry*. **78** (3): 167-177.

Han TM and De Vries GJ (2003). Organizational effects of testosterone, estradiol, and dihydrotestosterone on vasopressin mRNA expression in the bed nucleus of the stria terminalis. *J Neurobiol*. **54** (3): 502-510.

Hankin BL (2009). Development of sex differences in depressive and co-occurring anxious symptoms during adolescence: descriptive trajectories and potential explanations in a multiwave prospective study. *J Clin Child Adolesc Psychol*. **38** (4): 460-472.

Hardaway JA, Crowley NA, Bulik CM and Kash TL (2015). Integrated circuits and molecular components for stress and feeding: implications for eating disorders. *Genes Brain Behav*. **14** (1): 85-97.

Harris NA and Winder DG (2018). Synaptic plasticity in the bed nucleus of the stria terminalis: underlying mechanisms and potential ramifications for reinstatement of drug- and alcohol-seeking behaviors. *ACS Chem Neurosci*.

Haubensak W, Kunwar PS, Cai H, Ciocchi S, Wall NR, Ponnusamy R, Biag J, Dong HW, Deisseroth K, Callaway EM, Fanselow MS, Luthi A and Anderson DJ (2010). Genetic dissection of an amygdala microcircuit that gates conditioned fear. *Nature*. **468** (7321): 270-276.

Hazra R, Guo JD, Ryan SJ, Jasnow AM, Dabrowska J and Rainnie DG (2011). A transcriptomic analysis of type I-III neurons in the bed nucleus of the stria terminalis. *Mol Cell Neurosci*. **46** (4): 699-709.

Heilig M, Koob GF, Ekman R and Britton KT (1994). Corticotropin-releasing factor and neuropeptide Y: role in emotional integration. *Trends Neurosci*. **17** (2): 80-85.

Hein L (2006). Adrenoceptors and signal transduction in neurons. *Cell Tissue Res*. **326** (2): 541-551.

Heinsbroek RP, Van Haaren F, Feenstra MG, Endert E and Van de Poll NE (1991). Sex- and time-dependent changes in neurochemical and hormonal variables induced by predictable and unpredictable footshock. *Physiol Behav*. **49** (6): 1251-1256.

Herkenham M, Lynn AB, Little MD, Johnson MR, Melvin LS, de Costa BR and Rice KC (1990). Cannabinoid receptor localization in brain. *Proc Natl Acad Sci U S A*. **87** (5): 1932-1936.

Herman JP, Cullinan WE, Morano MI, Akil H and Watson SJ (1995). Contribution of the ventral subiculum to inhibitory regulation of the hypothalamo-pituitary-adrenocortical axis. *J Neuroendocrinol*. **7** (6): 475-482.

Herman JP, Figueiredo H, Mueller NK, Ulrich-Lai Y, Ostrander MM, Choi DC and Cullinan WE (2003). Central mechanisms of stress integration: hierarchical circuitry controlling hypothalamo-pituitary-adrenocortical responsiveness. *Front Neuroendocrinol*. **24** (3): 151-180.

Heuser I, Yassouridis A and Holsboer F (1994). The combined dexamethasone/CRH test: a refined laboratory test for psychiatric disorders. *J Psychiatr Res*. **28** (4): 341-356.

Hines M, Allen LS and Gorski RA (1992). Sex differences in subregions of the medial nucleus of the amygdala and the bed nucleus of the stria terminalis of the rat. *Brain Res*. **579** (2): 321-326.

Hoffman GE, Smith MS and Verbalis JG (1993). c-Fos and related immediate early gene products as markers of activity in neuroendocrine systems. *Front Neuroendocrinol*. **14** (3): 173-213.

Holleran KM, Wilson HH, Fetterly TL, Bluett RJ, Centanni SW, Gilfarb RA, Rocco LE, Patel S and Winder DG (2016). Ketamine and MAG Lipase Inhibitor-Dependent Reversal of Evolving Depressive-Like Behavior During Forced Abstinence From Alcohol Drinking. *Neuropsychopharmacology*. **41** (8): 2062-2071.

Howlett AC, Barth F, Bonner TI, Cabral G, Casellas P, Devane WA, Felder CC, Herkenham M, Mackie K, Martin BR, Mechoulam R and Pertwee RG (2002). International Union of Pharmacology. XXVII. Classification of cannabinoid receptors. *Pharmacol Rev*. **54** (2): 161-202.

Ide S, Hara T, Ohno A, Tamano R, Koseki K, Naka T, Maruyama C, Kaneda K, Yoshioka M and Minami M (2013). Opposing roles of corticotropin-releasing factor and neuropeptide Y within the dorsolateral bed nucleus of the stria terminalis in the negative affective component of pain in rats. *J Neurosci*. **33** (14): 5881-5894.

Inoue N (2014). Stress and atherosclerotic cardiovascular disease. *J Atheroscler Thromb*. **21** (5): 391-401.

Iwasaki-Sekino A, Mano-Otagiri A, Ohata H, Yamauchi N and Shibasaki T (2009). Gender differences in corticotropin and corticosterone secretion and corticotropin-releasing factor mRNA expression in the paraventricular nucleus of the hypothalamus and the central nucleus of the amygdala in response to footshock stress or psychological stress in rats. *Psychoneuroendocrinology*. **34** (2): 226-237.

Jennings JH, Sparta DR, Stamatakis AM, Ung RL, Pleil KE, Kash TL and Stuber GD (2013). Distinct extended amygdala circuits for divergent motivational states. *Nature*. **496** (7444): 224-228.

Jezova D, Kvetnansky R and Vigas M (1994). Sex differences in endocrine response to hyperthermia in sauna. *Acta Physiol Scand*. **150** (3): 293-298.

Johnston JB (1923). Further contributions to the study of the evolution of the forebrain. *The Journal of Comparative Neurology*. **35** (5): 337-481.

Ju G and Swanson LW (1989). Studies on the cellular architecture of the bed nuclei of the stria terminalis in the rat: I. Cytoarchitecture. *J Comp Neurol*. **280** (4): 587-602.

Ju G, Swanson LW and Simerly RB (1989). Studies on the cellular architecture of the bed nuclei of the stria terminalis in the rat: II. Chemoarchitecture. *J Comp Neurol*. **280** (4): 603-621.

Kanaya M, Tsuda MC, Sagoshi S, Nagata K, Morimoto C, Thu CK, Toda K, Kato S, Ogawa S and Tsukahara S (2014). Regional difference in sex steroid action on formation of morphological sex differences in the anteroventral periventricular nucleus and principal nucleus of the bed nucleus of the stria terminalis. *PLoS One*. **9** (11): e112616.

Kandel DB, Johnson JG, Bird HR, Canino G, Goodman SH, Lahey BB, Regier DA and Schwab-Stone M (1997). Psychiatric disorders associated with substance use among children and adolescents: findings from the Methods for the Epidemiology of Child and Adolescent Mental Disorders (MECA) Study. *J Abnorm Child Psychol*. **25** (2): 121-132.

Kano M, Ohno-Shosaku T, Hashimotodani Y, Uchigashima M and Watanabe M (2009). Endocannabinoid-mediated control of synaptic transmission. *Physiol Rev*. **89** (1): 309-380.

Kao CY, Stalla G, Stalla J, Wotjak CT and Anderzhanova E (2015). Norepinephrine and corticosterone in the medial prefrontal cortex and hippocampus predict PTSD-like symptoms in mice. *Eur J Neurosci*. **41** (9): 1139-1148.

Karkanias GB, Li CS and Etgen AM (1997). Estradiol reduction of alpha 2-adrenoceptor binding in female rat cortex is correlated with decreases in alpha 2A/D-adrenoceptor messenger RNA. *Neuroscience*. **81** (3): 593-597.

Kash TL, Pleil KE, Marcinkiewcz CA, Lowery-Gionta EG, Crowley N, Mazzone C, Sugam J, Hardaway JA and McElligott ZA (2015). Neuropeptide regulation of signaling and behavior in the BNST. *Mol Cells*. **38** (1): 1-13.

Kash TL and Winder DG (2006). Neuropeptide Y and corticotropin-releasing factor bi-directionally modulate inhibitory synaptic transmission in the bed nucleus of the stria terminalis. *Neuropharmacology*. **51** (5): 1013-1022.

Kaufling J, Girard D, Maitre M, Leste-Lasserre T and Georges F (2017). Species-specific diversity in the anatomical and physiological organisation of the BNST-VTA pathway. *Eur J Neurosci*.

Kelly DA, Varnum MM, Krentzel AA, Krug S and Forger NG (2013). Differential control of sex differences in estrogen receptor alpha in the bed nucleus of the stria terminalis and anteroventral periventricular nucleus. *Endocrinology*. **154** (10): 3836-3846.

Kessler RC, McGonagle KA, Zhao S, Nelson CB, Hughes M, Eshleman S, Wittchen HU and Kendler KS (1994). Lifetime and 12-month prevalence of DSM-III-R psychiatric disorders in the United States. Results from the National Comorbidity Survey. *Arch Gen Psychiatry*. **51** (1): 8-19.

Kessler RC, Petukhova M, Sampson NA, Zaslavsky AM and Wittchen HU (2012). Twelve-month and lifetime prevalence and lifetime morbid risk of anxiety and mood disorders in the United States. *Int J Methods Psychiatr Res*. **21** (3): 169-184.

Kessler RC, Sonnega A, Bromet E, Hughes M and Nelson CB (1995). Posttraumatic stress disorder in the National Comorbidity Survey. *Arch Gen Psychiatry*. **52** (12): 1048-1060.

Kim SY, Adhikari A, Lee SY, Marshel JH, Kim CK, Mallory CS, Lo M, Pak S, Mattis J, Lim BK, Malenka RC, Warden MR, Neve R, Tye KM and Deisseroth K (2013). Diverging neural pathways assemble a behavioural state from separable features in anxiety. *Nature*. **496** (7444): 219-223.

Kirschbaum C, Kudielka BM, Gaab J, Schommer NC and Hellhammer DH (1999). Impact of gender, menstrual cycle phase, and oral contraceptives on the activity of the hypothalamus-pituitary-adrenal axis. *Psychosom Med*. **61** (2): 154-162.

Kitay JI (1961). Sex differences in adrenal cortical secretion in the rat. *Endocrinology*. **68**: 818-824.

Knigge KM (1961). Adrenocortical response to stress in rats with lesions in hippocampus and amygdala. *Proc Soc Exp Biol Med*. **108**: 18-21.

Koob G and Kreek MJ (2007). Stress, dysregulation of drug reward pathways, and the transition to drug dependence. *Am J Psychiatry*. **164** (8): 1149-1159.

Koob GF (1999). Corticotropin-releasing factor, norepinephrine, and stress. *Biol Psychiatry*. **46** (9): 1167-1180.

Koob GF (2008). A role for brain stress systems in addiction. *Neuron*. **59** (1): 11-34.

Koob GF (2009). Brain stress systems in the amygdala and addiction. *Brain Res*. **1293**: 61-75.

Koob GF, Ahmed SH, Boutrel B, Chen SA, Kenny PJ, Markou A, O'Dell LE, Parsons LH and Sanna PP (2004). Neurobiological mechanisms in the transition from drug use to drug dependence. *Neurosci Biobehav Rev*. **27** (8): 739-749.

Koob GF and Heinrichs SC (1999). A role for corticotropin releasing factor and urocortin in behavioral responses to stressors. *Brain Res*. **848** (1-2): 141-152.

Kosten TA, Miserendino MJ and Kehoe P (2000). Enhanced acquisition of cocaine self-administration in adult rats with neonatal isolation stress experience. *Brain Res*. **875** (1-2): 44-50.

Krahn DD, Gosnell BA, Grace M and Levine AS (1986). CRF antagonist partially reverses CRF- and stress-induced effects on feeding. *Brain Res Bull*. **17** (3): 285-289.

Krawczyk M, Georges F, Sharma R, Mason X, Berthet A, Bezard E and Dumont EC (2011). Double-dissociation of the catecholaminergic modulation of synaptic transmission in the oval bed nucleus of the stria terminalis. *J Neurophysiol*. **105** (1): 145-153.

Kusumoto-Yoshida I, Liu H, Chen BT, Fontanini A and Bonci A (2015). Central role for the insular cortex in mediating conditioned responses to anticipatory cues. *Proc Natl Acad Sci U S A*. **112** (4): 1190-1195.

Kwako LE, Spagnolo PA, Schwandt ML, Thorsell A, George DT, Momenan R, Rio DE, Huestis M, Anizan S, Concheiro M, Sinha R and Heilig M (2015). The corticotropin releasing hormone-1 (CRH1) receptor antagonist pexacerfont in alcohol dependence: a randomized controlled experimental medicine study. *Neuropsychopharmacology*. **40** (5): 1053-1063.

Labus JS, Naliboff BN, Fallon J, Berman SM, Suyenobu B, Bueller JA, Mandelkern M and Mayer EA (2008). Sex differences in brain activity during aversive visceral stimulation and its expectation in patients with chronic abdominal pain: a network analysis. *Neuroimage*. **41** (3): 1032-1043.

Le AD, Harding S, Juzytsch W, Funk D and Shaham Y (2005). Role of alpha-2 adrenoceptors in stress-induced reinstatement of alcohol seeking and alcohol self-administration in rats. *Psychopharmacology (Berl)*. **179** (2): 366-373.

Lebow M, Neufeld-Cohen A, Kuperman Y, Tsoory M, Gil S and Chen A (2012). Susceptibility to PTSD-like behavior is mediated by corticotropin-releasing factor receptor type 2 levels in the bed nucleus of the stria terminalis. *J Neurosci*. **32** (20): 6906-6916.

Lebow MA and Chen A (2016). Overshadowed by the amygdala: the bed nucleus of the stria terminalis emerges as key to psychiatric disorders. *Mol Psychiatry*. **21** (4): 450-463.

Liberzon I, Taylor SF, Amdur R, Jung TD, Chamberlain KR, Minoshima S, Koeppe RA and Fig LM (1999). Brain activation in PTSD in response to trauma-related stimuli. *Biol Psychiatry*. **45** (7): 817-826.

Lin X, Itoga CA, Taha S, Li MH, Chen R, Sami K, Berton F, Francesconi W and Xu X (2018). c-Fos mapping of brain regions activated by multi-modal and electric foot shock stress. *Neurobiol Stress*. **8**: 92-102.

Liu CH, Jing B, Ma X, Xu PF, Zhang Y, Li F, Wang YP, Tang LR, Wang YJ, Li HY and Wang CY (2014). Voxel-based morphometry study of the insular cortex in female patients with current and remitted depression. *Neuroscience*. **262**: 190-199.

Louderback KM, Wills TA, Muglia LJ and Winder DG (2013). Knockdown of BNST GluN2B-containing NMDA receptors mimics the actions of ketamine on novelty-induced hypophagia. *Transl Psychiatry*. **3**: e331.

Lubbers LS, Zafian PT, Gautreaux C, Gordon M, Alves SE, Correa L, Lorrain DS, Hickey GJ and Luine V (2010). Estrogen receptor (ER) subtype agonists alter monoamine levels in the female rat brain. *J Steroid Biochem Mol Biol*. **122** (5): 310-317.

Lupien SJ, Maheu F, Tu M, Fiocco A and Schramek TE (2007). The effects of stress and stress hormones on human cognition: Implications for the field of brain and cognition. *Brain Cogn*. **65** (3): 209-237.

Luque JM, de Blas MR, Segovia S and Guillamon A (1992). Sexual dimorphism of the dopamine-beta-hydroxylase-immunoreactive neurons in the rat locus ceruleus. *Brain Res Dev Brain Res*. **67** (2): 211-215.

Malendowicz LK (1976). Sex differences in adrenocortical structure and function. III. The effects of postpubertal gonadectomy and gonadal hormone replacement on adrenal cholesterol sidechain cleavage activity and on steroids biosynthesis by rat adrenal homogenates. *Endokrinologie*. **67** (1): 26-35.

Malendowicz LK (1980). Sex differences in adrenocortical structure and function. VI. Long-term effect of gonadectomy and testosterone or estradiol replacement on rat adrenal cortex. *Endokrinologie*. **75** (3): 311-323.

Mantsch JR, Baker DA, Francis DM, Katz ES, Hoks MA and Serge JP (2008). Stressor- and corticotropin releasing factor-induced reinstatement and active stress-related behavioral responses are augmented following long-access cocaine self-administration by rats. *Psychopharmacology (Berl)*. **195** (4): 591-603.

Mantsch JR, Weyer A, Vranjkovic O, Beyer CE, Baker DA and Caretta H (2010). Involvement of noradrenergic neurotransmission in the stress- but not cocaine-induced reinstatement of extinguished cocaine-induced conditioned place preference in mice: role for beta-2 adrenergic receptors. *Neuropsychopharmacology*. **35** (11): 2165-2178.

Marcinkiewcz CA, Mazzone CM, D'Agostino G, Halladay LR, Hardaway JA, DiBerto JF, Navarro M, Burnham N, Cristiano C, Dorrier CE, Tipton GJ, Ramakrishnan C, Kozicz T, Deisseroth K, Thiele TE, McElligott ZA, Holmes A, Heisler LK and Kash TL (2016). Serotonin engages an anxiety and fear-promoting circuit in the extended amygdala. *Nature*. **537** (7618): 97-101.

Massi L, Elezgarai I, Puente N, Reguero L, Grandes P, Manzoni OJ and Georges F (2008). Cannabinoid receptors in the bed nucleus of the stria terminalis control cortical excitation of midbrain dopamine cells in vivo. *J Neurosci*. **28** (42): 10496-10508.

McBride D, Barrett SP, Kelly JT, Aw A and Dagher A (2006). Effects of expectancy and abstinence on the neural response to smoking cues in cigarette smokers: an fMRI study. *Neuropsychopharmacology*. **31** (12): 2728-2738.

McDonald AJ, Shammah-Lagnado SJ, Shi C and Davis M (1999). Cortical afferents to the extended amygdala. *Ann N Y Acad Sci*. **877**: 309-338.

McElligott ZA, Klug JR, Nobis WP, Patel S, Grueter BA, Kash TL and Winder DG (2010). Distinct forms of Gq-receptor-dependent plasticity of excitatory transmission in the BNST are differentially affected by stress. *Proc Natl Acad Sci U S A*. **107** (5): 2271-2276.

McElligott ZA and Winder DG (2008). Alpha1-adrenergic receptor-induced heterosynaptic long-term depression in the bed nucleus of the stria terminalis is disrupted in mouse models of affective disorders. *Neuropsychopharmacology*. **33** (10): 2313-2323.

McEwen BS (2016). In pursuit of resilience: stress, epigenetics, and brain plasticity. *Ann N Y Acad Sci*. **1373** (1): 56-64.

McEwen BS and Sapolsky RM (1995). Stress and cognitive function. *Curr Opin Neurobiol*. **5** (2): 205-216.

McReynolds JR, Christianson JP, Blacktop JM and Mantsch JR (2018). What does the Fos say? Using Fos-based approaches to understand the contribution of stress to substance use disorders. *Neurobiology of Stress*.

McReynolds JR, Vranjkovic O, Thao M, Baker DA, Makky K, Lim Y and Mantsch JR (2014). Beta-2 adrenergic receptors mediate stress-evoked reinstatement of cocaine-induced conditioned place preference and increases in CRF mRNA in the bed nucleus of the stria terminalis in mice. *Psychopharmacology (Berl)*. **231** (20): 3953-3963.

Meaney MJ, Brake W and Gratton A (2002). Environmental regulation of the development of mesolimbic dopamine systems: a neurobiological mechanism for vulnerability to drug abuse? *Psychoneuroendocrinology*. **27** (1-2): 127-138.

Meitzen J, Perry AN, Westenbroek C, Hedges VL, Becker JB and Mermelstein PG (2013). Enhanced striatal beta1-adrenergic receptor expression following hormone loss in adulthood is programmed by both early sexual differentiation and puberty: a study of humans and rats. *Endocrinology*. **154** (5): 1820-1831.

Meloni EG, Gerety LP, Knoll AT, Cohen BM and Carlezon WA, Jr. (2006). Behavioral and anatomical interactions between dopamine and corticotropin-releasing factor in the rat. *J Neurosci*. **26** (14): 3855-3863.

Micioni Di Bonaventura MV, Ciccocioppo R, Romano A, Bossert JM, Rice KC, Ubaldi M, St Laurent R, Gaetani S, Massi M, Shaham Y and Cifani C (2014). Role of bed nucleus of the stria terminalis corticotrophin-releasing factor receptors in frustration stress-induced binge-like palatable food consumption in female rats with a history of food restriction. *J Neurosci*. **34** (34): 11316-11324.

Miyawaki A, Llopis J, Heim R, McCaffery JM, Adams JA, Ikura M and Tsien RY (1997). Fluorescent indicators for Ca2+ based on green fluorescent proteins and calmodulin. *Nature*. **388** (6645): 882-887.

Mogil JS and Chanda ML (2005). The case for the inclusion of female subjects in basic science studies of pain. *Pain*. **117** (1-2): 1-5.

Morena M, Patel S, Bains JS and Hill MN (2016). Neurobiological Interactions Between Stress and the Endocannabinoid System. *Neuropsychopharmacology*. **41** (1): 80-102.

Myers B, Mark Dolgas C, Kasckow J, Cullinan WE and Herman JP (2014). Central stress-integrative circuits: forebrain glutamatergic and GABAergic projections to the dorsomedial hypothalamus, medial preoptic area, and bed nucleus of the stria terminalis. *Brain Struct Funct*. **219** (4): 1287-1303.

Myrick H, Anton RF, Li X, Henderson S, Drobes D, Voronin K and George MS (2004). Differential brain activity in alcoholics and social drinkers to alcohol cues: relationship to craving. *Neuropsychopharmacology*. **29** (2): 393-402.

Naqvi NH, Rudrauf D, Damasio H and Bechara A (2007). Damage to the insula disrupts addiction to cigarette smoking. *Science*. **315** (5811): 531-534.

Nestler EJ, Barrot M, DiLeone RJ, Eisch AJ, Gold SJ and Monteggia LM (2002). Neurobiology of depression. *Neuron*. **34** (1): 13-25.

Newport DJ and Nemeroff CB (2000). Neurobiology of posttraumatic stress disorder. *Curr Opin Neurobiol*. **10** (2): 211-218.

Nifosi F, Toffanin T, Follador H, Zonta F, Padovan G, Pigato G, Carollo C, Ermani M, Amista P and Perini GI (2010). Reduced right posterior hippocampal volume in women with recurrent familial pure depressive disorder. *Psychiatry Res*. **184** (1): 23-28.

Nobis WP, Kash TL, Silberman Y and Winder DG (2011). beta-Adrenergic receptors enhance excitatory transmission in the bed nucleus of the stria terminalis through a corticotrophin-releasing factor receptor-dependent and cocaine-regulated mechanism. *Biol Psychiatry*. **69** (11): 1083-1090.

Nolen-Hoeksema S, Larson J and Grayson C (1999). Explaining the gender difference in depressive symptoms. *J Pers Soc Psychol*. **77** (5): 1061-1072.

Ohm TG, Busch C and Bohl J (1997). Unbiased estimation of neuronal numbers in the human nucleus coeruleus during aging. *Neurobiol Aging*. **18** (4): 393-399.

Ohno-Shosaku T and Kano M (2014). Endocannabinoid-mediated retrograde modulation of synaptic transmission. *Curr Opin Neurobiol*. **29**: 1-8.

Oliver G and Wardle J (1999). Perceived effects of stress on food choice. *Physiol Behav*. **66** (3): 511-515.

Olsen CM and Winder DG (2010). Operant sensation seeking in the mouse. *J Vis Exp*. (45).

Pacak K, McCarty R, Palkovits M, Kopin IJ and Goldstein DS (1995). Effects of immobilization on in vivo release of norepinephrine in the bed nucleus of the stria terminalis in conscious rats. *Brain Res*. **688** (1-2): 242-246.

Palmiter RD (2018). The Parabrachial Nucleus: CGRP Neurons Function as a General Alarm. *Trends Neurosci*. **41** (5): 280-293.

Pang TY, Renoir T, Du X, Lawrence AJ and Hannan AJ (2013). Depression-related behaviours displayed by female C57BL/6J mice during abstinence from chronic ethanol consumption are rescued by wheel-running. *Eur J Neurosci*. **37** (11): 1803-1810.

Pankevich DE, Teegarden SL, Hedin AD, Jensen CL and Bale TL (2010). Caloric restriction experience reprograms stress and orexigenic pathways and promotes binge eating. *J Neurosci*. **30** (48): 16399-16407.

Patel S, Roelke CT, Rademacher DJ, Cullinan WE and Hillard CJ (2004). Endocannabinoid signaling negatively modulates stress-induced activation of the hypothalamic-pituitary-adrenal axis. *Endocrinology*. **145** (12): 5431-5438.

Paul S, Jeon WK, Bizon JL and Han JS (2015). Interaction of basal forebrain cholinergic neurons with the glucocorticoid system in stress regulation and cognitive impairment. *Front Aging Neurosci*. **7**: 43.

Penzo MA, Robert V, Tucciarone J, De Bundel D, Wang M, Van Aelst L, Darvas M, Parada LF, Palmiter RD, He M, Huang ZJ and Li B (2015). The paraventricular thalamus controls a central amygdala fear circuit. *Nature*. **519** (7544): 455-459.

Phelix CF, Liposits Z and Paull WK (1992). Monoamine innervation of bed nucleus of stria terminalis: an electron microscopic investigation. *Brain Res Bull*. **28** (6): 949-965.

Pinos H, Collado P, Rodriguez-Zafra M, Rodriguez C, Segovia S and Guillamon A (2001). The development of sex differences in the locus coeruleus of the rat. *Brain Res Bull*. **56** (1): 73-78.

Pitman RK, Rasmusson AM, Koenen KC, Shin LM, Orr SP, Gilbertson MW, Milad MR and Liberzon I (2012). Biological studies of post-traumatic stress disorder. *Nat Rev Neurosci*. **13** (11): 769-787.

Pleil KE, Rinker JA, Lowery-Gionta EG, Mazzone CM, McCall NM, Kendra AM, Olson DP, Lowell BB, Grant KA, Thiele TE and Kash TL (2015). NPY signaling inhibits extended amygdala CRF neurons to suppress binge alcohol drinking. *Nat Neurosci*. **18** (4): 545-552.

Polston EK, Gu G and Simerly RB (2004). Neurons in the principal nucleus of the bed nuclei of the stria terminalis provide a sexually dimorphic GABAergic input to the anteroventral periventricular nucleus of the hypothalamus. *Neuroscience*. **123** (3): 793-803.

Pomrenze MB, Fetterly TL, Winder DG and Messing RO (2017). The Corticotropin Releasing Factor Receptor 1 in Alcohol Use Disorder: Still a Valid Drug Target? *Alcohol Clin Exp Res*. **41** (12): 1986-1999.

Posternak MA and Zimmerman M (2001). Symptoms of atypical depression. *Psychiatry Res*. **104** (2): 175-181.

Puente N, Elezgarai I, Lafourcade M, Reguero L, Marsicano G, Georges F, Manzoni OJ and Grandes P (2010). Localization and function of the cannabinoid CB1 receptor in the anterolateral bed nucleus of the stria terminalis. *PLoS One*. **5** (1): e8869.

Rainbow TC, Parsons B and Wolfe BB (1984). Quantitative autoradiography of beta 1- and beta 2-adrenergic receptors in rat brain. *Proc Natl Acad Sci U S A*. **81** (5): 1585-1589.

Reed PL, Anthony JC and Breslau N (2007). Incidence of drug problems in young adults exposed to trauma and posttraumatic stress disorder: do early life experiences and predispositions matter? *Arch Gen Psychiatry*. **64** (12): 1435-1442.

Reilly S (1999). The parabrachial nucleus and conditioned taste aversion. *Brain Res Bull*. **48** (3): 239-254.

Riche D, De Pommery J and Menetrey D (1990). Neuropeptides and catecholamines in efferent projections of the nuclei of the solitary tract in the rat. *J Comp Neurol*. **293** (3): 399-424.

Robertson SD, Plummer NW, de Marchena J and Jensen P (2013). Developmental origins of central norepinephrine neuron diversity. *Nat Neurosci*. **16** (8): 1016-1023.

Roland BL and Sawchenko PE (1993). Local origins of some GABAergic projections to the paraventricular and supraoptic nuclei of the hypothalamus in the rat. *J Comp Neurol*. **332** (1): 123-143.

Roozendaal B (2002). Stress and memory: opposing effects of glucocorticoids on memory consolidation and memory retrieval. *Neurobiol Learn Mem*. **78** (3): 578-595.

Rosenberg N, Bloch M, Ben Avi I, Rouach V, Schreiber S, Stern N and Greenman Y (2013). Cortisol response and desire to binge following psychological stress: comparison between obese subjects with and without binge eating disorder. *Psychiatry Res*. **208** (2): 156-161.

Rosmond R (2005). Role of stress in the pathogenesis of the metabolic syndrome. *Psychoneuroendocrinology*. **30** (1): 1-10.

Rosso IM, Cintron CM, Steingard RJ, Renshaw PF, Young AD and Yurgelun-Todd DA (2005). Amygdala and hippocampus volumes in pediatric major depression. *Biol Psychiatry*. **57** (1): 21-26.

Rubin RT, Mandell AJ and Crandall PH (1966). Corticosteroid responses to limbic stimulation in man: localization of stimulus sites. *Science*. **153** (3737): 767-768.

Saffran M and Schally AV (1955). The release of corticotrophin by anterior pituitary tissue in vitro. *Can J Biochem Physiol*. **33** (3): 408-415.

Sallee FR, Lyne A, Wigal T and McGough JJ (2009). Long-term safety and efficacy of guanfacine extended release in children and adolescents with attention-deficit/hyperactivity disorder. *J Child Adolesc Psychopharmacol*. **19** (3): 215-226.

Sanford CA, Soden ME, Baird MA, Miller SM, Schulkin J, Palmiter RD, Clark M and Zweifel LS (2017). A central amygdala CRF circuit facilitates learning about weak threats. *Neuron*. **93** (1): 164-178.

Sato M, Ito M, Nagase M, Sugimura YK, Takahashi Y, Watabe AM and Kato F (2015). The lateral parabrachial nucleus is actively involved in the acquisition of fear memory in mice. *Mol Brain*. **8**: 22.

Scheinin M, Lomasney JW, Hayden-Hixson DM, Schambra UB, Caron MG, Lefkowitz RJ and Fremeau RT, Jr. (1994). Distribution of alpha 2-adrenergic receptor subtype gene expression in rat brain. *Brain Res Mol Brain Res*. **21** (1-2): 133-149.

Schwandt ML, Cortes CR, Kwako LE, George DT, Momenan R, Sinha R, Grigoriadis DE, Pich EM, Leggio L and Heilig M (2016). The CRF1 Antagonist Verucerfont in Anxious Alcohol-Dependent Women: Translation of Neuroendocrine, But not of Anti-Craving Effects. *Neuropsychopharmacology*. **41** (12): 2818-2829.

Selye H (1936). A syndrome produced by diverse nocuous agents. *Nature*. **138**: 32.

Shaham Y, Highfield D, Delfs J, Leung S and Stewart J (2000). Clonidine blocks stress-induced reinstatement of heroin seeking in rats: an effect independent of locus coeruleus noradrenergic neurons. *Eur J Neurosci*. **12** (1): 292-302.

Shanmugam M, Krett NL, Maizels ET, Cutler RE, Jr., Peters CA, Smith LM, O'Brien ML, Park-Sarge OK, Rosen ST and Hunzicker-Dunn M (1999). Regulation of protein kinase C delta by estrogen in the MCF-7 human breast cancer cell line. *Mol Cell Endocrinol*. **148** (1-2): 109-118.

Sher KJ, Gershuny BS, Peterson L and Raskin G (1997). The role of childhood stressors in the intergenerational transmission of alcohol use disorders. *J Stud Alcohol*. **58** (4): 414-427.

Shields AD, Wang Q and Winder DG (2009). alpha2A-adrenergic receptors heterosynaptically regulate glutamatergic transmission in the bed nucleus of the stria terminalis. *Neuroscience*. **163** (1): 339-351.

Shimada S, Inagaki S, Kubota Y, Kito S, Funaki H and Takagi H (1989). Light and electron microscopic studies of calcitonin gene-related peptide-like immunoreactive terminals in the central nucleus of the amygdala and the bed nucleus of the stria terminalis of the rat. *Exp Brain Res*. **77** (1): 217-220.

Shin LM, McNally RJ, Kosslyn SM, Thompson WL, Rauch SL, Alpert NM, Metzger LJ, Lasko NB, Orr SP and Pitman RK (1999). Regional cerebral blood flow during script-driven imagery in childhood sexual abuse-related PTSD: A PET investigation. *Am J Psychiatry*. **156** (4): 575-584.

Shonesy BC, Bluett RJ, Ramikie TS, Baldi R, Hermanson DJ, Kingsley PJ, Marnett LJ, Winder DG, Colbran RJ and Patel S (2014). Genetic disruption of 2-arachidonoylglycerol synthesis reveals a key role for endocannabinoid signaling in anxiety modulation. *Cell Rep*. **9** (5): 1644-1653.

Sidor MM, Davidson TJ, Tye KM, Warden MR, Diesseroth K and McClung CA (2015). In vivo optogenetic stimulation of the rodent central nervous system. *J Vis Exp*. (95): 51483.

Silberman Y, Matthews RT and Winder DG (2013). A corticotropin releasing factor pathway for ethanol regulation of the ventral tegmental area in the bed nucleus of the stria terminalis. *J Neurosci*. **33** (3): 950-960.

Silberman Y and Winder DG (2013). Corticotropin releasing factor and catecholamines enhance glutamatergic neurotransmission in the lateral subdivision of the central amygdala. *Neuropharmacology*. **70**: 316-323.

Sinha R (2007). The role of stress in addiction relapse. *Curr Psychiatry Rep*. **9** (5): 388-395.

Sinha R (2008). Chronic stress, drug use, and vulnerability to addiction. *Ann N Y Acad Sci*. **1141**: 105-130.

Sink KS, Walker DL, Freeman SM, Flandreau EI, Ressler KJ and Davis M (2013). Effects of continuously enhanced corticotropin releasing factor expression within the bed nucleus of the stria terminalis on conditioned and unconditioned anxiety. *Mol Psychiatry*. **18** (3): 308-319.

Sterrenburg L, Gaszner B, Boerrigter J, Santbergen L, Bramini M, Elliott E, Chen A, Peeters BW, Roubos EW and Kozicz T (2011). Chronic stress induces sex-specific alterations in methylation and expression of corticotropin-releasing factor gene in the rat. *PLoS One*. **6** (11): e28128.

Sterrenburg L, Gaszner B, Boerrigter J, Santbergen L, Bramini M, Roubos EW, Peeters BW and Kozicz T (2012). Sex-dependent and differential responses to acute restraint stress of corticotropin-releasing factor-producing neurons in the rat paraventricular nucleus, central amygdala, and bed nucleus of the stria terminalis. *J Neurosci Res*. **90** (1): 179-192.

Strohle A and Holsboer F (2003). Stress responsive neurohormones in depression and anxiety. *Pharmacopsychiatry*. **36 Suppl 3**: S207-214.

Stroud LR, Salovey P and Epel ES (2002). Sex differences in stress responses: social rejection versus achievement stress. *Biol Psychiatry*. **52** (4): 318-327.

Sullivan GM, Apergis J, Bush DE, Johnson LR, Hou M and Ledoux JE (2004). Lesions in the bed nucleus of the stria terminalis disrupt corticosterone and freezing responses elicited by a contextual but not by a specific cue-conditioned fear stimulus. *Neuroscience*. **128** (1): 7-14.

Sullivan RM and Gratton A (1999). Lateralized effects of medial prefrontal cortex lesions on neuroendocrine and autonomic stress responses in rats. *J Neurosci*. **19** (7): 2834-2840.

Swanson LW and Hartman BK (1975). The central adrenergic system. An immunofluorescence study of the location of cell bodies and their efferent connections in the rat utilizing dopamine-beta-hydroxylase as a marker. *J Comp Neurol*. **163** (4): 467-505.

Tamashiro KL, Sakai RR, Shively CA, Karatsoreos IN and Reagan LP (2011). Chronic stress, metabolism, and metabolic syndrome. *Stress*. **14** (5): 468-474.

Teegarden SL and Bale TL (2008). Effects of stress on dietary preference and intake are dependent on access and stress sensitivity. *Physiol Behav*. **93** (4-5): 713-723.

Tervo DG, Hwang BY, Viswanathan S, Gaj T, Lavzin M, Ritola KD, Lindo S, Michael S, Kuleshova E, Ojala D, Huang CC, Gerfen CR, Schiller J, Dudman JT, Hantman AW, Looger LL, Schaffer DV and Karpova AY (2016). A Designer AAV Variant Permits Efficient Retrograde Access to Projection Neurons. *Neuron*. **92** (2): 372-382.

Toth M, Gresack JE, Bangasser DA, Plona Z, Valentino RJ, Flandreau EI, Mansuy IM, Merlo-Pich E, Geyer MA and Risbrough VB (2014). Forebrain-specific CRF overproduction during development is sufficient to induce enduring anxiety and startle abnormalities in adult mice. *Neuropsychopharmacology*. **39** (6): 1409-1419.

Tran L, Schulkin J and Greenwood-Van Meerveld B (2014). Importance of CRF receptor-mediated mechanisms of the bed nucleus of the stria terminalis in the processing of anxiety and pain. *Neuropsychopharmacology*. **39** (11): 2633-2645.

Urwin RE, Bennetts B, Wilcken B, Lampropoulos B, Beumont P, Clarke S, Russell J, Tanner S and Nunn KP (2002). Anorexia nervosa (restrictive subtype) is associated with a polymorphism in the novel norepinephrine transporter gene promoter polymorphic region. *Mol Psychiatry*. **7** (6): 652-657.

Vale W, Spiess J, Rivier C and Rivier J (1981). Characterization of a 41-residue ovine hypothalamic peptide that stimulates secretion of corticotropin and beta-endorphin. *Science*. **213** (4514): 1394-1397.

Valentino RJ and Wehby RG (1988). Corticotropin-releasing factor: evidence for a neurotransmitter role in the locus ceruleus during hemodynamic stress. *Neuroendocrinology*. **48** (6): 674-677.

van den Pol AN (2012). Neuropeptide transmission in brain circuits. *Neuron*. **76** (1): 98-115.

van Gestel MA, Kostrzewa E, Adan RA and Janhunen SK (2014). Pharmacological manipulations in animal models of anorexia and binge eating in relation to humans. *Br J Pharmacol*. **171** (20): 4767-4784.

van Leeuwen FW, Caffe AR and De Vries GJ (1985). Vasopressin cells in the bed nucleus of the stria terminalis of the rat: sex differences and the influence of androgens. *Brain Res*. **325** (1-2): 391-394.

Vardy E, Robinson JE, Li C, Olsen RHJ, DiBerto JF, Giguere PM, Sassano FM, Huang XP, Zhu H, Urban DJ, White KL, Rittiner JE, Crowley NA, Pleil KE, Mazzone CM, Mosier PD, Song J, Kash TL, Malanga CJ, Krashes MJ and Roth BL (2015). A New DREADD Facilitates the Multiplexed Chemogenetic Interrogation of Behavior. *Neuron*. **86** (4): 936-946.

Vitlic A, Lord JM and Phillips AC (2014). Stress, ageing and their influence on functional, cellular and molecular aspects of the immune system. *Age (Dordr)*. **36** (3): 9631.

Volkow ND, Hampson AJ and Baler RD (2017). Don't Worry, Be Happy: Endocannabinoids and Cannabis at the Intersection of Stress and Reward. *Annu Rev Pharmacol Toxicol*. **57**: 285-308.

Wang GH (1923). The relation between 'spontaneous' activity and the oestrus cycle in the white rat. *Comp Psychol Monog*. **6**: 1-27.

Wang M, Ramos BP, Paspalas CD, Shu Y, Simen A, Duque A, Vijayraghavan S, Brennan A, Dudley A, Nou E, Mazer JA, McCormick DA and Arnsten AF (2007). Alpha2A-adrenoceptors strengthen working memory networks by inhibiting cAMP-HCN channel signaling in prefrontal cortex. *Cell*. **129** (2): 397-410.

Wang X, Cen X and Lu L (2001). Noradrenaline in the bed nucleus of the stria terminalis is critical for stress-induced reactivation of morphine-conditioned place preference in rats. *Eur J Pharmacol*. **432** (2-3): 153-161.

Wang Z, Guo Y, Bradesi S, Labus JS, Maarek JI, Lee K, Winchester WJ, Mayer EA and Holschneider DP (2009). Sex differences in functional brain activation during noxious visceral stimulation in rats. *Pain*. **145** (1-2): 120-128.

Weissman MM, Bland RC, Canino GJ, Faravelli C, Greenwald S, Hwu HG, Joyce PR, Karam EG, Lee CK, Lellouch J, Lepine JP, Newman SC, Rubio-Stipec M, Wells JE, Wickramaratne PJ, Wittchen H and Yeh EK (1996). Cross-national epidemiology of major depression and bipolar disorder. *Jama*. **276** (4): 293-299.

Wichmann S, Kirschbaum C, Bohme C and Petrowski K (2017). Cortisol stress response in post-traumatic stress disorder, panic disorder, and major depressive disorder patients. *Psychoneuroendocrinology*. **83**: 135-141.

Wills TA, Vaccaro D and McNamara G (1992). The role of life events, family support, and competence in adolescent substance use: a test of vulnerability and protective factors. *Am J Community Psychol*. **20** (3): 349-374.

Wing RR and Phelan S (2005). Long-term weight loss maintenance. *Am J Clin Nutr*. **82** (1 Suppl): 222s-225s.

Yang L, Zhao Y, Wang Y, Liu L, Zhang X, Li B and Cui R (2015). The Effects of Psychological Stress on Depression. *Curr Neuropharmacol*. **13** (4): 494-504.

Yehuda R, Giller EL, Southwick SM, Lowy MT and Mason JW (1991). Hypothalamic-pituitary-adrenal dysfunction in posttraumatic stress disorder. *Biol Psychiatry*. **30** (10): 1031-1048.

Young AH, Sahakian BJ, Robbins TW and Cowen PJ (1999). The effects of chronic administration of hydrocortisone on cognitive function in normal male volunteers. *Psychopharmacology (Berl)*. **145** (3): 260-266.

Yu K, Ahrens S, Zhang X, Schiff H, Ramakrishnan C, Fenno L, Deisseroth K, Zhao F, Luo MH, Gong L, He M, Zhou P, Paninski L and Li B (2017). The central amygdala controls learning in the lateral amygdala. *Nat Neurosci*. **20** (12): 1680-1685.

Zhou JN, Hofman MA, Gooren LJ and Swaab DF (1995). A sex difference in the human brain and its relation to transsexuality. *Nature*. **378** (6552): 68-70.

Zhu H, Aryal DK, Olsen RH, Urban DJ, Swearingen A, Forbes S, Roth BL and Hochgeschwender U (2016). Cre-dependent DREADD (Designer Receptors Exclusively Activated by Designer Drugs) mice. *Genesis*. **54** (8): 439-446.